Optimization of nanoporous silicon anodes with high ionic conductivity argyrodite solid electrolytes in solid state batteries

A comparative study of battery performance between silicon types, solid electrolytes and electrode preparation methods

Niels Bergsma

Optimization of nanoporous silicon anodes with high ionic conductivity argyrodite solid electrolytes in solid state batteries

A comparative study of battery performance between silicon types, solid electrolytes and electrode preparation methods

Thesis report

by

Niels Bergsma

to obtain the degree of Master of Science
at the Delft University of Technology
to be defended publicly on January 20, 2025

Thesis committee:

Chair:	Prof. dr. ir. Marnix Wagemaker
Supervisors:	Prof. dr. ir. Marnix Wagemaker
	Postdoc. Ajay Gautam
External examiner:	Prof. dr. Stephan Eijt
Place:	TU Delft Reactor Institute, Delft
Project Duration:	November, 2023 - January, 2025 at 10:00
Student number:	4715128

Faculty of Applied Sciences
Department Radiation Science and Technology | Storage of Electrochemical Energy (SEE) Group

Acknowledgments

I really enjoyed the time i spend within the SEE group during the process of my masters thesis. I learned a lot from watching and working alongside the other members of the group, and the weekly presentations on Thursday morning, where i got a very nice insight into what everybody was working on. I also want to thank the members of the inorganic group and the members of the battery now project for letting me take part in their meetings so i could see how everybody works together on different topics, and for giving me the opportunity to also show my own works and give me feedback which really helped me with my research.

In particular I want to thank Wenxuan, Zhu and Pranav for answering a lot of questions and giving advice for operations in the lab. And also special thanks to Frans, Katarina and Nirmal the lab technicians for keeping everything in the lab running smoothly and creating a good work environment. And especially to Frans for providing new solid state battery tips when i needed new ones. And thanks to Vignesh who worked along side me often in the glove box or in the student rooms, for all the nice chats we had and for going trough this thesis process together.

Then I want to thank the members of my thesis committee for taking the time to read this thesis and for agreeing to look at my presentation and for asking question at my defense. And thanks to Martina for arranging the room and arranging the date and time planning around my defense.

And the person who i should tank the most is my daily supervisor Ajay Gautam. You where always kind, and enthusiastic and ready to answer all my questions or tell me who to talk to in the group for help or information on certain topics. I really enjoyed having you as my supervisor and will look back on our time working together fondly.

And of course special thanks to my friends, family, colleagues and roommates for my time outside this process which kept me motivated and going until the finish line!

Niels Bergsma
Delft, The Netherlands
January, 2025

Abstract

We are currently undergoing an energy transition, in which batteries are playing a vital role. Their cost is quickly decreasing and they provide a way of storage for electricity generated by renewable energy sources such as wind and solar power generation. With the increase in demand for battery capacity comes the demand for safer, more energy dense, higher power output and faster charging batteries. To meet these demands researchers are now focusing on solid state batteries. And in these batteries on the anode side on a specif material called silicon (Si).

With its abundance in the earth's crust and a gravimetric energy density of more then 10 times that of graphite, which is currently most used as the anode in lithium ion batteries, this material seems very promising. But the silicon material expands up to 300-400% when fully charged/lithiated. This of course brings challenges for using silicon in solid state batteries, where the expansion could destroy the battery from within. Multiple solutions have been tried to deal with this volume expansion, and one of the solutions is to add nanopores into the silicon material so the material expands into the pores and not outwards. Such a material is provided by a company called E-magy, they have already shown this material to be effective in liquid lithium-ion batteries. But this thesis will focus on how this material performs in solid state batteries by comparing the galvanostatic battery cycling and electrochemical impedance spectroscopy data, to solid state-batteries that use silicon particles of the same size without the nanopores (called Com Si). For the solid electrolyte (SE) in these batteries a Cl rich version of lithium argyrodite is chosen with the chemical formula $Li_{5,5}PS_{4,5}Cl_{1,5}$. This material combines properties of halides and sulfides resulting in a deformable high ionic conductivity solid electrolyte that can form a stable interface in the battery operating potentials and accommodate the volume expansion of the silicon. Regular lithium argyrodite (Li_6PS_5Cl) and the Cl rich variant where synthesized with respective ionic conductivities of 2,9 and 7,5 mS/cm, to compare there performance in the Si solid state batteries.

Si/SE/CNF (Carbon nano fiber to increase the electronic conductivity) composite powder mixture electrodes where made with varying compositions, where the 6/3/1 composition showed the best performance with a initial discharge capacity of 2410 mAh/g with a current density of 0,229 mA/cm^2 for Com Si . After the formation cycles this battery showed a capacity retention of 73% going from 1680 mAh/g to 1230 mAh/g at a current density of 0,458 mA/cm over the span of 45 cycles. The CNF was shown to not have a positive and possibly a negative impact on the battery performance and with the results from the Si/SE/CNF batteries there was not a clear difference between the performance of porous and non porous silicon.

The switch was made to using Si deposited on Cu electrodes with a PVDF binder instead of the Si/SE/CNF composite electrodes. The best battery performance was achieved with a non porous 1,2 mg Si electrode showcasing a initial discharge capacity of 2700 mAh/g, and a capacity retention of 81,3% after the formation cycles going from 2250 to 1830 mAh/g with the same current densities as before. This test was done with both SE's showcasing a clear improvement in capacity retention with the $Li_{5,5}PS_{4,5}Cl_{1,5}$ but still no clear difference between the porous and non porous material.

Then, to better preserve the nano porous Si structure, the Si deposited on Cu electrodes where only charged to a capacity of 1000, 1500 and 2000 mAh/g by using time constraints. This showed clear improvements for the nanoporous Si material over the regular Si for capacities of 1000 and 1500 mAh/g over 50 cycles. The 1000 mAh/g E-magy Si battery showed a coulombic efficiency of 99% and a stable minimum negative potential of -0,5 V vs In/LiIn for 50 cycles. Using $Li_{5,5}PS_{4,5}Cl_{1,5}$ of Li_6PS_5Cl lead to more stable battery performance and less of an increase in the required potentials to reach the same capacities each cycle.

This study provides a insight into how the battery performance of Si solid state batteries is influenced by: Nanopores in the Si material, different Si electrode preparation methods, Si composite electrode composition ratio's, choice of the olid electrolyte, and the utilized capacity of the Si electrode. And thereby makes a contribution to the large amount of research that is currently being done to allow for Si anodes to successfully be utilized in solid state batteries.

Contents

Nomenclature

List of Abbreviations

AC	Alternating Current
CC	Constant Current
CE	Coulombic Efficiency
CNF	Carbon Nano Fibre
CNT	Carbon Nano Tube
CPE	Constant Phase Element
CV	Constant Voltage
DC	Direct Current
EIS	Electrochemical impedance spectroscopy
LE	Liquid Electrolye
NCM	Nickel Cobalt Manganese
NMP	N-methylpyrrolidon
NMR	Nuclear Magnetic Resonance
OCV	Open Circuit Voltage
PEIS	Potentiostatic Electrochemical Impedance Spectroscopy
PVDF	Polyvinylideenfluoride
RQ	Research Question
SE	Solid Electrolyte
SEI	Solid Electrolyte Interface
SEM	Scanning Electron Microscopy
Si	Silicon
SOC	State Of Charge
TR	Thermal Runaway
XPS	X-ray photoelectron spectroscopy
XRD	X-ray diffraction

List of Figures

List of Tables

1

Introduction

Its becoming more and more clear to the world that CO2 emissions will have to be reduced in order to stop or at least mitigate the effects of global warming. According to the statistical review of world energy from 2023 [1], the energy used in the world is still for 82% being generated by using fossil fuels like coal, oil and natural gas. That means that in 2023 only 14,8% of the total primal energy consumption was generated by renewable energy sources. The missing 3,2% comes form nuclear energy, this is singled this out since not every one is of the same opinion whether or not this counts as renewable energy. 14,8% might sound like a small number but if you take a look at figure(1.1) you can see that the amount of renewable energy generation has more then doubled since 2010 [2] with especially large growths in solar and wind energy generation. But this growth will have to increase even more to meet goals, like for example the Paris agreement [3], to realise net zero emissions by 20250.

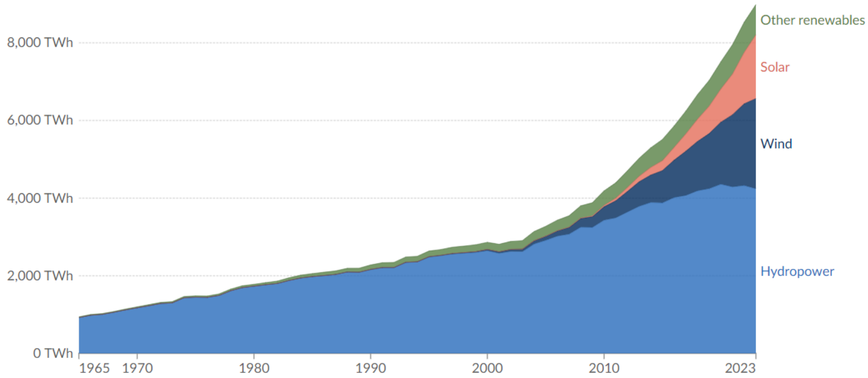

Figure 1.1: The amount of renewable energy generated in the world throughout the years [2]

An important part of reaching these goals is increasing the generation capacity of renewable energy sources, like solar and wind power generation capacity. But with only renewable renewable energy your not quite there yet. You still need a way to actually use this energy. And since the most prominent renewable energy generation techniques produce electricity, a large electrification of the current energy sector will have to take place. You can think of the change from cars that drive on gasoline or diesel to cars that use electricity to drive. Now you got a way to generate the energy, and you can use it but there has to be kept in mind that the most prominent renewable energy sources are intermittent. Which means that power production is dependent on outside factors like solar radiation and wind speed, unlike coal and gas power plants which can can more easily scale power production up and down to meet the current energy demand. To accommodate for this, without having to build an enormous access amount of renewable energy generation capacity, energy storage techniques will be necessary to deal with these fluctuations.

And this finally brings us to the topic of this thesis: Batteries. Or to be more precise: Optimization of nanoporous silicon anodes with high ionic conductivity argyrodite solid electrolytes in solid state batteries. But more on that later. The battery industry has blown up over the last couple of years which can be seen in figure(1.2) and this trend is not slowing down, figure(1.3) shows that the total battery capacity in the world is predicted to keep growing rapidly the next 25 years [4]. This quickly increasing total installed battery capacity is made possible by a price drop of 85% for lithium-ion batteries over the last decade [5]. And the price is predicted to drop even further with a reduction of 50% predicted in 2030 compared to 2020 [5]. This makes it financially more and more interesting to choose batteries as a storage technique over other energy storage techniques like pumped hydro, which is also very dependent on the location where it is used [6]. The demand for batteries in general has not only increased, the demand for better batteries has too. Take electric cars as an example: You want a battery with a large amount of energy storage capacity, but you also want it to be light and not take up to much space, you want it to be able to charge quickly, but you also want it to not lose capacity during cycling to ensure a long life time. Its important to realize that there is a trade-off between these properties and that a perfect battery which maximizes all off them does not exist. To deal with the enormous expansion of the battery industry and meet the ever increasing list of battery requirements, a lot of research will be necessary.

This thesis will take a small part in this by looking at how a specific material called silicon can be used on the anode side of solid state batteries. In particular to be able to increase the energy density compared to current lithium ion batteries. This material has the ability to store a lot more lithium per weight then materials that are currently being used, but it has a large volume change upon charging and discharging. In this thesis we will try to still make use of a nanoporous version of this material to see if this can limit the volume changes and there negative effects in solid state batteries.

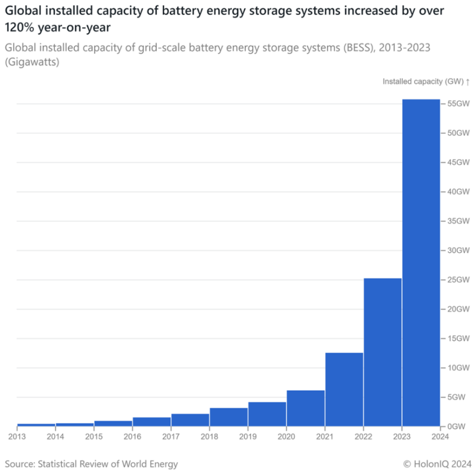

Figure 1.2: The total installed battery capacity in the world from 2013 to 2024 [4]

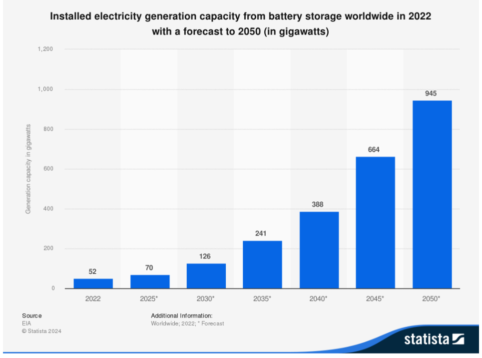

Figure 1.3: Projected global battery storage capacity from 2022 to 2050 [4]

This will be done by first discussing in chapter 2 the theory behind solid state lithium-ion batteries, and by looking what role silicon can play in them and what research has already been done regarding using silicon in batteries. Then in chapter 3, the main research question will be formulated together with some smaller research questions which will help to answer the main question. The techniques and methods that are used during this research will be explained in the methodology in chapter 4. Chapter 5 will discuss the results gained by the application of these techniques. And at last in chapter 6 a conclusion will be drawn and some recommendations for future research on this topic will be given.

2

Solid state lithium ion batteries

In this chapter we will go over some theory related to this research project. This will be done by first going over how lithium-ion batteries work, then we will take a look at a more specific type of battery, the solid state lithium-ion battery and what these have to offer. And what follows is an explanation of some important terms often used in battery research. Then we will take a look at the components used in solid state lithium-ion batteries and what materials are used. After which we will look at the failure mechanisms occurring in lithium-ion batteries. This then finally brings us to discuss the silicon material and the opportunities and challenges it brings for use in solid-state batteries. And to close of we will take a look at solution and research that has already been done for using silicon in solid state batteries.

2.1. What are, and how do lithium ion batteries work

You are probably already familiar with the concept of a battery being able to somehow store energy. And also with the concept of charging and discharging them multiple times so you don't have to buy a new phone everyday. But how do they actually work? Lets find out.

Like many things, explaining how a battery works is easiest done with a picture, so see figure(2.1). A battery consists mainly of 3 parts: The cathode (positive electrode), anode (negative electrode) and the electrolyte in between them. The cathode and anode are both electrodes at which redox reactions can take place. These are reactions where a transfer of electrons between 2 species takes place. When you discharge (take power out of) a battery, a redox reaction occurs at the anode which releases anions (positively charged ions and negatively charged electrons. These electrons then flow through the external circuit towards the cathode. The electron flow through the external circuit from anode to cathode is what generates the electrical current that provides power to a device, like your phone. The electrons can not travel through the electrolyte between the anode and the cathode because they are blocked by the electrolyte itself or by a separator. That is why they are forced to travel through the external circuit. For the ions it is actually the other way around. They are able to travel freely from cathode to anode and vise versa, through the electrolyte and the separator. Unlike the electrons they can not move through the external circuit.

The electrons that arrive on the cathode side during this discharging are then used in a second redox reaction. Its important to realize that the reason that the electrons flow like this is to ensure charge balance in the battery. So the ions move first and the electrons follow to ensure charge balance. The positively charged cations will simultaneously move from the anode through the electrolyte towards the cathode. The redox reaction at the cathode and anode occur simultaneously. [6].

If you are using a rechargeable battery, this mechanism can also be reversed. An external power source (like your phone charger) applies a voltage to the battery and forces the redox reactions to happen in the opposite direction making the ions move from cathode to anode and again making the electrons follow to ensure charge balance.

Ideally you would be able to keep charging and discharging for ever. But sadly batteries degrade over time which will prevent this from being possible. The mechanisms that cause this degradation will be discussed later in section(2.5)

An example of the redox reactions occurring in a Li-ion battery will now be given to make the workings of the battery more clear. In this example a lithium metal-metal oxide, in this case lithium-cobal oxide ($LiCoO_2$) acts

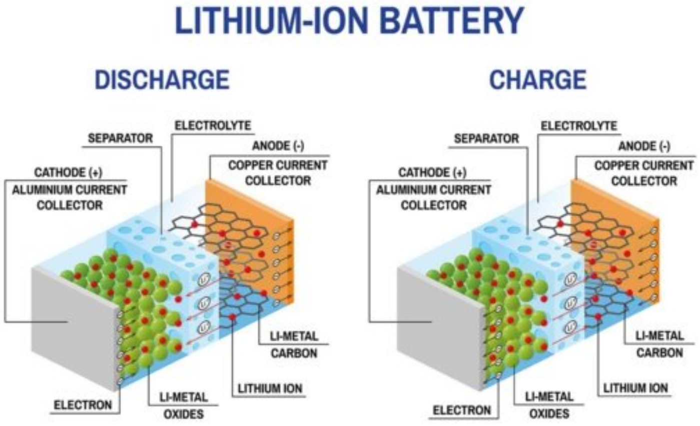

Figure 2.1: Depiction of a lithium-ion battery during both the charge and discharge state [7]

as the cathode and graphite(C_6) will act as the anode [8]. So the Lithium will travel between the graphite and the cobalt oxide during charging/discharging. During discharging, a reduction will take place at the cathode and the lithium ions combine with the cobalt oxide to form $LiCoO_2$. The half reaction taking place is shown below.

$$CoO_2 + Li^+ + e^- \longrightarrow LiCoO_2 \tag{2.1}$$

As you can see in the half reaction, an electron is necessary for this reaction to take place. This electron is provided by the redox reaction that is occurring on the other side of the battery, the anode side. On this side a reduction reaction occurs where LiC_6 gets reduced to C_6 and a Li-ion. This half reaction is shown below.

$$LiC_6 \longrightarrow C_6 + Li^+ + e^- \tag{2.2}$$

These two half reactions add up to the following full reaction:

$$LiC_6 + CoO_2 \longleftrightarrow C_6 + LiCoO_2 \tag{2.3}$$

So during discharging the reaction occurs from left to right and, and during charging from right to left. There are different ways for the lithium to intercalate alloy or react with the electrodes but more more on that can be found in the anode section(2.4.2)

2.2. Solid state batteries

The previous section discussed lithium-ion batteries in general. But in this thesis the focus will be on a more specific lithium-ion battery type, the solid state lithium-ion battery. The working principle is the same, you still have a anode and cathode with lithium ions traveling between them and a electronic circuit that facilitates the flow of electrons. But in solid state batteries the liquid electrolyte (LE) is replaced with a solid electrolyte (SE). This solid electrolyte then also acts as the separator since it is has a high ionic conductivity but a very low electronic conductivity. But why do we suddenly want to switch from liquid to solid state batteries? There are multiple reasons for this, some of them are:

Liquid lithium-ion batteries are running into physicochemical limitations [9] which will limit further improvements and therefore limit further energy density improvements that are wanted by consumers. Solid state batteries allow for new materials to be used like lithium metal or silicon as the anode which have a capacity that is a lot higher then graphite that is mostly used in liquid Li-ion batteries.

Another aspect that has to be taken into account is the safety of the batteries. Current lithium ion batteries use liquid electrolytes which are often very flammable which causes a safety risk. Especially for larger battery systems. You have probably heard of electric car fires which can go on for days or even weeks and which can even cause explosions. These fires are very hard to put out and are cause by a phenomenon called thermal runaway (TR) [10]. This can be a result of either thermal, mechanical or electrical abuse of the battery. These terms mean respectively: The battery being exposed to high temperatures which leads to accelerated chemical reactions, the battery getting punctured or crushed causing internal short circuit and with electrical abuse is meant that the battery can be charged or discharged further then was intended in its design. In all these cases extra heat is being generated, and current liquid lithium-ion batteries mostly use liquid electrolytes which evaporate into highly flammable gasses above temperatures of 200 degrees Celsius [11]. And once this burning starts more and more electrolyte will keep evaporating and fueling the fire, which makes it very hard to put out. To prevent incidents like these, solid state batteries are preferred since they replace the flammable liquid electrolyte with less or non flammable SE. The use of a SE also eliminates the possibility of leaking of the electrolyte which could start unwanted side reactions.

It was first believed that the use of SE over LE would also stop the problem of dendrite formation in batteries [12]. Dendrites are formed during cycling of the battery and form a lithium pathway between both electrodes that allows the conduction of electrons. This causes the cell to short circuit when the dendrite gets so long that it connects both electrodes. And this can start the thermal runaway process discussed above. Theses dendrites can still be formed between the electrodes in the solid electrolyte but as was discussed previously. The chance of a fire getting started in case these dendrites get formed is reduced with the use of solid SE over LE. But choosing the right materials for the solid state battery can still help to prevent this problem.

Figure (2.2) shows the structure of a solid state battery. As you can see this is almost exactly the same as the lay out of a liquid battery. One thing to note is that the use of a separator is not necessary in solid state batteries. This is because the SE already functions as a separator between the anode and cathode because the SE has a high ionic conductivity but a very low electronic conductivity, so it allows the conduction of ions and blocks the flow of electrons.

Of course there are not only benefits when it comes to solid state batteries compared to there liquid counterpart. Downsides such as sluggish kinetics between the SE and electrode interfaces due to the nature of the contact between a solid/solid interface [13]. And a large obstacle in the commercialization of solid state batteries is the high resistances at the solid to solid interfaces [14]. An other downside is that the manufacturing of these surfaces that have to maintain good contact throughout the batteries life time with constant expansion and shrinking has been proven to be difficult, which makes manufacturing more expensive [15].

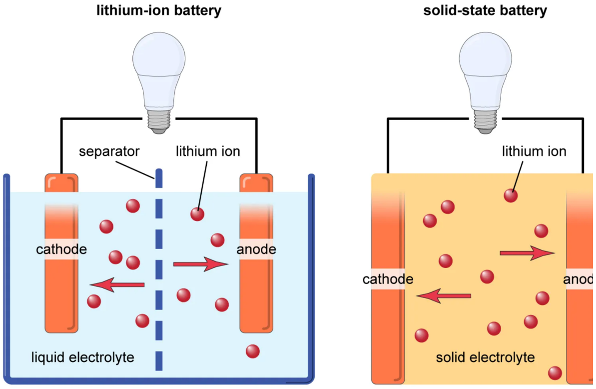

Figure 2.2: Solid state battery Vs liquid lithium-ion battery [16].

2.3. Ionic conductivity, electronic conductivity and the electrochemical stability window

Ionic conductivity, electronic conductivity and the electrochemical stability window are all terms used a lot in this thesis. So before the different components of the battery are discussed in more detail, a look will be taken at what is meant with these 3 terms.

2.3.1. Ionic conductivity

Ionic conductivity is a measure of a materials ability to transport ions (such as lithium ions in a Li-ion battery) through its structure. In the context of battery materials, ionic conductivity is essential because it determines how efficiently ions move between the electrodes during charge and discharge cycles, through the solid electrolyte. High ionic conductivity facilitates faster ion movement, which improves the batteries power output and reduces internal resistance [17]. The unit of ionic conductivity is Siemens per centimeter (S/cm). This unit is the same for both ionic and electronic conductivity. Since both are a measure of current flow in response to an applied electric field. The difference between them is just wether the charge carriers are ions or electrons. Both the electronic and ionic conductivity are gained from the following equation:

$$Conductivity(\sigma) = \frac{Currentdensity(J)}{Electricfield(E)} \tag{2.4}$$

And the units of the conductivity are derived as follows:

$$\frac{A/cm^2}{V/cm} = S/cm \tag{2.5}$$

With A being the current in Ampere (A)

And V being the Voltage in Volts (V)

If your remember that Ohms law is:

$$R(\Omega) = \frac{I(Ampere)}{V(Volts)} \tag{2.6}$$

With R being the Resistance in Ohm(Ω)

You can now see that the conductivity is inversely proportional with the resistance from Ohms law.

In solid electrolytes ions mostly move by the vacancy hopping mechanism [18] where the Li^+ ions hop from vacancy to vacancy in the SE to move between the anode and the cathode. So the ionic conductivity will be higher if its easier for ions to hop to the next vacancy. Ionic conductivity is influenced by factors like the materials crystal structure, the presence of dopants, temperature, all of which affect the pathways available for ions to move inside the material (ion migration). In solid electrolytes, achieving high ionic conductivity is critical for fast charge-discharge rates and overall battery performance. Currently commercial liquid electrolytes still have higher ionic conductivities in the order of 10^{-3} to10^{-2} S/cm, or 1 to 10 mS/cm, compared to the conductivity in SE which is mostly around 10^{-3} S/cm or 1 mS/cm [19]. But with all the research that is being done, the ionic conductivity of new SE's seems to actually start to be comparable to there liquid counterparts.

2.3.2. Electronic conductivity

Electronic conductivity refers to a materials capacity to conduct electrons. Unlike ionic conductivity, which is critical for ion movement, electronic conductivity is necessary to transfer electrons to the external circuit during battery operation. Like mentioned before electronic conductivity share the same unit with ionic conductivity which is S/cm. In a battery cell, the electrodes need high electronic conductivity to support effective electron flow and reduce resistive losses. Conductive additives, like carbon materials in the anode, are often incorporated to enhance electronic conductivity when the primary active material has limited ability to conduct electrons. A high electronic conductivity in electrodes and current collectors reduces overall cell resistance, allowing for improved charge/discharge efficiency and enhanced cycle life.

2.3.3. Electrochemical stability window

The electrochemical stability window is the range of voltages within which a material is electrochemically stable. So it is the voltage range between the reduction potential and the oxidation potential of the material. For an electrolyte, this stability window is crucial, as it defines the voltage range over which it can operate without decomposing or reacting with the electrode materials. A wide electrochemical stability window is especially desirable in solid-state batteries, where electrolytes must withstand the high voltages of cathodes and low potentials of anodes without breaking down. If the voltage exceeds this window, unwanted side reactions can occur, leading to capacity fade, increased cell resistance, and possibly even thermal runaway. The stability window depends on the properties of the electrolyte, like its chemical composition and structure. The electrochemical stability window is essential for defining the safe operating limits of a battery cell. The electrochemical stability window of some different SE groups is shown in figure(2.3). The electrochemical stability windows are shown for Li-M-X SE's. So M represents the metal cation shown at the bottom and X represent the groups shown at the top, so halides(which includes fluorides, chlorides, bromides and iodides), oxides, sulfides and nitrides [20]. In the section about solid electrolyte there will be taken a look at the other properties that distinguish these groups of solid electrolytes from each other.

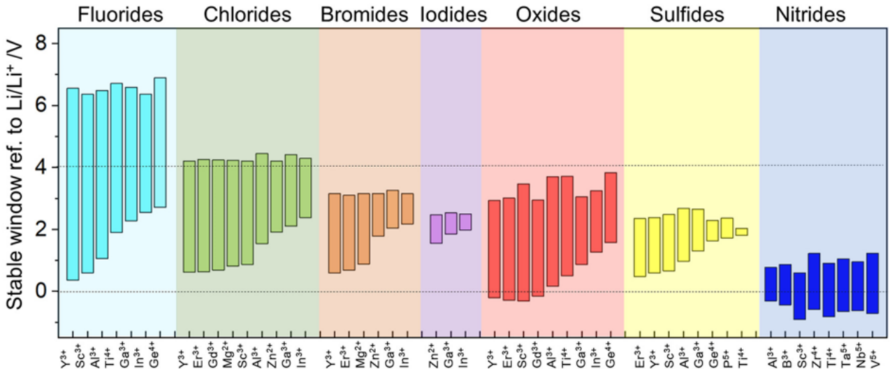

Figure 2.3: The electrochemical stability windows of different groups of solid electrolyte, the Li-M-X solid electrolytes are depicted with M being the metal cations at the bottom and X being one of 7 groups at the top of the figure [20].

2.4. Components of a (solid state) lithium ion battery

This section will give a more detailed description of the most important components of a (solid state) lithium-ion battery. The focus will be on the cathode, anode, solid electrolyte and the current collectors.

2.4.1. Cathode

The cathode is the positive electrode of a battery. When the battery is discharged the lithium ions will be on the cathode side of the battery and upon charging the ions will migrate towards the anode side. A cathode material in a lithium ion battery of course has to consist of lithium, to facilitate the lithium ions. And this Li is often combined with the transition metals cobalt(Co), manganese (Mn), and nickel and with oxygen(O_2) to form metal oxides like: Lithium cobalt oxide ($LiCoO_2, LCO$), Lithium Manganese oxide ($LiMn_2O_4, LMO$) and Lithium Nickel Manganese Cobalt Oxide ($LiNiMnCoO_2, NMC$) [21]. Which cathode material is chosen for a specific battery will depend on specific requirements like energy density, longevity, thermal stability and of course cost.

2.4.2. Anode

The anode is the negative electrode of the battery. The Lithium ions will be be stored on the anode side of the battery when the battery is considered to be fully charged. The most common anode battery material is graphite. Graphite consists of the element carbon (C) in a crystalline form. Graphite is made out of layers of graphene stacked on top of each other and the Lithium ions can be stored in between these layers. Some of the qualities that make graphite such an attractive anode material are high abundance, a low electrochemical potential, good electronic conductivity, low toxicity and low costs. It has capacity of 372 mAh/g and and good electrochemical stability at low potentials (like 0.1 V compared to the Li/Li+ reference) [22]. This results in the capacity remaining intact for a large amount of cycles thus ensuring a long battery life time. Anode materials can be divided into 3 categories based on the mechanism they use to store lithium. These mechanisms are intercalation, alloying and conversion. Figure(2.4) shows some popular anode materials grouped by which lithium storing mechanism they use.

During the intercalation process, ions (in this case lithium) are reversibly integrated into the vacant sites of the crystal lattice without significantly altering the crystal structure. This results into anodes with a relatively lower capacity but a long life time since mechanical strain and volume change caused by the insertion and extraction of the ions is minimized [24]. An example of a anode material that use the intercalation mechanism is graphite. The weak van der Waals forces allow the graphene layers to move slightly so the lithium ions can be reversibly taken up into in the vacant sites of the crystal lattice.

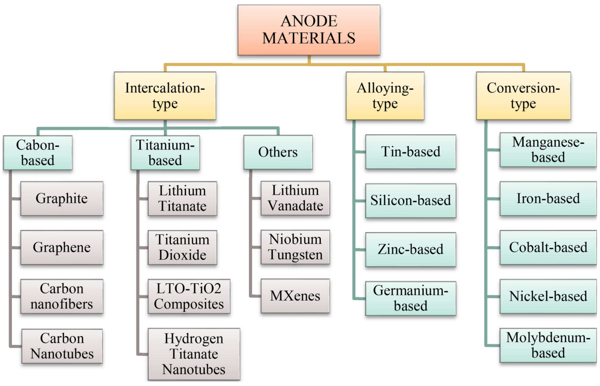

Figure 2.4: Various anodes grouped based on the lithium storing mechanism they exhibit [23].

During the alloying mechanism the ions actually insert into the host material and form a lithium-metal alloy. This alloying mechanism allows these types of anodes to store a higher fraction of lithium ions then the anodes that use the intercalation mechanism [25]. This results in materials like silicon which have a capacity of up to 3600 mAh/g. The downside of these materials is that the continuous alloying and de-alloying of lithium and the metal results in large volume changes, 400% for silicon. which leads to mechanical stress, contact loss and therefore negatively impact the life time of the cell.

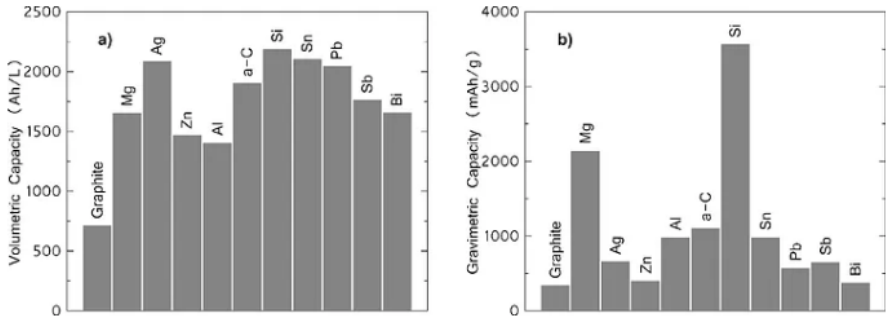

Figure 2.5: Different materials that are used as electrodes, showing there volumetric and gravimetric energy densities [26].

The last type of anodes use the conversion mechanism. In conversion materials, lithium storage occurs through a chemical reaction that transforms the original material into new compounds rather than simply inserting lithium ions into an existing lattice. For instance, during lithiation, lithium ions react with a host compound (such as Fe_2O_3) and break it down, forming metallic iron (Fe) and lithium oxide (Li_2O). This transformation involves the reduction of metal ions (e.g., Fe^{3+} is reduced to Fe^0) and results in significant structural changes, unlike alloying materials that maintain a consistent basic structure. Conversion reactions, just like alloying leads to high volume changes due to the breakdown and reformation of different compounds within the electrode. As a result, these structural transformations can create internal stress and degrade battery performance over time. Despite the complexity of these reactions, conversion materials can store a high number of lithium ions, giving them a high theoretical capacity, often comparable to or even exceeding alloying materials.

The 3 type of anodes and and a picture depicting the different ways they store lithium is shown in figure(2.6)

In this thesis the focus will be on alloying type anodes and silicon in particular. Since these anodes show very promising high capacities but still require a lot of research to increase the stability and cycle life of batteries using them.

2.4.3. (Solid) Electrolyte

The electrolyte functions as medium for ion conduction between the anode and the cathode but also as a blockade that prevents electrons from moving through it. So it has to have a high ionic conductivity but a low

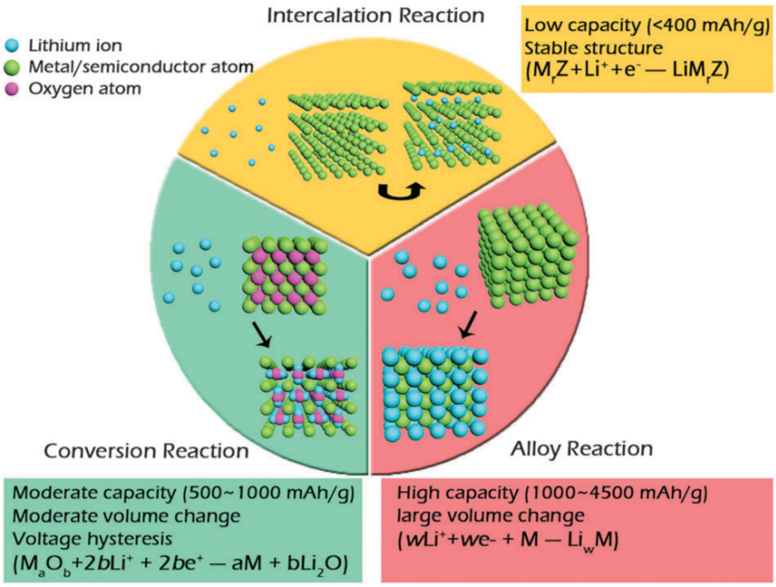

Figure 2.6: A display of the intercalation, conversion and alloying mechanisms and the capacity ranges of the accompanying materials [25].

electronic conductivity. A lot of different solid electrolytes are being used and they all have different ionic conductivity's, chemical stability's, thermal stability's, mechanical properties, costs, etc. Just like with the anode and cathode material, a trade off between these properties exist and no perfect material exists, or at least is not found yet. Figure(2.7) shows a graph indicating some common type of solid electrolytes and shows there advantages and disadvantages.

Oxides, sulfides and halides

Oxides are generally stable in air and have a large electrochemical stability window with high stability at high voltages [28]. But they have lower ionic conductivities compared to sulfides. They are also brittle which provides difficulties with cell production and with the contact of the SE and the electrodes. And this contact plays an important role, especially for solid state batteries since it is more difficult to create good uniform contact between 2 solid layers then between a solid and a liquid layer.

In contrast to the oxide SE, Sulfide SE's provide higher ionic conductivities which can even reach above 10 mS/cm. This is in the same order of magnitude as liquid electrolytes that are being used right now. Sulfide SE are also softer and more deformable then oxides which is important for ensuring good surface contact between the SE and the cathode/anode during charging and discharging. The ionic radius and polarizability of S^{2-} is higher then O^{2-} . This polarizability difference results in the the attraction of Li+ ions to be weaker in the sulfide SE. And this causes the sulfide SE to provide better mobility for the Li+ ions [29]. And thus ensuring a higher ionic conductivity.

A downside of using sulfide SE is that they have a narrow electrochemical stability window compared to oxides. Which makes it unable to operate at high voltages and therefore not fit to use with some electrode materials that perform best at these higher voltages. Sulfides are also not stable in air and can react to form solid by products like Li_3PO_4 and LiOh which form a solid layer that increase the interfacial impedance of the battery [30]. They also react with water in the air to create toxic hydrogen sulfide H_2S gas. Which makes large scale production of the material more difficult [30].

Halide SSE's are more balanced between oxide and sulfide materials according to the following aspects, electrochemical stability window, moisture resistance and ionic conductivity [27]. They are called halides because they include halogen elements, fluorine (F), chlorine (Cl), bromine (Br) or iodine (I).

Lithium argyrodites

A very promising material that belongs to the family of sulfide SE's but also has halide components is lithium argyrodite. This material has the Li_6PS_5X (X = Cl, Br, I) formula and provides conductivities of 1-10 mS/cm at

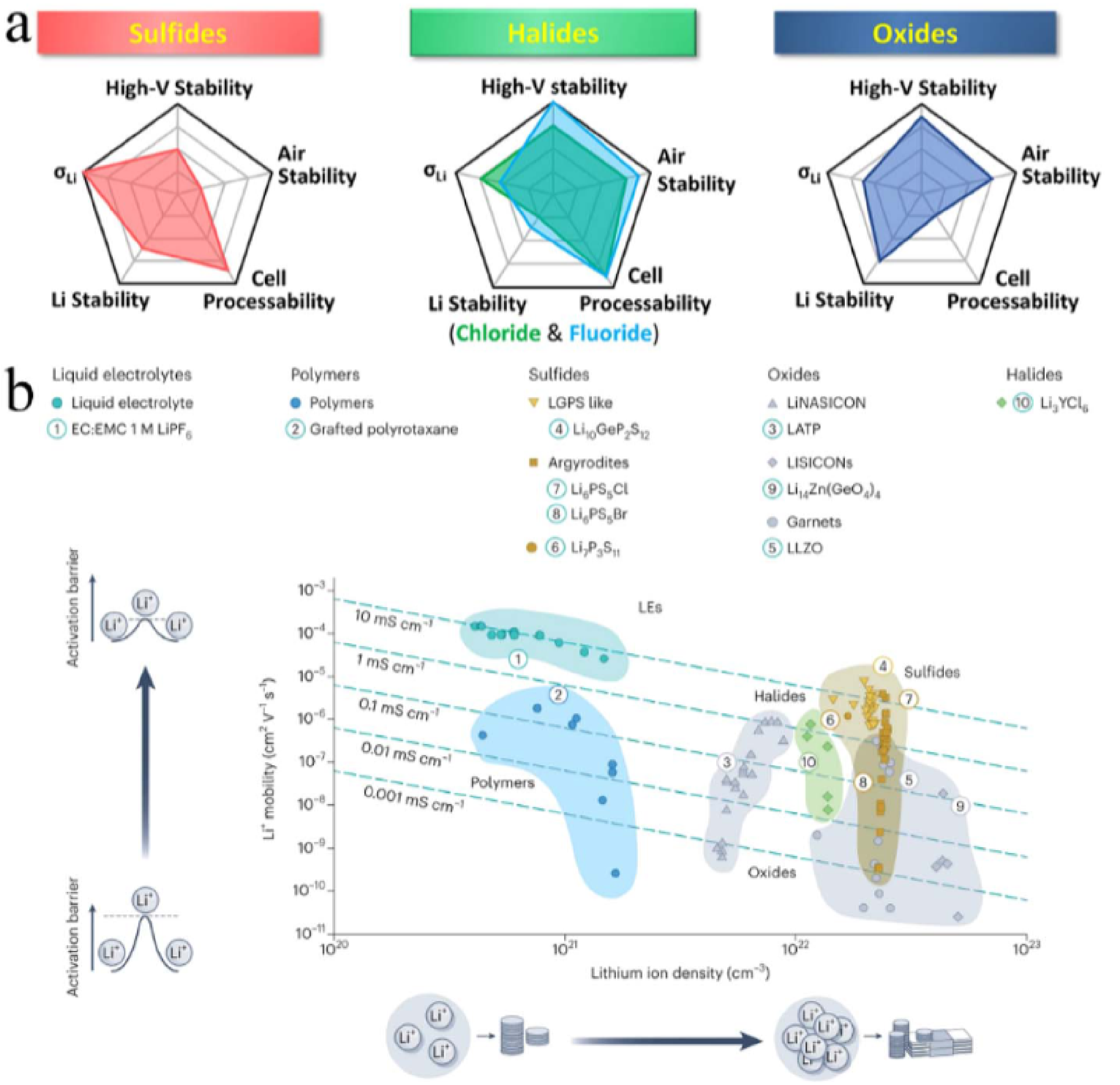

Figure 2.7: (a)Spider plots showcasing some of the properties of sulfide, halide and oxide solid electrolytes.(b) A plot showing the Li-ion mobility vs the density and lines showcasing the ionic conductivity for for material groups like sulfides, halides and oxides [27].

room temperature [28]. The properties of the synthesized material, like the conductivity and air stability will depend on how and what composition was synthesized exactly. For example the ball milling time or the oven heating and ramping time can be changed which all can have a large effect on the properties of the final material. [31] shows how replacement of the sulfide by chloride increases the ionic conductivity by decreasing the overall lower charge in the Li cages which lowers there interaction with the moving Li-ions, and the extra Cl- makes these cages better connected. Take for example the regular argyrodite Li_6PS_5Cl which has a ionic conductivity of 2.9 mS/cm but only a slight adjustment of the composition gives the material $Li_{5,5}PS_{4,5}Cl_{1,5}$ a conductivity of 7 mS/cm which is more then twice as high [32]. It was also shown by [33] using $C-Li_2S/Li_{5,5}PS_{4,5}Cl_{1,5}/LiIn$ and $C-Li_2S/Li_6PS_5Cl/LiIn$ solid state batteries that the use of $Li_{5,5}PS_{4,5}Cl_{1,5}$ instead of Li_6PS_5Cl lead to lower solid to solid interface resistance and that this lead to better cycling performance and higher discharge capacities. [32] also showed an overall enhancement of the cell performance with the $Li_{5,5}PS_{4,5}Cl_{1,5}$ used in a study of these electrolytes with NCM cathodes (Nickel-Cobalt-Manganese, with the full chemical name being lithium nickel manganese cobalt oxides). However at lower potentials $Li_{5,5}PS_{4,5}Cl_{1,5}$ showed more electrochemical decompositions then Li_6PS_5Cl and this was the case for cells cycled in a potential range of 2 to 3,6 (V vs In/LiIn). The batteries cycled in thesis use even lower potentials of -0,6 to 0,5 (V vs In/LiIn) so it will be interesting if these low potentials will increase the electrolyte decomposition even more and if the higher ionic conductivity provided by $Li_{5,5}PS_{4,5}Cl_{1,5}$ will then still be worth it for the battery performance overall.

2.4.4. Current collectors

The current collectors are the parts of the battery that electronically connect the electrodes to the electrical circuit of the battery. On the anode side of lithium-ion batteries copper (Cu) is the most used current collector. This is because copper has a high electronic conductivity, has abundant reserves, a soft texture which is good for interface connection with the electrode and it is stable in the voltage range anodes of lithium ion-batteries tend to operate [34]. On the cathode side of the battery where the materials experience higher voltages aluminum(Al) is often used [35] because it's electrochemical stability window lies at higher voltages. In this thesis mostly half cells are assembled with a lithium/indium alloy (LiIn on one side and a silicon, with sometimes other additives, on the other side. These batteries are operated in in a voltage range of about 0 - 1,1 V vs Li/Li^+. And because Cu is stable in this voltage range against both LiIn and Si, Cu will be mostly used as the current collector for the batteries that are tested.

2.5. failure mechanisms in lithium-ion batteries

With all the different components working together in a battery, there is of course a lot that can go wrong inside a battery. If we want to be able to design batteries that have a long life time it will be important to understand what failure mechanisms occur inside the battery and how these can be prevented or minimized. So the most important failure mechanisms in lithium ion batteries will briefly be discussed here:

- Loss of lithium: There are multiple ways that the lithium that was first used in the cell can no longer be utilized. One of these is SEI formation. In solid-state batteries, the SEI forms due to reactions between the anode and the solid electrolyte during the initial cycles. What type of layer is formed exactly will depend on the materials that are chosen for the SE and the anode but to form this layer some lithium is irreversibly used. So this lithium can no longer be used to move from anode to cathode and vice versa. This SEI layer will form on the surface of the anode active material. But upon lithiation anode materials are know to expand, especially the anodes using the alloying or conversion mechanism to store lithium like discussed in section(2.4.2). This shrinking and expanding of the anode will cause the already formed SEI layer to crack. These cracks then form new surfaces to form more SEI on. And this process will continue to happen every battery cycle, therefore consuming more and more lithium and thus reducing the battery's capacity [36].
  The lithium can also get isolated if the material cracks, causing the lithium to be stuck in place due to no longer having sufficient electrical and ionic conductivity in the whole electrode.
- Loss of active material mass on the anode side making it no longer available for lithium insertion. This can occur due to particle cracking, which is again a result of the large volume changes. The active anode material can also get isolated if electrical contact is lost making it no longer able to to store lithium. [37]
- The same failures happening to the anode material can of course also happen to the cathode active material. But in this thesis the focus will be on the anode side of the battery.
- Contact loss of the different layers of material in a battery plays a big roll especially for solid state batteries since it is harder to maintain contact between 2 solid layers then between a liquid/ solid interface since the liquid can deform more easily then the solid. This degradation between the active material and solid electrolyte surfaces increase the interfacial resistance and negatively impact the cell performance [14].
- Dendrites can form and grow larger and larger during battery cycling, this dendrite of course consumes lithium making it no longer available for charging the battery. But the dendrite can also grow so large that it pierces all the way through the solid electrolyte layer [38]. This creates a pathway for the electrons to now travel through the dendrite from the anode to the cathode and vice versa, so the external circuit is no longer the only path the electrons can take. And this causes the cell to short circuit, possibly starting the thermal runaway process discussed in section(2.2).

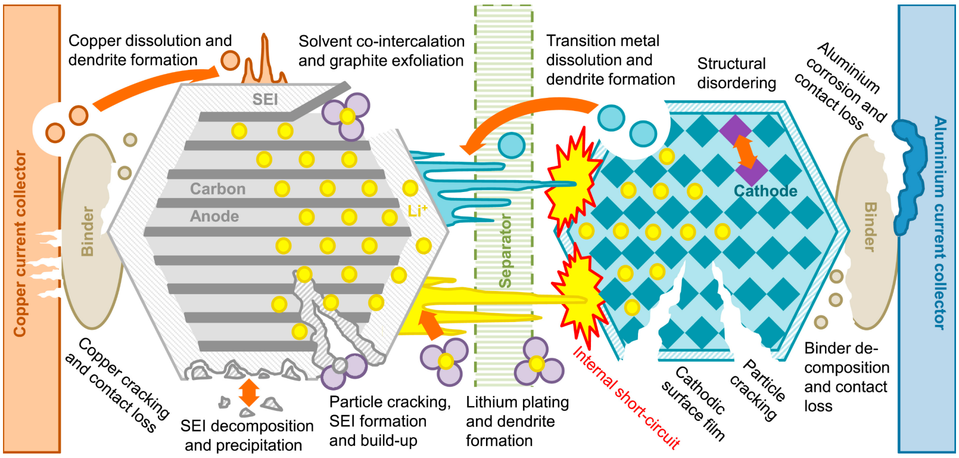

Figure 2.8: The multiple degradations mechanisms of a lithium-ion battery cell [37].

2.6. Silicon anodes, promising, but there are difficulties

In the section about anodes (2.4.2) there was already a brief mention of a material called silicon (Si) which uses the alloying mechanism to store lithium. Silicon has a theoretical capacity of 4200 mAh/g for $Li_{4},{}_{4}Si$ [39] (at room temperatures a capacity of 3590 mAh/g with Li $Li_{3},{}_{75}Si$ [40]), it has a low reaction potential of 0.5 V vs Li/Li^{+} and what is also very important, it is abundant. Since it is making up 27,7 % of the earth crust [41]. But since silicon is an alloying anode it has a large volume expansion and contraction of 300-400% upon lithiation and delithiation. You can probably imagine that such a large volume change of the material inside your battery can lead to some problems, some of which where already mentioned in the section failure mechanisms in lithium-ion batteries (2.5). This volume change leads to cracking and pulverization of the silicon anode particles and it also leads to cracks and breaking apart of the SEI layer around these particles, which will result in a continuously growing SEI layer, and with more SEI being formed more lithium is being continuously consumed which reduces the capacity of the battery during cycling. This is visualized in figure(2.9)

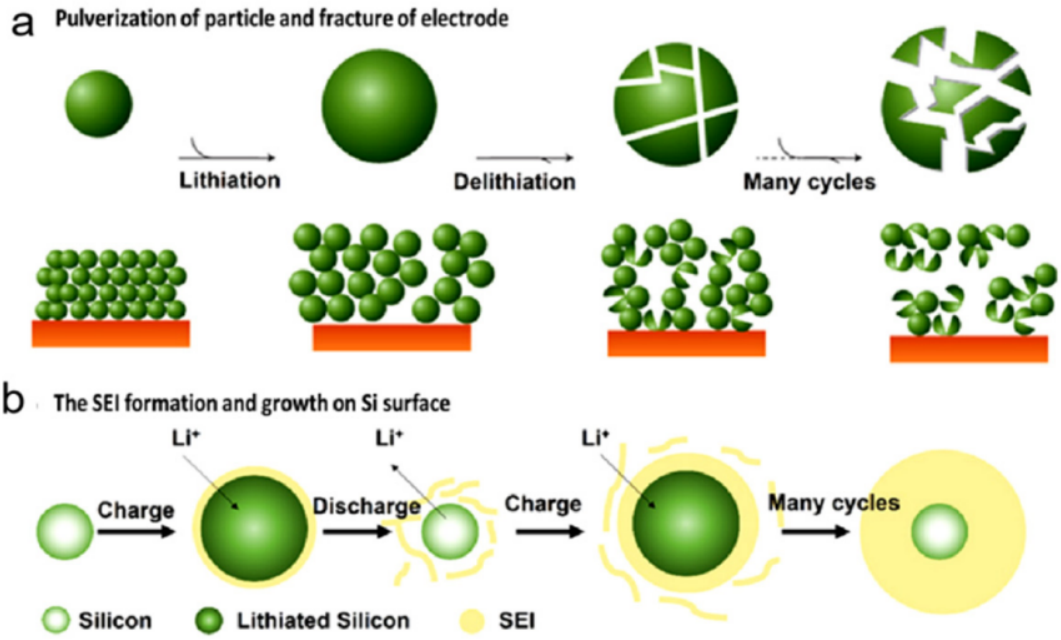

Figure 2.9: The failure mechanisms of Silicon upon repeated cycling with a) showcasing particle pulverization and electrode fracture cause by the expansion, and b) showing the process of continuous SEI formation caused by SEI cracking [42]

There are a lot of different solutions that are tried over the last decade that try to minimize or help cope with the large volume expansion of silicon. A few of these solutions are discussed in the section below. The nanoporous silicon that is mentioned there will help with the problem of the large volume change of the silicon material upon lithiation, and this nanoporous material will be the main focus of this thesis. Some of the other main challenges and the strategies that help to overcome them are shown with the help of some simplified pictures in figure(2.10)

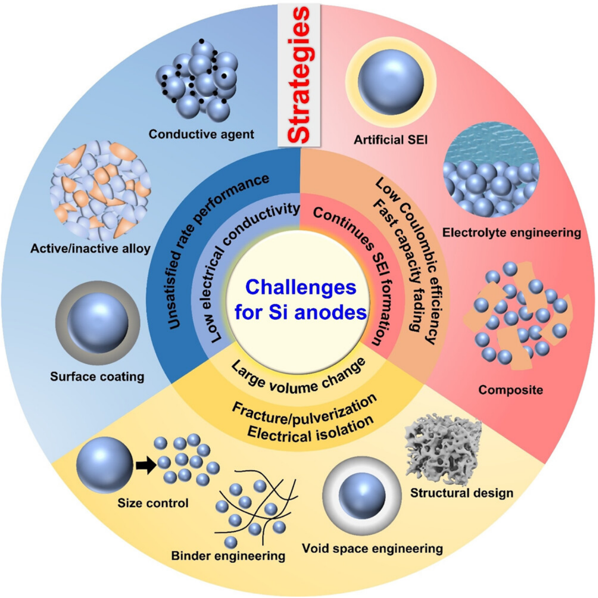

Figure 2.10: Some of the main challenges for silicon anodes [43].

2.7. Trends and research about silicon anodes in solid state batteries

In this section we will go over some of the things that influence the performance of silicon anodes in batteries and the different solutions and research other people have already done to improve the performance of silicon anodes.

2.7.1. Particle size of the silicon

One of the methods to prevent the fracture and pulverization of silicon particles is to use smaller particles. But why is this the case? Well:

- Smaller particles have smaller absolute volume changes then larger ones and therefore have smaller internal stress
- Smaller particles have a higher surface area / volume ratio, so there is more surface available to accommodate the expansion allowing for better stress distribution.
- Larger particles are less homogeneous and have more defects where stress will concentrate at to form cracks.
- During charging and discharging, the larger particle are also more likely to suffer from uneven delithiation causing uneven expansion and contraction in the particles which can cause fracture.
- smaller particles can also deform elastically to a larger extent then larger particles preventing permanent structural damage [44].

So why should we not just make the Si particles as small as possible then to make sure no fracture or pulverization occurs? Smaller particles give a larger active area. Like just mentioned, smaller particles have a larger surface area/ volume ratio then larger ones. This larger area area will cause more SEI to be formed, and therefore consume more lithium.

So the smaller particles provide a larger area for SEI to be formed on. But the SEI that gets formed on these smaller particles seems to actually be more stable then the SEI that gets formed on larger particles. So larger particles do form less initial SEI, but because the SEI is more unstable then for small particles, it will consume more lithium over time during cycling. Smaller particles lead to the decrease of the tensile hoop strains in the outer portion of the SEI and simultaneously make the overall elastic strains in the inner portion more compressive [45]. Because of this there seems to be an optimum particles size with a good balance between the amount of SEI that gets formed and the stability of it. This particles size is about 150 nano-meter for silicon. This is also small enough to prevent the pulverization and fracture of the silicon particles. [46].

So that brings us to the question of why the industry does not just use this nano sized silicon if it has all these benefits compared to micro-sized silicon. The answer to this is comes down too, as usual, money. The production and processing of nano sized silicon is not currently commercially competitive compared to micro sized silicon, even if the nano material has better performance. In 2020 the nano sized silicon was around 10 times more expensive then micro sized silicon [47].

2.7.2. Nanoporous silicon

So can we get the benefits of nano silicon without paying the higher price? The next solution tries to use nano pores inside micro size silicon to do this. The idea is that the pores allow the material to expand into the pores instead of just outwards. And this could help to reduce cracking of the SEI layer that is formed around the particles, since the particles expand less outwards with this method. A downside of this solution is that if the silicon contains pores the volumetric energy density of the electrode will be reduced since there is less active material mass per volume. An example of such a nano porous structure is shown in figure(2.11).

This thesis will focus on how nano-porous silicon like this can be used in all solid state batteries. The nanoporous material is provided by a company called "E-magy" [48]. They are trying to solve the expansion issue of silicon upon lithiation by designing a nanoporous material. The pores can then allow the material to expand into the pores itself so it doesn't expand outwards and destroy the battery. The material has already been extensively tested in combination with liquid electrolytes, showing very stable battery cycling and near zero volume expansion in these liquid electrolyte using batteries [49]. But not yet in combination with solid electrolytes in all solid state batteries. So the main goal of this thesis will be to test if this promising material can be utilized in all solid state batteries to get both the benefits of the nanoporous silicon and the benefits of solid state batteries compared to liquid electrolyte batteries.

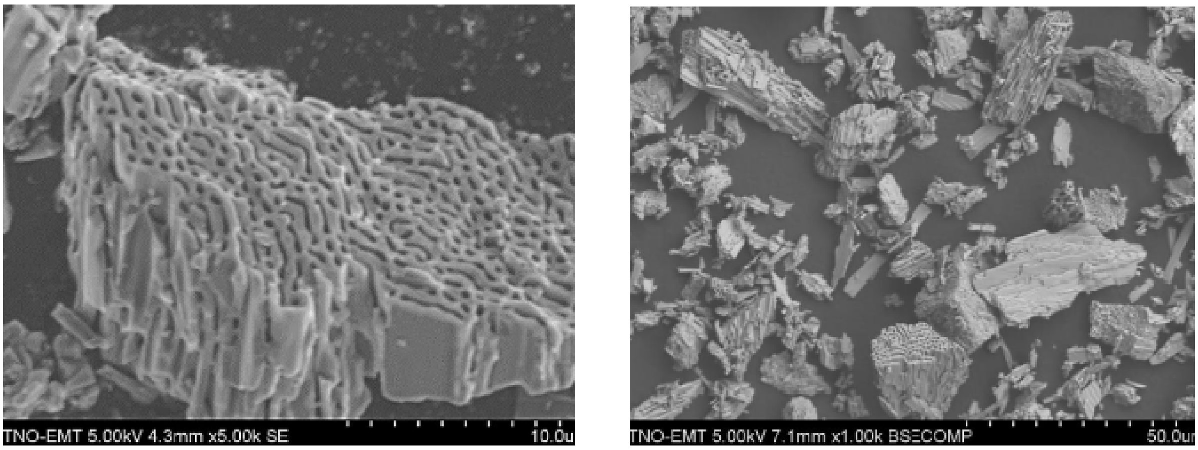

Figure 2.11: SEM image of the porous silicon material provided by E-magy with the more zoomed in version on the left.

2.7.3. Mix silicon with solid electrolyte and carbon additive

To improve the ionic and electronic conductivity of the electrode, the active material can be mixed with all kinds of additives. The ionic conductivity can be improved with the help of SE, this can be the same SE that is used in the cell but it doesn't have to be necessarily. This makes sense of course since SE is designed specifically to have a high ionic conductivity. In the case of silicon it is important to choose a solid electrolyte that can mitigate the damage done by volume changes of the silicon. As discussed before in the section about solid electrolytes (2.4.3), sulfide and halide solid electrolytes like argyrodite are very soft and compressible compared to there oxide counterparts, making them a good choice.

To also get a good electronic conductivity in the electrode often a carbon additive is added, this also helps with a better current distribution in the electrode [50]. This has been done universally in the electrodes of lithium ion batteries [51]. A downside of using carbon to increase the overall electronic conductivity of the anode mixture is that carbon has a negative effect on the stability of sulfide SSE's [52] [53]. [52] Showed a comparison between solid state batteries where a pure silicon mixture was compared against a silicon mixture with 20% weight percentage of carbon added. Mircro Si(C) || SSE || NCM811 cells where made with both compositions and the cells with carbon additive showed severe electrolyte decomposition and SEI growth. [53] showed that for the SSE decomposition it does matter a lot which type of carbon is used, but that no carbon added resulted in the least amount of decomposition. In the cells that where made for this thesis that did contain carbon the choice was made to use carbon nano fibers (CNF) because compared to other carbon additives, such as carbon black or super P, CNF's have a high aspect ratio and robust mechanical properties, which reduce contact resistance with silicon and the solid electrolyte and also create a more resilient and stable conductive matrix throughout cycling. Carbon nano tubes (CNT) hold these same benefits but there costs can be, depending on many factors of course, up to 100 times more expensive then CNF's [54]. So with this in mind the choice was made to use CNF as a conductive additive.

2.7.4. Pressure effects on battery performance

External pressure has a big influence on solid state battery behavior and therefore a large impact on the battery performance [55] [56]. The pressure can help to maintain the solid to solid contact of solid state batteries which increase the ionic transport. But a pressure that is to high can also have negative effects. In the case of lithium metal anodes for example, a lower pressure can help decrease the growth of dendrites but a higher pressure can force the lithium metal through the solid electrolyte and cause short circuiting. [57] showed for an NMC/graphite pouch cell that there was an optimum pressure. A pressure of 1 MPa seemed to enhance the stability of the solid electrolyte and improve the battery performance, but pressures above that resulted in a decrease in the capacity caused by non-uniform SEI formation and an increase in lithium dendrite growth. Another example that showed the role of external pressure is the 2D silicon carbon free sulfide solid electrolyte battery which was mentioned before [52]. This battery showed incredible performance with an average coulombic efficiency of 99,95% and a capacity retention of 80% after 500 cycles using a 99.9 weight % silicon anode. But this result was obtained by using a cell with a large stack pressure of 50 Mpa contionously

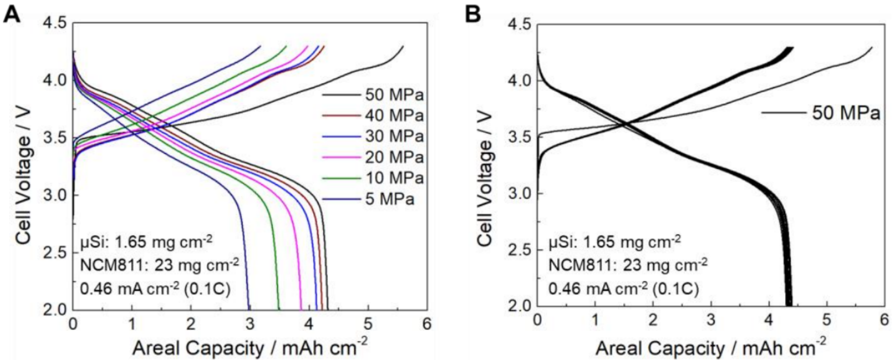

Figure 2.12: A figure showcasing the capacity vs voltage graphs of a 2 identical batteries where A is subjected to a decreasing pressure every cycle and B being subjected to the same pressure of 50 Mpa every cycle [52]. As you can see the battery A where the pressure gets reduced every cycle shows a lot more capacity loss then battery B.

being applied to the battery. The results obtained with the same battery chemistry but now with a decrease in pressure every cycle are shown in figure(2.12). So an extra device has to apply this external pressure. And taking into account the extra space this device will have to take in of course reduces the energy density of the battery. So whether or not the use of this pressure is worth it will have to be looked into further.

2.7.5. Limited capacity cycling

One relatively simple solution that helps deal with the large expansion of silicon is to just not use the full capacity of the material so it will expand less. This will lower the energy density of the battery since less lithium will be stored per gram of silicon, but since silicon has the ability to store more then 10 times the amount of lithium then graphite per gram, which is currently often used on the anode side, this could still be an improvement even if part of the silicon capacity remains unutilized. [58] modeled silicon nano particles of different sizes and mixing those sizes to see how much the particles could be lithiated without fracturing. They showed for 1 and 2 micrometer particles that the lithiation shouldn't exceed 66 and 60 % respectively. Some actual batteries where also made by [59] to test this, this was done by using a composite anode of Si micro particles with carbon additive, Li_6PS_5Cl SE and a NMC cathode. The anode was only charged to 800 mAh/g of Si which showed good electrochemical performance while still having a 28% higher energy density with the partially charged silicon then a graphite anode would have. And this was done without a device that maintained a external pressure on the battery while it was cycling. The people from E-magy also suggested to only use part of the silicon materials capacity to preserve the crystalline backbone [48] of the material that keeps the nanopores intact.

Ideally we want to make use of as much of the available capacity of the Si as possible, so it will be interesting to see what amount of capacity utilization is best suited for the batteries made in this thesis with the use of the nanoporous E-magy Si material and the high ionic conductivity $Li_{5},_{5}PS_{4},_{5}Cl_{1},_{5}$ solid electrolyte.

3

Thesis research question and sub questions

In this small chapter we will formulate the research question that this thesis will try to answer. This will be followed by formulating some smaller questions that will help with answering the main question.

3.1. Research question

The main research research question is:

Research Question 1, Main question

How can nanoporous silicon be used to improve the performance of solid state batteries using argyrodite solid electrolyte?

The E-magy nanoporous material has already been proven to improve the cycling stability compared to regular silicon in liquid electrolyte batteries. And because of the many benefits of all solid state batteries, it will be interesting to see if this is also the case for solid state batteries.

3.2. Sub questions

To answer the main question, batteries will be made using high conductivity SE with sulfide and halide properties called lithium argyrodite (Li_6PS_5Cl), a small modification to his materials composition leads to the creation of $Li_{5,5}PS_{4,5}Cl_{1,5}$ which has a greatly improved ionic conductivity, but has been shown to behave less stable at lower potentials. This brings us to the first sub question:

Research Question 2, Sub-question

Can the use of $Li_{5,5}PS_{4,5}Cl_{1,5}$ help to improve the battery performance when compared to Li_6PS_5Cl in solid state batteries using silicon?

Silicon is often combined with other additives, meant to improve the ionic and electronic conductivity, to create a composite powder mixture electrode. In this research we will use the $Li_{5,5}PS_{4,5}Cl_{1,5}$ SE and carbon nanofiber as additives. Which precise composition is the best and if these additives are even necessary will have to be seen. So that brings us to the following question:

Research Question 3, Sub-question

Will the addition of $Li_{5,5}PS_{4,5}Cl_{1,5}$ and CNF as additives to the powder silicon composite electrode improve the battery cycling results and what composition performs the best?

But a dry powder mixture is not the only way of making a silicon electrode, another way is by mixing the silicon with a binder and a solvent to make a wet slurry and deposit the mixture on a Cu sheet that can be punched to make Si electrodes. It can be interesting to see how these 2 techniques compare to each other, which gives us the following question:

Research Question 4, Sub-question

How does the battery performance change when silicon deposited on Cu electrodes is used instead of the Si/SE/CNF dry powder mixture electrode?

A way of reducing battery degradation resulting from silicons large volume changes is, only partially lithiating the silicon so not the full capacity is utilized. This does however reduce the energy density of the material, but the increased stability and capacity retention could outweigh this downside. So the following question arises:

Research Question 5, Sub-question

How does partial lithiation of the silicon by limiting the utilized capacity influence the battery performance?

These are some of the questions that we we will try to answer to help come to a conclusion about the main research question in the conclusion chapter(6). But before that the methodology (4) will be discussed and the results on which these answer will be based are discussed in the results chapter(5).

4

Methodology

This chapter will discuss which techniques where used to get an answer to the research questions from the previous chapter. First an explanation will be given about the materials inside the batteries and how the solid electrolyte was synthesized. How the purity of the SE was tested using XRD is up next. Then a detailed description of the solid state battery making process is given, which is followed by an explanation of the battery cycling procedure. After which a explanation of the mixing methods that are used is given. Then the step by step procedure of creating the Si on Cu deposited electrodes will be explained. Afterwards electronic impedance spectroscopy (EIS) will be discussed and how it can be utilized for this research. And to close off how the ionic conductivity of the solid electrolytes was determined is discussed. All techniques are performed under room temperature and a atmospheric pressure unless it is mentioned otherwise.

4.1. Materials inside the battery

This section will go over the materials that are used inside the batteries throughout this thesis project

4.1.1. Solid state synthesis for the solid electrolyte

The solid electrolyte used in the battery cells had to be synthesized. This was done by first calculating the right amount of each chemical that has to be added together to form the right composition. This composition is then made in the glove box by weighting the chemicals in powder form and adding them together so they can be mixed using a mortar and pestle. After mixing/grinding the material mix for 10 minutes a homogeneous powder should be left. This powder mix can now be pressed into 500 mg pellets using 49 MPa created by a hand press machine in the glove box. The pellets now should be added inside a glass testing tube. The testing tube will be sucked into a vacuum state using a pump and the testing tube with the pellet inside is then closed off using a blowtorch. The vacuum closed of tubes with the the pellets inside can now be placed into the oven to continue the synthesis process. The temperature, duration and ramp time of the oven can all be tuned to get the preferred material properties. In this case a maximum oven temperature of $450^{\circ}C$ with the oven ramping up to this temperature by increasing the temperature 1 $100^{\circ}C$ every hour. Once $450^{\circ}C$ is reached the oven will remain that temperature for 2 hours. And then the oven will continuously cool down again $100^{\circ}C$ every hour until $20^{\circ}C$ is reached. These parameters can of course be optimized for each material to try to maximize the ionic conductivity. But that is not the focus of this thesis project so oven conditions where taken from my supervisor Ajay Gautam who has had a lot of experience with this synthesis process and with synthesizing SE's in general in for example [31]. This synthesis process resulted in ionic conductivities of 2,9 mS/cm for Li_6PS_5Cl and 7,5 mS/cm for $Li_{5,5}PS_{4,5}Cl_{1,5}$. How these conductivities where determined is explain in the separate section ionic conductivity of the solid electrolyte (4.8)

After the synthesis process has been completed the material purity has to be checked using XRD-analysis which is explained further in the XRD section(4.2). The conductivity is also checked using electrochemical impedance spectroscopy. If the material purity and conductivity are sufficient the material can now be used in the solid state battery cells.

Both the regular argyrodite and the Cl rich variant where synthesized with this method. The other powders that where used where all already available in the lab, and in the case of the E-magy silicon, it was provided by the company [48].

Figure 4.1: The pellets SE pellets after they have been heat treated overnight, they are now ready to be removed from the glass tube to be ground into SE powder in the glove box.

4.1.2. E-magy Vs non porous silicon

Both silicon powders where readily provided. To see if the nanopores improve the performance of the silicon material, it will be best to compare the material from E-magy with a silicon material that is similar but without the nanopores. That way, if we see any difference between the performance of the materials we can say with more certainty that this difference is caused by the nanopores and not by other factors. The other silicon that is used throughout this research project has a particle size of 1-5 microns which was the most comparable size to the E-magy silicon which has a particle size distribution where 90% of the particles are smaller then 7,3 μm, 50% is above and 50% is below 3,4 μm and only 10% is below 1,6 μm. So the particle sizes of both silicon types are very similar. This other silicon type will be referred to as "Commercial" or "Com" silicon throughout this project.

4.1.3. Lithium indium (LiIn) and Cu current collectors

The materials on the silicon side and the SE have now been discussed, but there is also materials on the other side of the SE that makes up the other electrode. Not just lithium, but a lithium indium alloy is used as the electrode on this side of the battery. The indium is added instead of using pure lithium because of undesired reactions occurring between the sulfide SE and the lithium, and because of more lithium dendrite formation when pure lithium is used [60]. LiIn also forms a more stable interface at the SE and maintains a more stable potential which is important when using a two-electrode measurement set up since then the reference electrode and counter electrode are not separate so it should be very stable to get reliable measurements [61]. The equilibrium redox potential at room temperature of the LiIn electrode is 0,62 V vs Li^+/Li [62]. Because all batteries we made us LiIn instead of Li, the potentials will be displayed against LiIn in the results graphs. In the batteries a LiIn composition is made by putting a 8 mm diameter and 42 mg indium pellet on the SE Pellet in the cylinder PEEK, then adding a 5 mm diameter 2-3 mg lithium pellet, and then adding a 10 mm diameter 6,8 mg Cu pellet on top of the lithium pellet. Then the cell is closed and the materials are pressed together. The exact step by step procedure of making the entire battery is discussed in the Solid state battery preparation section(4.3). Cu is used since it is very stable in the potential windows the batteries will be cycled in as was discussed in the Current collector section)2.4.4).

4.2. X-ray diffraction (XRD) to check material composition/purity

Powder XRD is a powerful lab technique that can provide us with information about the sample such as: Phase identification, sample purity, crystallite size, and in some cases, morphology [63]. This information is gained by emitting X-rays on the sample we want to research and then detecting the X- rays after they leave the sample again with a detector. The wave length of x-rays is similar to the wavelength of the crystal structures that make up the material. The X rays will scatter inside the sample and it is important to note that crystals have a structure that repeats itself. And the x-rays interact with each other by either destructive or constructive interference. Constructive will increase the intensity of the x-ray and the opposite will happen for destructive interference. This x-ray pattern is then detected by the detector after it went thought the sample. And this pattern can then be used to trace back what the d-spacing between the crystal planes of the material was. This is possible since each material has a different d-spacing, so each material also has a specific pattern [64]. This can be done with the help of Bragg's law since this relates the d-spacing to the scattering angle.

$$n\lambda = 2dsin(\theta) \tag{4.1}$$

In this law n is an integer, $\lambda$is the wavelength of the x-ray, d is the lattice spacing and $2\theta$is the difference between the scarred beam and the angle of incidence. See the left side of figure(4.2) to get a better understanding of what $\theta$and d mean. If n is a whole number, so an integer, it will mean that the x rays interfere constructively which can be seen as a high intensity peak in the graph which is created as a result of the XRD measurement. The graph i am referring to shows the intensity vs 2θ. These peaks and there intensities can now be used to identify the structure of the material of the powder that we are analyzing.

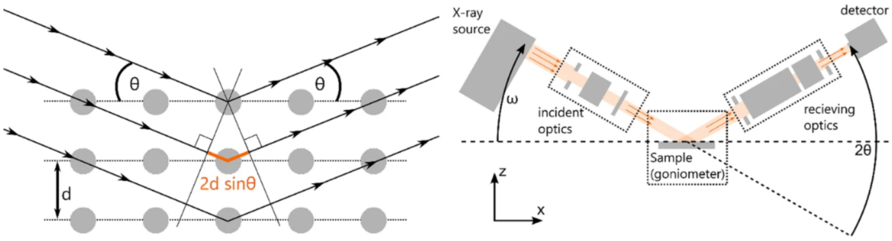

Figure 4.2: Visualization of the way X rays are diffracted in a sample on the left, and a simplified depiction of an XRD machine setup on the right [65].

XRD was used to check composition of the synthesized solid electrolytes to make sure no or at least a minimal amount of impurities were present. In order for the XRD spectrum to be accurate the sample that you put into the machine must have a very flat surface. So the XRD would be done with the synthesized sample. And the resulting intensity vs θgraph we get from that is compared to the XRD spectrum of sample of a pure Li_6PS_5Cl or $Li_5,_5PS_4,_5Cl_1,_5$ sample to be certain that it is pure. If the graph overlaps with the graph from the pure sample we can say that the material we synthesized is free of impurities.

The XRD measurements where done with a XPert-Pro diffractometer from Malvern Panalytical. It had a radiation source which emitted Cu Kαradiation at 45 kV and 40 mA. The samples are put into a airtight XRD holder in the glove box and then transported to the XRD-measurement machine. The measurement is done under atmospheric pressure and at room temperature.

4.3. Solid state battery preparation

Battery cell cycling and preparation was a big part of the experimental work that lead to this thesis report, therefore this will be treated extensively in this section. First there will be a quick overview of the components a solid state battery cell consists off, then how the to be cycled cells are prepared.

4.3.1. Cell Components

- 2 stainless steel metal holders with 10 mm diameter tips.
- 2 o rings
- 10 mm inner diameter air tight cylinder made from PEEK (Polyether-ether-ketone)
- 3 screws with 3 metal rings and 3 plastic washers.

figure(4.3) shows all the cell components both disassembled and assembled.

The cathode / anode description might be a bit confusing here since silicon was always mentioned as a material that is used as the anode for solid state lithium ion batteries. But in these cells that we are making the electrochemical potential of the Li/In alloy is even lower then the electrochemical potential of the silicon. So by the definition of anode and cathode we should then call silicon the cathode material in these specific experiments.

The small metal tips from the 2 metals parts can be detached by undoing the small screws at the bottom. This is necessary for the cleaning, and the small screws need to be replaced if you see that rust is starting to form on them. If you don't replace it when it starts rusting it gets very difficult to turn the small screw. And you want to be able to remove these tips since using high pressures causes them to deform a bit after a few cycling instances. Then they will no longer fit in the cylinder and you wont be able to close the cell of anymore.

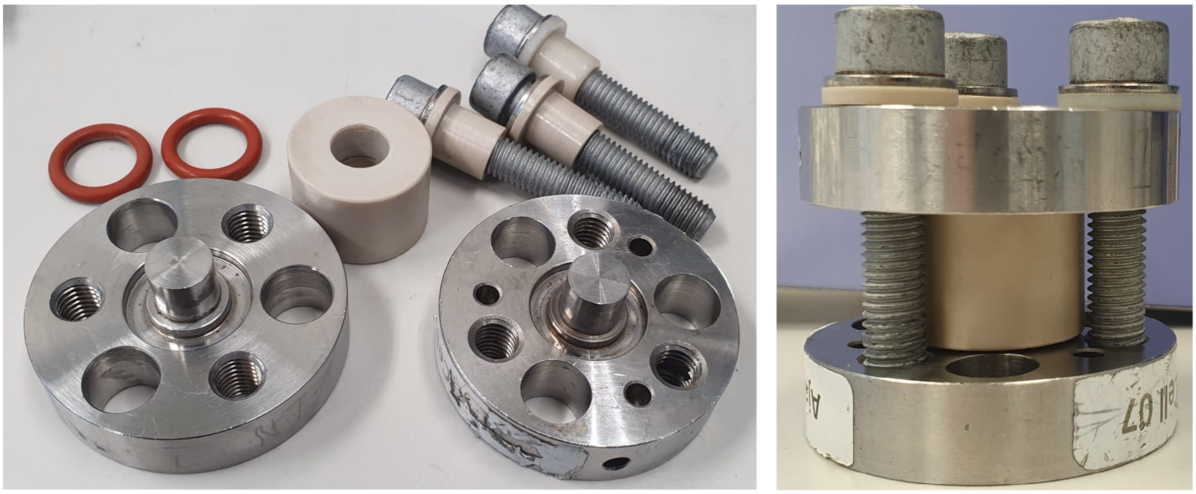

Figure 4.3: The components of a solid state battery testing cell, disassemble on the left and assembled on the right.

4.3.2. Preparation of the Cell

We will now go through the process of making a solid state testing battery step by step:

1. Remove the battery cell parts from the 80 degrees vacuum oven after they have dried there overnight.
2. Move the cells into the glove box by following the necessary steps of vacuuming and flushing the antechamber at least three times with argon gas.
3. Now it is save to move the cells into the glove box.
4. After you moved the cells into the glove box make sure to put the antechamber on vacuum again to minimize the possibility of air leakage.
5. Before you start making the cells make sure you have all your necessary tools, powders and pellets available to prevent having to go in and out of glove box multiple times while you are working.
6. Put on extra gloves over the glove box gloves to keep them clean and prevent punctures. Now its finally time to start making battery cells.
7. Remove the O rings from the metal assembly parts if they are still in there.
8. Put the cylinder on one of the metal assembly parts.
9. Weight the correct amount of solid electrolyte material, in all batteries we use 80 mg of SE which is a similar amount as [66], and add it in the cylinder.
10. Close the cylinder off with the other metal part.
11. Use the electric machine press to apply 1 ton of pressure for 5 seconds to get a nice and evenly distributed solid electrolyte pellet. This pressure of 1 ton is equivalent to a pressure of 124,8 Mpa for the surface area in the 10 mm diameter cylinder.
12. Take off one off the metal parts.
13. Weight and add the correct amount of active material, this could be a mixture of silicon/SE/CNF or a copper pellet with silicon coated on it, depending on which experiment you are conducting.
14. Add one O ring in the metal part you removed before and put it on the cylinder again.
15. Use the electrical mechanical press for 5 minutes at 2,5 ton (312 MPa).
16. Take out the cell and turn it upside down. Make sure not to remove the wrong metal part of the cell since this will break the contact of the active material and the solid electrolyte that was just formed by pressing them together. This mistake in some earlier cells of the project seemed to lead to worse cell performance. That is why it is important to already add the O ring on that side, so you don't have to open that side again to add the O ring later.
17. Now open the cell on the side that has no active material, in other words take off the metal part that has no O ring added yet.

18. Put the indium pellet of 42 mg and 8 mm diameter in the middle of the SE surface inside the cylinder. These pellets can be pressed outside of the glove box since indium does not undergo a spontaneous reaction in air.
19. Punch a 5 mm diameter 2-3 mg lithium pellet out of the flat rolled lithium metal, or roll it flat yourself if its not there yet. This can not be done outside the glove box since lithium will react in an environment of normal air. Make sure to place the pellet of lithium in the middle of the indium pellet and check if it is stable and wont slide of the indium. This is important since the lithium should not be in direct contact with the SE.
20. Add a 10 mm diameter 6,8 mg copper pellet on top of the lithium pellet, drop this pellet in carefully so it does not push the lithium off the indium.
21. Add an O ring to the remaining metal part and put the part in the cylinder to close off the cell.
22. Add the screws with metal rings and the plastic washers pieces to fit tight through the hole and and turn them to close the cell.
23. Put the cell in the electric mechanical press with a pressure of 0,5 ton (62,4 MPa) . While the press is on use the hex key to tighten the screws further. You might have to turn the press off to turn the cell 180 degrees and then turn it back on so you can tighten all screws. The screws should be so tight that you can't turn the hex key by lightly pressing it to the side with one finger.
24. Remove the cell from the press and write with a marker what the composition of the material inside the cell is so you don't get your cells mixed up.
25. Put each cell in a separate latex glove so they can't make contact with each other or other metal that could short circuit them.
26. Take the cells outside of the glove box. Make sure the antechamber you use to take out the cell is flushed with argon gas so no regular air will enter the glove box when taking out the cell.
27. Now the cell is ready to be used for impedance measurements and cell cycling, but more on that in the next sections.

All cell compositions are made at least twice to make sure the results are reliable and reproducible. If a certain compositions performs other then is expected or both of the same cells show a large deviation in performance, so capacity and capacity retention, more cells are made to get more certainty about the results.

4.4. Solid state battery cell cycling

This section will discuss the battery cycling process by first explaining some key concepts for battery cycling, then showing some graphs that use the data we get from battery cycling and then giving some values and calculations on what specifications are used for the battery cycling that is done in this research project.

4.4.1. Battery cycling theory

Now that the batteries are made and tested with EIS, the cell cycling can finally begin. Galvanostatic cycling measurements are made with the batteries, where a constant current is applied and the resulting voltage is measured. The current applied will be determined by the capacity we want to reach and the C-rate that is defined. A C-rate of 1 means that the battery will charge in 1 hour, and a C-rate of 1/20 will mean that the battery will charge in 20 hours, so a full charge/discharge cycle takes 40 hours. The applied current is calculated so that the capacity we are trying to reach will be reached in the time defined by the C-rate.

The potential will change during the cycling process and sometimes the potential will start to become either to low or to high, which can have negative effects for the material in the cell. For example to low potentials can start lithium plating, where metallic lithium forms on the anode side instead of the lithium intercalating or alloying with the electrode [12]. Or unintended potentials could lead to unwanted side reactions and electrolyte decomposition when the voltage gets out of the electrochemical stability window of the material. For reasons like this voltage limits are set to make sure the voltage stays in that range. If the voltage limit is reached while the battery is charging the machine will force the battery to start the discharge process, and if the limit is reached while discharging it will start the charging process, even if the intended capacity cycling time is not reached yet. If no voltage limits are set the machine will eventually stop the measurement if the potential gets to high or to low at for example -5 V vs Li/LiIn.

If we take a look at Ohms law, which is:

$$I = \frac{V}{R}$$

With I being the current in Ampere, V being the voltage in Volts and R being the resistance in Ohm. Then it becomes clear that if we want to charge and discharge the battery with a constant current I, the voltage V will have to go up if the resistance R goes up. This is why the voltage range between charging and discharging will grow further apart if a cell keeps being cycled and the battery starts to degrade. So that means the voltage limits that are set for the experiment will be reached quicker and quicker if the resistance in the battery increases, so the battery will get less time being charged/discharged, which will result in the capacity of the battery getting lower and lower every cycle.

Instead of only limiting the battery cycling with voltage limits, time limits can also be applied. This method was used to charge the batteries to only a certain amount of there capacity. This is done by calculating how much time the battery will need to reach that capacity with the chosen current, and then setting that time as a limit. A backup voltage limit can still be used when using this time limited cycling in case the voltage gets to high or to low.

4.4.2. Graphs made from battery cycling data

The battery cycling data can be shown in a graph with the battery charge and discharge capacities on the y-axis and the cycle number on the x-axis. This type of graph will give insight into how fast the capacity of the battery fades and on the coulombic efficiency since both the charge and discharge capacities are registered by the machine. Another graph that gives insight in the battery performance is the potential vs capacity graph. Multiple cycles of the same battery can be displayed on this graph to see how the capacity and the voltages that are needed to reach certain capacities change for each cycle. A lot of these two types of graphs are shown in the results chapter (5) for all the different batteries that where made. Figure(4.4) already gives an example of what these types of graphs, that are made from the battery cycling data look like.

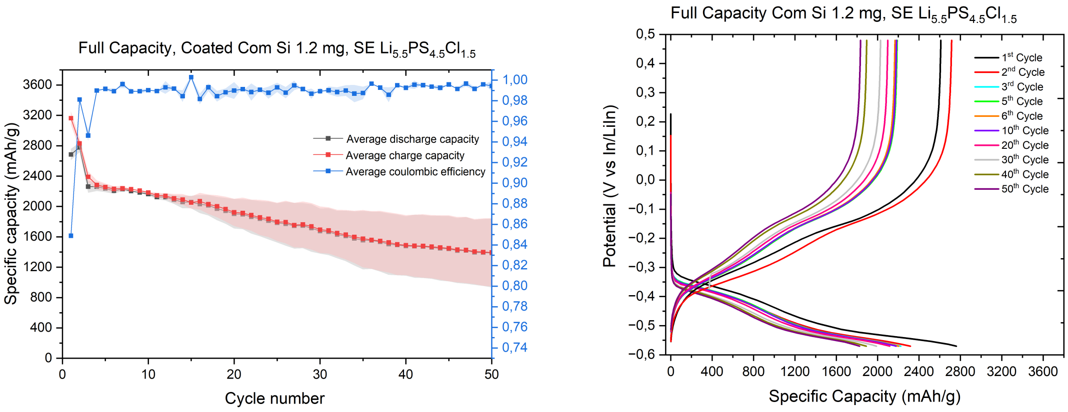

Figure 4.4: An example showcasing a capacity vs cycle number vs coulombic efficiency graph on the left and a potential vs capacity graph on the right.

4.4.3. Values used for battery cycling

The voltage limits set for the batteries are -0,57 to 0,48 V vs In/LiIn for all batteries unless it is specifically mentioned for a certain test in the results section(5). This voltage window should allow a targeted capacity of 3000 mAh/g to be reached while keeping the potential in a range where the materials in the battery remain stable, these values where chosen since similar values where used by [66], [61] and other people in the SEE research group who where cycling Si/Argyrodite/LiIn solid state batteries.

For the first set of batteries that was made 2 mg of silicon was present in the electrode. So a capacity of 3000 x 0,002 = 6 mAh is the target. If the C rate is 1/20 the capacity should be reached in 20 hours. So the current will have to be 6/20 = 0,3 mA. To be able to compare this number with other solid state batteries we want to know the current per cm^2 so this number will have to be divided by the area of the surface between the electrodes and the SE which is πx 0,5^2 =0,7854 cm^2. So the current density for a cell with 2 mg Si and a C-rate of 1/20 is

0,3/0,7854 = 0,382 mA/cm^2, this current density is similar to the areal densities used in [52]. For all batteries the first few cycles are done at C/20 so stable interfaces can be slowly formed. First 5 of these C/20 cycles where done but later from the test results we could see this was not necessary so then only 2 C/20 cycles where used. After the formation cycles the C-rate is doubled to C/10 (so for 2 mg Si this gives 0,764 mA/cm^2) for the rest of the 50 remaining battery cycles. The amount of 50 was chosen just like in [66] to get a good idea about the cycling stability of the cell. These test take a lot of time and many different battery compositions are tested so the cycle number can't be to high because of practical time constraints.
Later on the switch was made from 2 to 1,2 mg Si in the batteries to reduce the current density, to improve the performance without having to lower the C-rate and having to wait longer for the batteries to cycle. This change results in a current density of 0,229 mA/cm^2 for C/20 and a current density of 0,458 mA/cm^2 for the C/10 cycles.

4.5. Silicon/SE/CNF powder mixing methods

For the first battery experiments of this thesis a powder mixture of silicon (E-magy and Commercial silicon where both used to compare them), solid electrolyte (either $Li_{5,5}PS_{4,5}Cl_{1,5}$ or Li_6PS_5Cl) and CNF where used. These mixtures would vary the amount of SE and CNF added to the Si to see which composition was the best. Similar to how it was done by [66]. These mixtures are called names like 631 Si E-magy Cl1,5. This means that the mixture contains 60 wt% silicon form the E-magy company, 30 wt % $Li_{5,5}PS_{4,5}Cl_{1,5}$ and 10 wt % carbon nano fiber.

Two different mixing methods where used to create these mixtures. For most cells a simple mortar and pestle where used, shown on the left in figure(4.5) to grind the different powders together until a uniform mixture with the same color was created. This grinding was done for 10 minutes for each new composition. After which the mixture could be removed from the mortar by scraping it out with a spatula and storing the material in a vile.

Some experiments used another mixing method to see how this would affect the battery performance. For these batteries the mixture was made with the help of ball milling. All powders are then put into a ball mill jar inside the glove box with the correct proportions. Ball mill jars with balls are shown on the right of figure 4.5. But instead of grinding it by hand, small balls are added to the powder mixture, the jar is then closed of air tight and taken out of the glove box and placed in the ball mill machine. This machine rotates very quickly making the balls and the powder move inside the jar to mix the material. A time of 5 min spinning and 5 min rest was chosen for each ball mill cycle, with 48 cycles being completed in succession. The 14 balls in each jar had a diameter of 10 mm and are made of tungsten carbide.

After the ball mill machine was finished, the ball mill jars are placed back in the glove box and the material can be scraped out of the jar using a spatula. The jars can the then be removed from the glove box and be cleaned by filling them with some water and sand, and then running the ball mill machine again. Repeat this process until the balls and jars are all clean again and don't look dusty anymore.

Figure 4.5: On the left a mortar and pestle are shown and on the right 2 opened ball mill jars are shown.

4.6. Coated Si on Cu

After the pour results of the powder Si battery cycling tests it was decided to take a look at how the material performs when the silicon is applied as a coating instead of a powder mix. Before silicon powder was mixed with electronic and ionic conductive additive powders and then simply mixed with a mortar and pestle inside of the glove box. Now the silicon powder will be mixed with a binder powder and and a liquid solvent to create a slurry. This slurry can then be deposited on a copper foil sheet which will act as the current collector. The copper foil with the slurry on top of it will then be heated, and the solvent will evaporate out of the material. The end result is a copper foil sheet with a layer of silicon deposited onto it. Circles can be punched out of this sheet to create electrodes which can be used in the solid state battery cells.

There are a few parameters that have to be taken into account during this procedure.

- The Binder: For the binder polyvinylidene fluoride (PVDF) was chosen since this was also used by [52] to create there carbon free silicon anodes. One weight percentage of PVDF was added since this amount was recommended and led to good Si coatings within the research group.
- The Solvent: N-Methylpyrrolidone (NMP) liquid was chosen as a solvent to mix together with the PVDF and the silicon. The NMP is necessary because the PVDF binder only dissolves into NMP and not in water [67]
- The Mixing speed: A mixing speed of 900 RPM for one hour was chosen to make sure the powder/liquid mixture would turn into a thick homogeneous slurry. Figure(4.6) shows the mixing setup.

Figure 4.6: The setup used for mixing the silicon, NMP and PVDF into a slurry.

- The Coating thickness: The coating thickness is directly correlated to the amount of active material on the electrode you end up with. And the active material mass directly affects the capacity and the battery degradation so to be able to compare the different batteries we want to be able to make electrodes with the same thickness. This is done by using a doctor blade that has a gap with a predefined thickness on each side, this tool is shown in figure(4.7). The blade is then moved over the slurry to spread it out over the Cu foil. The thicknesses of gaps in the blade that was used are 50, 100, 150 and 200 micrometer. The first time 50, 100 and 150 micrometer were all used to see what silicon weight those thicknesses would give. After punching the electrodes, it became clear that using the 50 micrometer thickness gave silicon masses of around 1,2 mg. Take note that we say around 1.2 mg. The weight would vary between 0,9 and 1,5 mg. This is the case because it proved quite difficult to get the coatings as a uniform thickness. But this was not a problem since a lot of coating was made at once. So the the pellets could be weighted on a scale outside of the glove box to select only the pellets that had a weight of 1,2 mg silicon deposited onto them. The weighting of the pellets is shown in figure(4.8).
- The slurry drying temperature and time: After the slurry is spread out over the Cu sheet, the sheets are first quickly dried with the setup shown on the right side of figure(4.7). If the material is then dried enough so it doesn't move anymore when tilting the sheets, it can be moved to a large vacuum drying oven. During the drying of the coated electrodes the solvent (NMP) will dissolve and evaporate out of the material. To make sure all solvent is evaporated the coatings are dried in a vacuum oven with 100 degrees Celsius overnight. The dried coating and the dried coating after the electrodes are punched out of it are shown in figure(4.9).

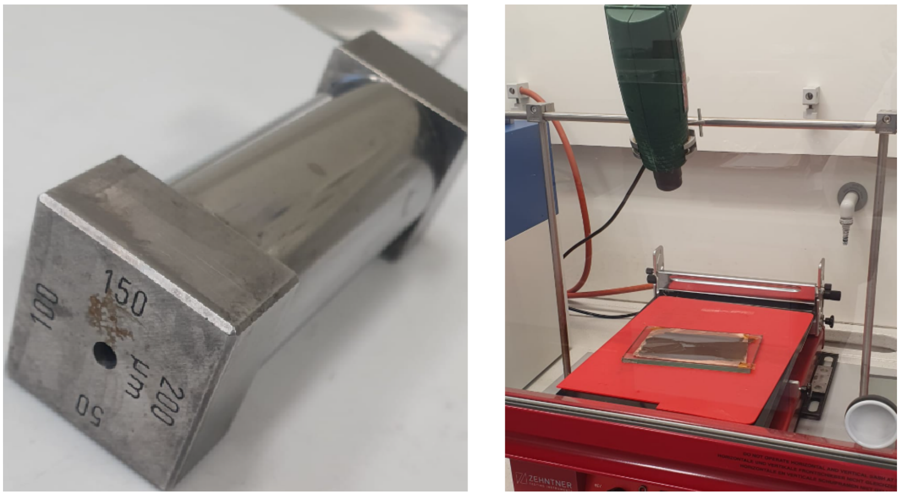

Figure 4.7: On the left the doctor blade is shown. An don the right side the drying setup where the slurry covered sheets are dried is shown.

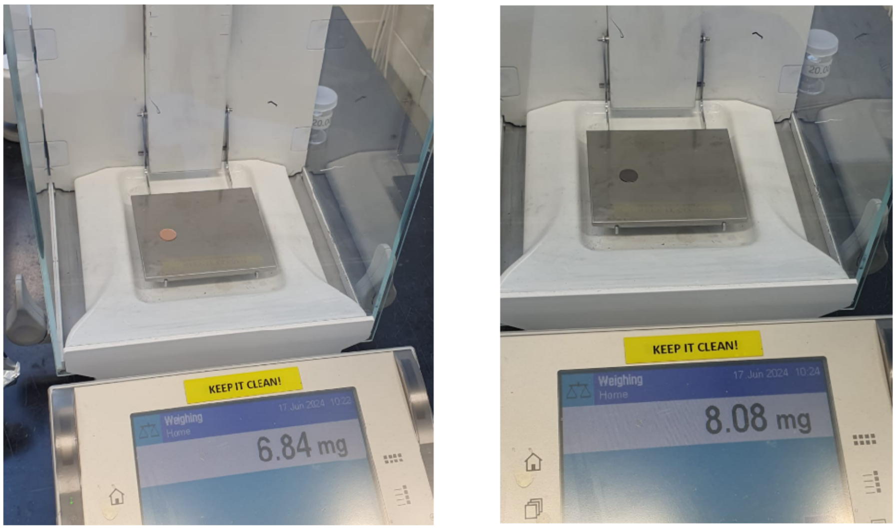

Figure 4.8: Weighting of the pure Cu pellet and the Cu with Si deposited pellet, showcasing a weight difference of 1.2 mg.

Figure 4.9: Si on Cu before and after the electrodes have been punched out.

4.7. Electrochemical impedance spectroscopy EIS

Electrochemical impedance spectroscopy is a powerful method we can use for analyzing electrochemical systems in a non destructive way. So that means a battery can be subjected to this testing method without it influencing how the battery will perform when cycling it in the future, or it can also be done in between battery cycles without influencing the cycling process. During EIS a small sinusoidal perturbation voltage called E(t) is applied to the battery. This small voltage perturbation result in a linear current density called j(t). This j(t) has the same frequency as input E(t) but the amplitude and phase can be different [68] The ratio of E(t) and j(t) is defined as the impedance, see the formula below. A easier definition of impedance according to [69] is: 'the resistance that interrupts the current flow when an AC voltage is applied to the circuit'.

$$Z(t) = E(t)/j(t) \tag{4.2}$$

What makes EIS so useful is that by varying the frequency of the voltage E(t), we can see how the battery responds at different frequencies/timescales. For example at low frequencies slow processes like diffusion will be dominant on the spectrum while at high frequencies faster processes like ion migration are more dominant. The way we actually use this Impedance data is by looking at Nyquist and Bode plots. For these plots it is important to realize that E(t) and j(t) are sinusoidal signals so they contain phase and magnitude information so they can be written as complex numbers, so the impedance Z is also a complex number consisting of a real R(Z) (or Z') and a imaginary Im(Z) (or Z") part. This Re(Z) and Im(Z) can then act as the y and x axis of a Nyquist plot. We can now try to recreate this Nyquist plot by modeling the battery as an equivalent circuit. This circuit is made out of components which are shown in figure 4.10. If we then create a circuit that correctly models the batteries behavior we can fit the EIS data to this circuit. This can then tell us for example about the ionic resistance of the solid electrolyte by modeling it with a resistor element or about the charge transfer resistance and double-layer capacitance at the silicon/solid electrolyte interface by modeling it with a resistor in parallel with a Constant Phase Element(CPE).

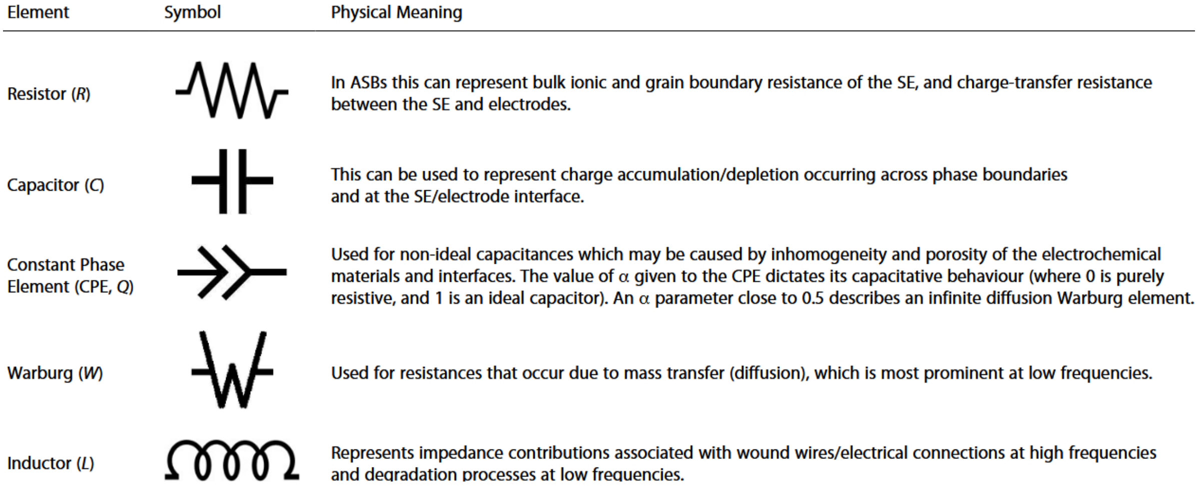

Element	Symbol	Physical Meaning
Resistor (*R*)		In ASBs this can represent bulk ionic and grain boundary resistance of the SE, and charge-transfer resistance between the SE and electrodes.
Capacitor (*C*)		This can be used to represent charge accumulation/depletion occurring across phase boundaries and at the SE/electrode interface.
Constant Phase Element (CPE, *Q*)		Used for non-ideal capacitances which may be caused by inhomogeneity and porosity of the electrochemical materials and interfaces. The value of α given to the CPE dictates its capacitative behaviour (where 0 is purely resistive, and 1 is an ideal capacitor). An α parameter close to 0.5 describes an infinite diffusion Warburg element.
Warburg (*W*)		Used for resistances that occur due to mass transfer (diffusion), which is most prominent at low frequencies.
Inductor (*L*)		Represents impedance contributions associated with wound wires/electrical connections at high frequencies and degradation processes at low frequencies.

Figure 4.10: A showcase of the circuit elements which are used in EIS. For each circuit element an explanation is given about its physical meaning, or in other words what the element is trying to model/represent [68].

Before doing the impedance measurements the cells where first let to rest for 2 hours. This was necessary because if the cells where immediately connected to the machine after being prepared in the glove box, the OCV was not stable and slowly going up. After 2 hours it could be seen that the OCV got to a stable number for all the cells. EIS was performed on all battery cycles both before and after cycling to see what kind of effect the battery cycling had on the different compositions.

The EIS measurements are done with an EC lab Potentiostat. All measurements done in this study make use of a small voltage perturbation, so to be more precise we can say Potentiostatic Electrochemical Impedance Spectroscopy (PEIS) The measurements are done in a frequency range between of 7 MHz and 100 mHz. With 15 frequency points per decade and the amplitude of the signal was 10 mV. The results are shown on Nyqsuist plots showing the real vs the imaginary impedance. To analyze the data, easily compare the Nyquist plots and to fit the equivalent circuits to the data, RelaxIS 3 [70] software is used.

4.8. Ionic conductivity determination solid electrolyte

Before the synthesized electrolyte can be used, the ionic conductivity should be checked to make sure it is similar to the conductivity other people report so we can use it in the batteries. To do this a battery cell is made but with only SE inside it. The SE powder is then pressed into a pellet with the same pressure cycles as all the other solid state batteries where subjected to, so first 1 ton for 5 seconds to check if a smooth pellet is being formed and then 5 minutes at 2,5 ton. The cell should then be closed with the pellet inside it and the battery can be connected inside the glove box to do a EIS measurement. For $Li_{5,5}PS_{4,5}Cl_{1,5}$ this gives a spectrum like shown in figure(4.11).

The conductivity can be calculated by using the resistance we get from the EIS measurement with the following formula's [68]:

$$\sigma = \frac{L}{(R \cdot A)} \tag{4.3}$$

$$A = \pi r^2 \tag{4.4}$$

In this formula L represents the thickness of the SE pellet in cm, R is the resistance in Ω gathered from the EIS and A is the area of the circular surface of the pellet in cm^2. The resistance is gathered from the EIS data by looking at the Nyquist plot. The point where the line crosses the x-axis at Z" is 0, and this shows the resistance caused by the solid electrolyte [71]. The Nyquist plot shown in figure(4.11) shows a resistance of 24,85 Ω. The thickness of the pellet is determined by carefully opening the cell again after the EIS measurement is done. The pellet can then be removed from the cell and the thickness can be measured as show in figure(4.11). Parts of the pellet break off quite easily during this process. So there has to be made sure that the surface you are measuring is the thickness between the most outer smooth surfaces of the pellet, since that was the thickness of the whole pellet before it got removed from the cell. The area of the pellet is know since we know that the inner diameter of the cylinder where the pellet it pressed into is 1 cm.

To give an example we now fill in all these values we got from $Li_{5,5}PS_{4,5}Cl_{1,5}$ into the equation, we get:

$$\sigma = \frac{L}{(R \cdot A)} = \frac{0,1472cm}{24,85 \cdot \pi \cdot 0,5^2} = 7,546 \cdot 10^{-3} S/cm = 7,546 mS/cm \tag{4.5}$$

This value agrees with the ionic conductivity of 7 mS/cm found in [32] and 9,5 mS/cm from [72] [73]. The same procedure was followed for the Li_6PS_5Cl powder and this showed a ionic conductivity of 2,87 mS/cm which is also in agreement with conductivity of 2,9 mS/cm for the same material reported by [32].

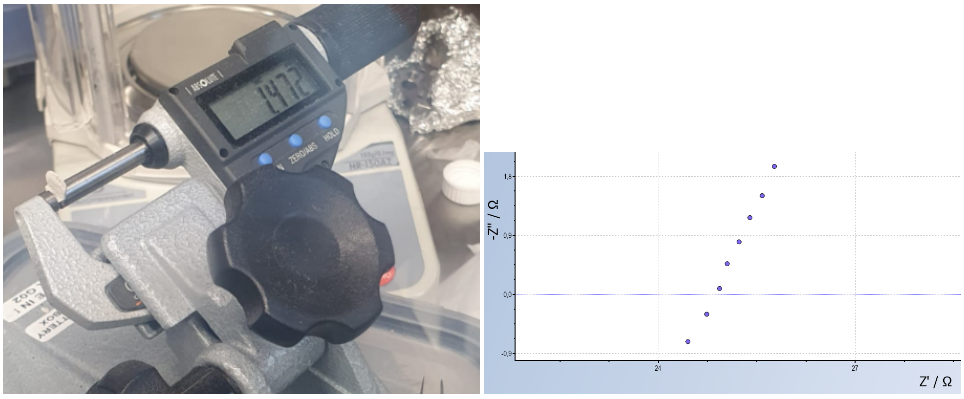

Figure 4.11: On the left device that was used to determine the thickness of the SE pellets is shown, and on the right part of the EIS graph is shown that shows how the cell resistance can be read of the point where the Nyquist plot crosses the x-axis at Z" is 0.

5

Results

In this chapter an overview of the results obtained with the solid state battery cells is shown. Like mentioned in the research question chapter, multiple factors where varied in these batteries to make a comparative study. This chapter for the most part, follows the chronological timeline in which the experiments where conducted throughout the project.

5.1. timeline of the completed experiments

The first set of experiments was aimed at finding the best composition by changing the ratio of silicon, SE, and CNF in the electrode mixture. This was done for bot the commercial (Com) and E-magy silicon material. The best composition was selected to be used in experiments that followed. Next up a comparison was made between batteries of the same composition but with a different current density applied to them to see how much impact this had on the battery performance. After this some cells where made to see how the performance would change if Li_6PS_5Cl was used instead of $Li_{5,5}PS_{4,5}Cl_{1,5}$. And the final experiments done with the dry powder Si/SE/CNF composite electrode where about the mixing method of the mixture, by comparing hand grinding with a mortar and pestle with mixing by using a ball mill machine.

The results of those experiments where interesting but the battery capacity and degradation where still not up to par with the results we where trying to achieve. For his reason a switch was made from using a powder mixture of Si/SE/CNF, to now use silicon deposited on Cu pellets as a electrode instead. This was done for both the E-magy and Com silicon. And also with both the $Li_{5,5}PS_{4,5}Cl_{1,5}$ and the Li_6PS_5Cl solid electrolytes. This gave some promising results but it was still difficult to reproduce the good cycling stability that was observed in some of the batteries. The final set of experiments aimed at looking how the battery performance would change if the capacity of the silicon was limited to only part of its total storage capacity. This set of experiments was done for both types of silicon and both types of solid electrolyte.

The following tables give an overview of the conducted series of experiments. These tables are shown in each result section where they belong. But they are also shown here to give a quick and easy overview of the different experiments.

The first tests where done to see which composition of Silicon/SE/CNF would perform the best. This was done both for the E-magy silicon and the commercial silicon.

Silicon type	Silicon mass	Capacity	Solid Electrolyte	Compositions	Mixing method
E-magy	2 mg	3000 mAh/g	$Li_{5,5}PS_{4,5}Cl_{1,5}$	5/4/1 6/3/1 7/2/1 8/1/1	hand ground
Commercial	2 mg	3000 mAh/g	$Li_{5,5}PS_{4,5}Cl_{1,5}$	5/4/1 6/3/1 7/2/1 8/1/1	hand ground
E-magy	2 mg	3000 mAh/g	$Li_{5,5}PS_{4,5}Cl_{1,5}$	7/2 No Carbon	hand ground

The first 5 Cycles have a C rate of 1/20, all other cycles have a C-rate of 1/10
The cycling is potential limited with a lower and upper limit potential of -0,57 to 0,48 (V vs In/LiIn)

Table 5.1: This table summarizes some of the important parameters of the composition testing experiment series.

From these tests 6/3/1 seemed to perform the best. But the initial battery capacities where very low and faded quickly during the battery cycling. Because of this, the decision was made to lower the amount of active Si material to 1.2 instead of 2 mg. And the applied current was adjusted accordingly. This had the desired effect which becomes very clear if you compare the data between 1.2 and 2 mg.

Next a comparison was made between the 2 dry mixing methods: Hand grinding and ball milling.

Silicon type	Silicon mass	Capacity	Solid Electrolyte	Compositions	Mixing method
E-magy	1.2 mg	3000mAh/g	$Li_{5,5}PS_{4,5}Cl_{1,5\cdot 5}$	6/3/1	Hand ground
Commercial	1.2 mg	3000mAh/g	$Li_{5,5}PS_{4,5}Cl_{1,5}$	6/3/1	Hand ground
E-magy	1.2 mg	3000mAh/g	$Li_{5,5}PS_{4,5}Cl_{1,5}$	6/3/1	Ball milled
Commercial	1.2 mg	3000mAh/g	$Li_{5,5}PS_{4,5}Cl_{1,5}$	6/3/1	Ball milled

The first 5 Cycles have a C rate of 1/20, all other cycles have a C-rate of 1/10
The cycling is potential limited with a lower and upper limit potential of -0,57 to 0,48 (V vs In/LiIn)

Table 5.2: This table summarizes some of the important parameters of the ball mill vs hand grind experiment series.

Now instead of making a Si/SE/CNF powder mixture, the silicon is deposited directly on a Cu foil current collector. This resulted in higher initial capacities and less degradation during the cycling then the powder mixtures. A comparison is made between Com and E-magy Si and between regular and Cl rich argyrodite.

Silicon type	Silicon mass	Capacity	Solid Electrolyte	Compositions	Electrode type
E-magy	1.2 mg	3000 mAh/g	$Li_{5,5}PS_{4,5}Cl_{1,5}$	1% PVDF	Si deposited on Cu
Commercial	1.2 mg	3000 mAh/g	$Li_{5,5}PS_{4,5}Cl_{1,5}$	1% PVDF	Si deposited on Cu
E-magy	1.2 mg	3000 mAh/g	Li_6PS_5Cl	1% PVDF	Si deposited on Cu
Commercial	1.2 mg	3000 mAh/g	Li_6PS_5Cl	1% PVDF	Si deposited on Cu

The first 2 Cycles have a C rate of 1/20, all other cycles have a C-rate of 1/10
The cycling is potential limited with a lower and upper limit potential of -0,57 to 0,48 (V vs In/LiIn)

Table 5.3: This table summarizes some of the important parameters of the Si deposited on Cu full capacity testing experiment series.

Limited capacity testing: The conditions with these tests are the same as for previous one but now we want to see what happens if we try to limit the capacity of the material. This is done by using time constraints. The tests are done for capacities of 1000, 1500 and 2000 mAh/g. Again for both E-magy and Com Si, and for Li_6PS_5Cl and $Li_{5,5}PS_{4,5}Cl_{1,5}$

Silicon type	Silicon mass	Capacity	Solid Electrolyte	Compositions	Electrode type
E-magy	1.2 mg	1000, 1500, 2000 mAh/g	$Li_{5,5}PS_{4,5}Cl_{1,5}$	1% PVDF	Si deposited on Cu
Commercial	1.2 mg	1000, 1500, 2000 mAh/g	$Li_{5,5}PS_{4,5}Cl_{1,5}$	1% PVDF	Si deposited on Cu
E-magy	1.2 mg	1000, 1500, 2000 mAh/g	Li_6PS_5Cl	1% PVDF	Si deposited on Cu
Commercial	1.2 mg	1000, 1500, 2000 mAh/g	Li_6PS_5Cl	1% PVDF	Si deposited on Cu

The first 2 Cycles have a C rate of 1/20, all other cycles have a C-rate of 1/10
The cycling is time limited to control the amount of capacity that is utilized. There is still a upper voltage limit in place for all batteries at 0,48 (V vs In/LiIn) and for the Li_6PS_5Cl experiments there is also a lower voltage of -0,57 (V vs In/LiIn) in case the potential limit is reached before the time limit

Table 5.4: This table summarizes some of the important parameters of the Si deposited on Cu limited capacities experiment series.

5.2. Short explanation of graphs

Here we will give short explanation about the graphs that are used to show the results in this section

5.2.1. Capacity vs capacity vs coulombic efficiency

For each experiment the specific capacity (mAh/g) vs cycle number vs columbic efficiency (CE) graphs are shown. These graphs give insight in the initial capacity of the battery, the battery degradation and on how the coulombic efficiency changes during the cycling process. Most of these graphs are made with the results of two or more batteries, so the lines in these graphs are the averaged result of multiple batteries. The colored area around these lines shows the error of the average. So if a graph consists of the results of two batteries, then the top edge of the colored area shows the capacity and coulombic efficiency of one battery, and the bottom edge of the colored area shows the capacity and coulombic efficiency for the other battery, together they combine into the averaged line in the middle. So if the colored area is very small it means that the batteries for that experiment had very similar results. Some graphs show only the result of one battery cycling test so then no colored area indicating the error is displayed but this will be explicitly mentioned later.

5.2.2. Voltage vs capacity curves

The second plot that is shown for most batteries shows the voltage vs the capacity in (mAh/g). This graph helps us see how the voltage changes as the battery charges and discharges and how the capacity changes for each battery cycle. Some things to keep in mind when looking at these graphs is that the discharge capacity of the first cycle is usually lower then that of the second cycle since the SEI layer is being formed which consumes part of the lithium and therefore lowers the coulombic efficiency of the first cycle to around 80%. After this first cycle the lines typically follow the trend of the earlier cycles being on the right at the higher capacities and the later cycle being on the left at the lower capacities. The bottom part of the graph shows the potential when the Si is being lithiated and lithium is moving away from the LiIn alloy, and the top part of the graphs show when the lithium is moving out of the silicon and back towards the LiIn side. So the first process is defined as charging and the second process discharging. This convention is kept in the graphs and used for calculating the coulombic efficiency as follows:

$$\mathrm{CE} = \frac{Q_{\mathrm{discharge}}}{Q_{\mathrm{charge}}} \tag{5.1}$$

Usually a larger capacity drop between 2 cycles can be seen when the C rate goes up. In the first set of experiments the first 5 cycles have a C rate of 1/20 which then drops to 1/10 for the remaining cycles. In later experiments only the first 2 cycles have a C-rate of 1/20 and all the other cycles are C 1/10. But this will be mentioned later in the specif results per experiment too. For the capacity vs cycle number graphs, averages of multiple batteries are shown together in one plot. But in the potential vs capacity graphs showing average lines with errors made the graphs very cluttered and hard to understand. That is why the choice was made to show only the data of one battery in the potential vs capacity graphs at the time. If 2 batteries had the same composition, the potential vs capacity of the best performing battery is shown or it is specified if a worse performing battery is shown if that gave a more interesting and insightful graph.

5.2.3. EIS spectra, graphs and tables

An EIS measurement was done for each battery before and after cycling. This allowed us to look at the imaginary and real impedance values in a Nyquist plot, and compare them for the different batteries. The higher frequency processes are shown on the left of the Nyquist plot and the as the frequency gets lower we move to the right side of the plot. EIS was done for all batteries but in this results chapter we are mostly focusing on the EIS spectra of the batteries with the silicon deposited on copper electrodes. So for some batteries the Nyquist plots will be shown together with the fitted spectra. We also take a look at the values attributed to the equivalent circuit components of the fitted spectra.

5.3. Composition testing powder mixture

The first experiment series that was done was aimed at achieving the best performance of the silicon in combination with a carbon additive and SE. And then to see which ratio of these materials would lead to the best performance. For these tests Carbon Nano Fibres (CNF) are used to enhance the electronic conductivity and $Li_{5,5}PS_{4,5}Cl_{1,5}$ to improve the ionic conductivity. Ideally we want to have to add as little additives as possible to the silicon since this will reduce the energy density of the material, since the SE and CNF can store less lithium then the silicon (volumetric and gravimetric). [66] conducted a similar experiment but with 50, 40 ,30, 20 and 10% solid electrolyte, but they used a mixture of 92-93% graphite and only 8-7% silicon for the remainder of the mixture. They showed that for their compositions the more SE was added the higher the capacity of the cell was for all the 50 charge and discharge cycles.

Since we ideally want to add less SE in the electrode mixture to keep the energy density of battery high, we wanted to tee see if it was necessary to add a high amount of SE to get a good performance or if lower amounts of SE could be used. In our experiments we use $Li_{5,5}PS_{4,5}Cl_{1,5}$ with a conductivity of 7,7 mS/cm instead of the Li_6PS_5Cl they used which had a ionic conductivity of 2,16 mS/cm. Since the electrolyte we use has a lot higher ionic conductivity we predict that a lower percentage of SE will have to be added to the silicon to ensure good enough ionic conductivity of the mixture.

It was chosen to use 10% CNF in all cells. The amount of silicon was changed from 50% up to 80% with steps of 10%. The rest of the material was SE. This lead to the following cell configurations: 5/4/1, 6/3/1, 7/2/1 and 8/1/1. With the first number being the amount of silicon, the second number the amount of SE and the last number being the 10% CNF. Each composition was used in 2 solid state battery cells, or more if it was observed that the cell short circuited at the start, which still happened sometimes since this where the first cell that where made and there is quite a lot that can go wrong during the cell assembly.

The composition testing was done for both the commercial silicon as the E-magy silicon. A brief summary of some of the important parameters of the composition testing experiments is summarized in the table below.

Silicon type	Silicon mass	Capacity	Solid Electrolyte	Compositions	Mixing method
E-magy	2 mg	3000mAh/g	Li5.5PS4.5Cl1.5	5/4/1 6/3/1 7/2/1 8/1/1	hand ground
Commercial	2 mg	3000mAh/g	Li5.5PS4.5Cl1.5	5/4/1 6/3/1 7/2/1 8/1/1	hand ground
E-magy	2 mg	3000-mAh/g	Li5.5PS4.5Cl1.5	7/2 No Carbon	hand ground

The first 5 Cycles have a C rate of 1/20, all other cycles have a C-rate of 1/10
The cycling is potential limited with a lower and upper limit potential of -0,57 to 0,48 (V vs In/LiIn)

Table 5.5: This table summarizes some of the important parameters of the composition testing experiment series.

The results of the composition test with Com silicon are shown in figure(5.1) by using capacity vs cycle number vs coulombic efficiency, and potential vs capacity graphs. The same graphs are made for the cycling results of the composition testing with the E-magy material, which are displayed in figure(5.2)

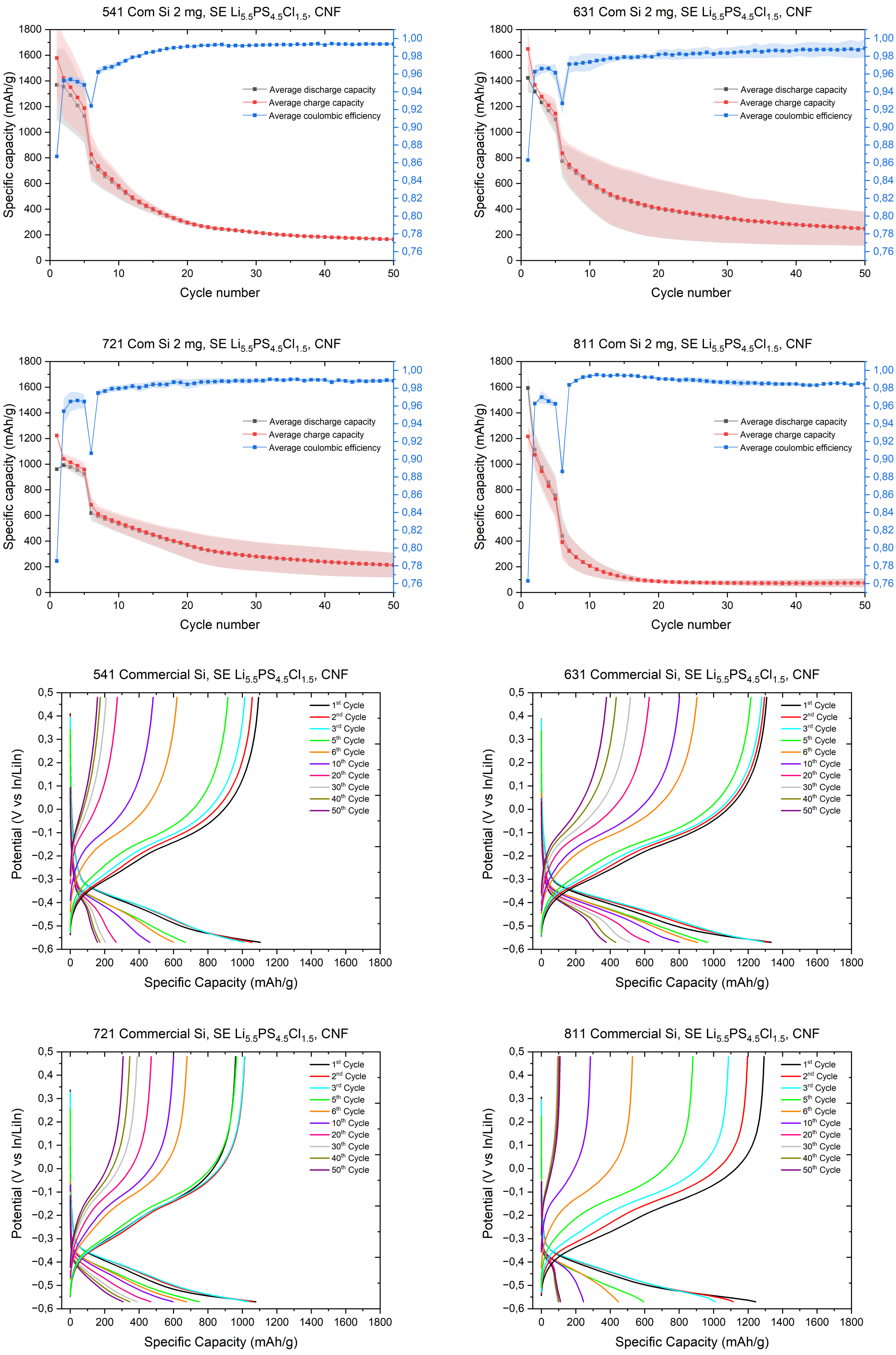

Figure 5.1: This figure shows the capacity vs cycle number vs coulombic efficiency graps at the top and the potential vs capacity graphs at the bottom. For each individual graph is indicated to which composition it belongs too. 5/4/1 6/3/1 7/2/1 and 8/1/1 compositions where tested in this test series with Com Si.

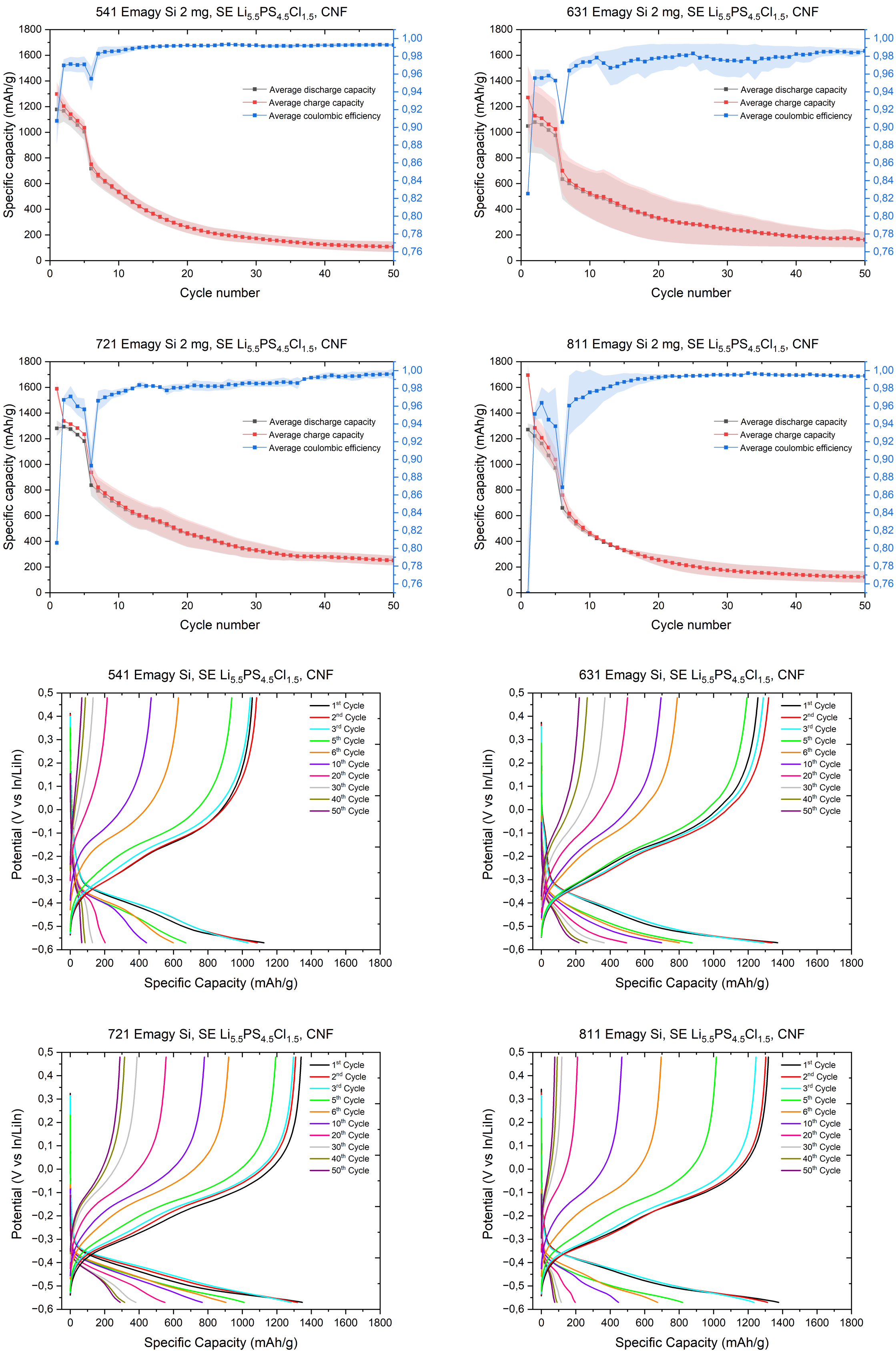

Figure 5.2: This figure shows the capacity vs cycle number vs coulombic efficiency graps at the top and the potential vs capacity graphs at the bottom. For each individual graph is indicated to which composition it belongs too. 5/4/1 6/3/1 7/2/1 and 8/1/1 compositions where tested in this test series with E-magy Si.

From the figures(5.1) and (5.2) regarding the composition testing of both the types of silicon a few things can be seen, these will be displayed by bullet points for clarity:

- The initial capacities of most batteries are around 1500 mAh/g. And this per gram means per gram of silicon. This initial capacity was lower then expected with the set voltage limits. It was expected that close to the full capacity of the silicon could be utilized, so a capacity around 3000 mAh/g.
- The capacity of all batteries seems to drop quickly until the capacity is only left to about 20% of the initial capacity.
- For the first battery cycle it shows that the higher the amount SE mixed with the Si, the higher the coulombic efficiency of the first cycle. This was a clear trend with no outliers for the first cycle, but this trend did not continue for the rest of the cycles.
- A big drop in capacity is seen for all batteries after 5 cycles but this was to be expected since the C- rate then doubles form 1/20 to 1/10. The coulombic efficiency slowly grew as the capacity of the cells got lower and lower, so less and less lithium kept being lost % wise.
- From the area size around the average capacity charge and discharge curves you can see how much difference there was between batteries with the same composition. The 6/3/1 composition shows the largest red/gray area so the biggest difference between the 2 cells with the same composition. But for both silicon types the single battery that performed the best was of the 6/3/1 type, showing better capacity retention. For this reason it was chosen to continue from now on with the 6/3/1 battery composition.
- The 8/1/1 composition performed the worse overall showing the lowest coulombic efficiencies and quick capacity loss. This indicates that there is a benefit of adding more then 10% of SE to the mixture.
- From the low initial capacities and the large capacity loss it seems that the current density that is applied is to high. The area of the cell cant be changed, and we don't want to make the C-rate of the material even lower since the batteries already take a lot of time to cycle. So it was chosen to reduce the amount of silicon (but also the amount of CNF and SE in the mixture to keep the same composition) so a lower current density could be used with the same C-rates.

So for the experiments that follow the 6/3/1 composition will be used and the amount of active material (Si) will be reduced from 2 to 1.2 mg. To keep the composition the same 6/3/1 the amount of SE and CNF will also be reduced according to the Si mass reduction. This allows us to reduce the current density the material experiences while keeping the C-rates the same to prevent even longer testing times.

5.4. Different solid electrolytes and current density change

It seems unlikely, but we wanted to test if for some reason the poor performance was maybe correlated to the change from Li_6PS_5Cl which was also used by [66], to $Li_{5,5}PS_{4,5}Cl_{1,5}$. It was decided to also use this test to already get an indication of how the battery performance changes with lowering the amount of active material from 2 to 1,2 grams as was suggested at the end of the composition testing experiments. Figure(5.3) shows the cycling results of this experiment

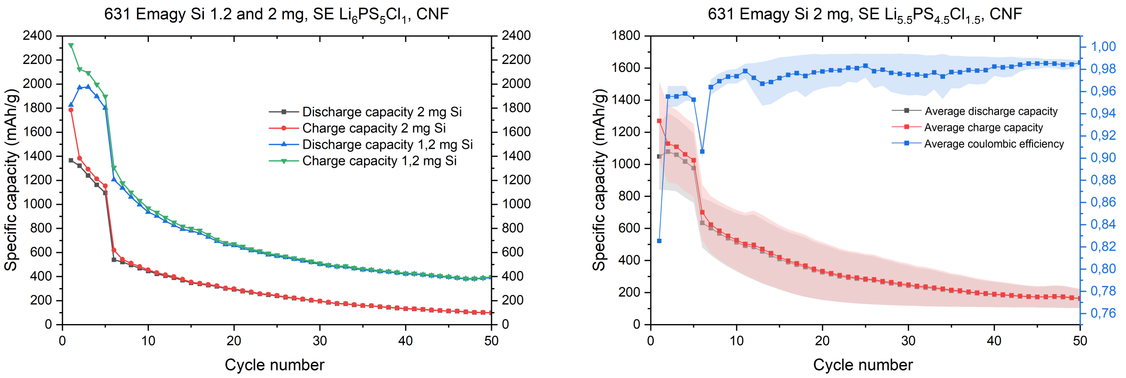

Figure 5.3: This figure shows the Capacity vs Cycle number curve for 2 batteries aimed at comparing Li_6PS_5Cl to $Li_{5,5}PS_{4,5}Cl_{1,5}$ and a loading of 2 to a loading of 1,2 mg. Next to it on the right a picture is shown copied form the composition testing for comparison.

If we compare the results from the new tests with a 631, 2 mg E-magy Si graph from the previous section in figure(5.1) we can see the following:

- The change from 2 to 1,2 mg seems to increase the capacity by about 30% and makes the capacity drop slightly slower at the beginning but overall the shape of the graph does not change much and the battery capacity still drops fast.
- The 1,2 mg Si cell with Li_6PS_5Cl falls on the lower side of the capacity if we compare it to the 631 E-magy composition testing cells using $Li_{5,5}PS_{4,5}Cl_{1,5}$ we previously made. However, we will need more results to conclude how much these different electrolytes really have an effect on the battery performance.

This was only a quick look to see if the $Li_{5,5}PS_{4,5}Cl_{1,5}$ SE was having some bad effect on the battery performance for some reason we didn't take into consideration. But this does not seem to be the case. A more in depth comparison between the battery performance of $Li_{5,5}PS_{4,5}Cl_{1,5}$ and Li_6PS_5Cl will be given from section(5.7 on wards where we will compare both solid electrolytes in solid state batteries using Si deposited on Cu instead of the composite powder mixture that is used now, but more on that later.

5.5. Current density and active material amount influence on battery performance

To see the influence of the current density and the active material amount on the battery performance, new batteries where made for both the E-magy and Com silicon, but instead of using 2 mg Si now 1,2 mg Si is used in each cell. The proportions are still the same so the new cells also have less SE and CNF in the electrode powder mixture in the cell. Again, the capacity vs. cycle number and the coulombic efficiency are shown in figure(5.4) and from this we can see that:

- The batteries with 1,2 mg silicon have not only a capacity shift upwards which was already shown for the battery comparison between 1,2 and 2 mg with the cells using Li_6PS_5Cl. But the capacity also drops a lot slower for the cells using less active material (and are therefore experiencing a smaller current density). The 2 mg Si cells would often lose more than 75% of their discharge capacity after 50 cycles, whereas the 4 cells that are now made with the 1,2 mg Si only lose 50% or even less. This is of course still too much and should be reduced further. But it is interesting that the current density change did not just shift the capacity curves but actually slows the battery degradation.
- The results also seem to have gotten more reproducible with less amount of active material, you can see this from the colored area around the average capacity graphs being a lot smaller indicating less variance in the performance for the new series of batteries that was made.

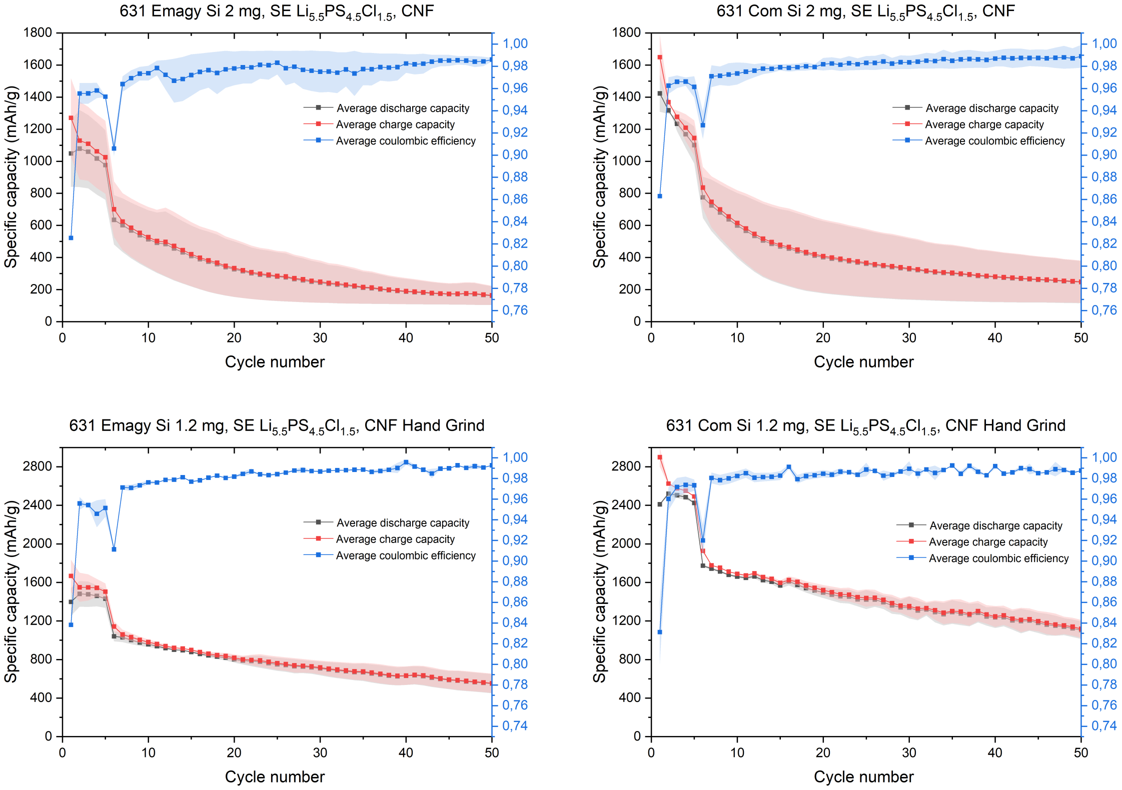

Figure 5.4: The capacity vs cycle number vs coulombic efficiency graphs comparing batteries with a 6/3/1 composition of Si E-magy and Com Si, $Li_5,_5PS_4,_5Cl_1,_5$ and CNF. The amounts of active material is changed from 2 mg in the top graphs to 1,2 mg in the bottom graphs.

5.6. Ball milling VS hand ground silicon

All the previous experiments were carried out with Si / SE / CNF mixtures that were made by hand grinding with the use of a mortar pestle. In this section, we will take a look at how ball milling instead of hand grinding with the pestle influences the performance of the cells. To compare both techniques, all cells were made with the same 6/3/1 compositions, this experiment was again done for both the E-magy and the Com silicon. So the only difference between the cells is the mixing method and which type of silicon they use.

The mortar pestle hand grinding was done by grinding the powder mixture for 10 minutes. The ball milling method has a lot more parameters that can be changed like: The milling time, RPM of the machine, type and amount of balls, amount of milling cycles. The hand grind and ball mill parameters are mentioned in the the methodology chapter in the section silicon anode powder mixture (4.5). The experiment parameters are summarized in the table below.

Silicon type	Silicon mass	Capacity	Solid Electrolyte	Compositions	Mixing method
E-magy	1.2 mg	3000 mAh/g	$Li_{5,5}PS_{4,5}Cl_{1,5}$	6/3/1	Hand ground
Commercial	1.2 mg	3000 mAh/g	$Li_{5,5}PS_{4,5}Cl_{1,5}$	6/3/1	Hand ground
E-magy	1.2 mg	3000 mAh/g	$Li_{5,5}PS_{4,5}Cl_{1,5}$	6/3/1	Ball milled
Commercial	1.2 mg	3000 mAh/g	$Li_{5,5}PS_{4,5}Cl_{1,5}$	6/3/1	Ball milled

The first 5 Cycles have a C rate of 1/20, all other cycles have a C-rate of 1/10
The cycling is potential limited with a lower and upper limit potential of -0,57 to 0,48 (V vs In/LiIn)

Table 5.6: This table summarizes some of the important parameters of the ball mill vs hand grind experiment series.

The results are shown with capacity vs cycle number vs coulombic efficiency, and potential vs capacity graphs in figure(5.5). From the graphs we can see the following:

- The colored area around the average charge and discharge capacity graphs is a lot smaller for the hand ground material then for the ball milled material, showing more consistent battery performance for the hand grind mixture.
- The hand ground Com Si shows the highest initial capacity we have seen yet, and it actually maintains this capacity relatively well with the capacity dropping from 1680 to 1230 showing a capacity loss of 27% after 45 cycles (if we take the first capacity after the first 5 formation cycles). The E-magy silicon is also showing a lot less capacity reduction during the cycling now the switch is made to a lower current density. The shape of both hand ground capacity vs cycling graphs is the same but the E-magy graph is shifted down since the batteries showed lower capacities.
- The ball milled batteries however showed the opposite result with E-magy giving higher capacities now instead of the Com Si.
- The ball milled samples showed worse performance overall compared to the hand ground samples. This could be because of the ball mill parameters being to extreme, destroying the crystalline silicon backbone and making the material more amorphous [74]. Smaller amorphous silicon particles have a larger surface area for SEI to form around which would explain why the initial capacities are lower for the ball milled samples. The smaller particles should also have a better cycling stability then larger particles as discussed in section(2.7.1). This seems to be true for the Com ball milled sample since it reduces capacity slower then the hand ground com batteries but it has a lower initial capacity. But for the E-magy Si the ball milled samples degrades quicker then the hand ground samples, this could be because the ball milling amorphasizes the crystalline Si destroying the nano-porous structure and therefore eliminating the whole benefit the E-magy material was supposed to provide for dealing with the expansion of the silicon by letting the silicon expand into the nanopores.

The results of this mixing comparison experiment show that for these ball milling parameters the performance is worse then when you compare it to simple hand grinding with a mortar and pestle. And especially since we are working with the nano porous Si material from E-magy, there has to be precisely looked at which ball mill parameters sufficiently mix the material but don't destroy the porous structure. We could have continued to explore ball milling of the electrode mixture further but we started to experiment with another technique where the silicon is deposited on a Cu sheet via slurry drying. This technique showed more promising results then what we got so far with the dry Si powder mixtures. For this reason the choice was made to not spend any more time on optimizing the ball mill parameters for the Si/SE/CNF powder mixture but to instead focus on the Si on Cu coated technique.

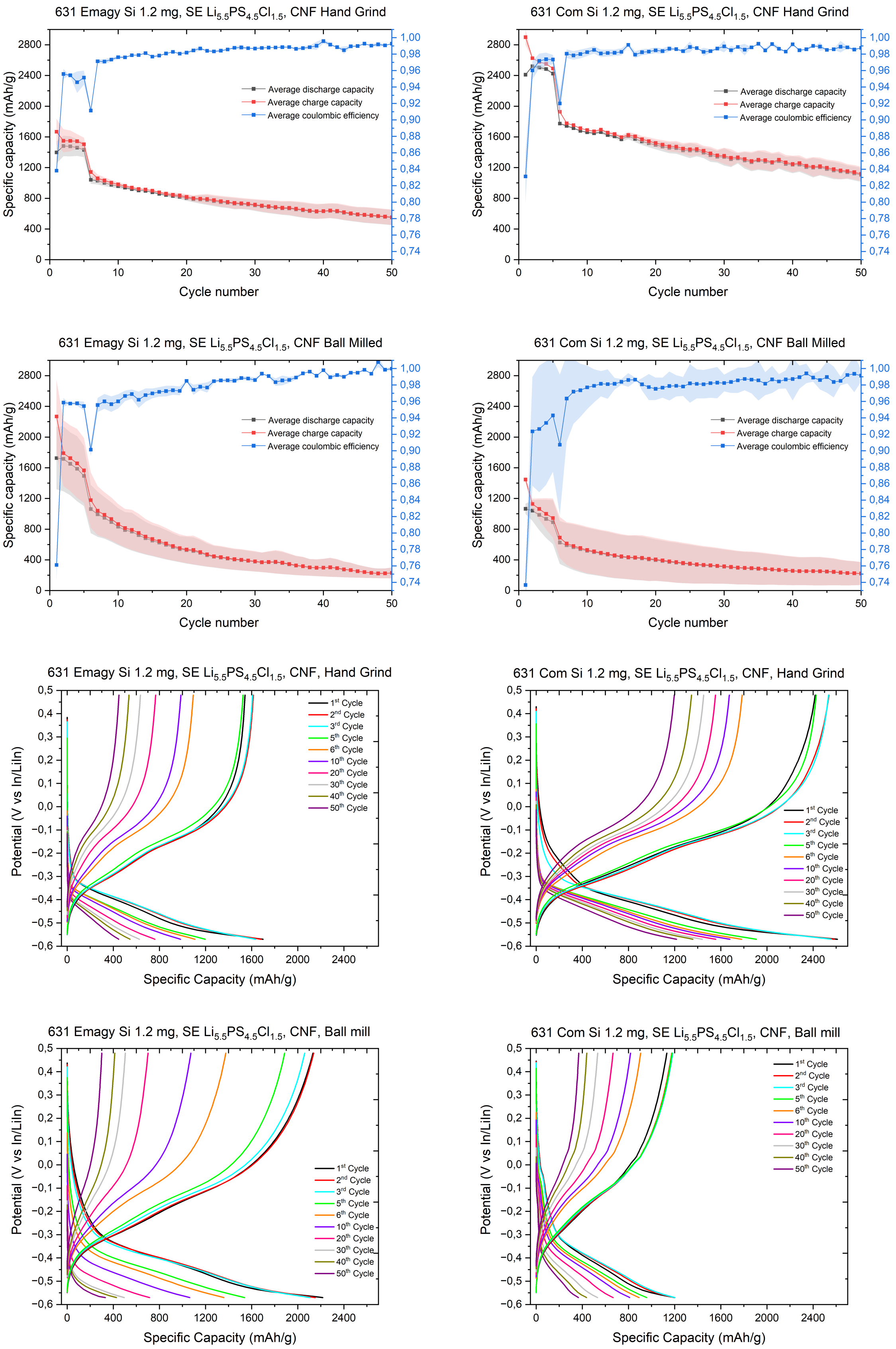

Figure 5.5: The capacity vs cycle number vs coulombic efficiency graphs for the purpose of comparing the ball milling vs the hand grinding mixing technique are shown at the top of the figure, and the potential vs capacity graphs of these measurements are shown at the bottom. These test where done with Com and E-magy Si and all of them use $Li_5,_5PS_4,_5Cl_1,_5$ SE.

5.6.1. No CNF

As was mentioned in the theory section 'mixing silicon with solid electrolyte and carbon additives (2.7.3)', the presence of carbon can have a negative effect on the battery cycling capacity and capacity retention since it promotes other side reactions and SEI formation. So to see if CNF was actually necessary or if it had a positive or negative effect on the battery performance, two 6/3/0 E-magy $Li_{5,5}PS_{4,5}Cl_{1,5}$ batteries where made without adding any CNF to the electrode mixture. In these batteries 2 mg of Si was still used since they where made before the results showed that it would be better to reduce the active material amount to 1,2 mg Si. The results of these test are shown in figure(5.6) together with the 631 E-magy result from the E-magy composition tests.

The batteries without any CNF actually showed higher initial capacities then the previous test where CNF was used. But the capacity still dropped at similar rates. This shows that it might not actually be necessary to add CNF and that the silicon has sufficient enough electronic pathways for the electrons to be conducted. It was shown by [75] and [76] that the electronic conductivity of lithiated (so charged) silicon thin films was more then 3 magnitudes higher then the pure non lithiated silicon. This was for thin films but it shows that there is a large difference in electronic conductivity of a charged or non charged silicon electrode. With this in mind we would expect that for the first cycle when there is no lithium present in the silicon yet, the cell without CNF would perform worse since the mixture of silicon and $Li_{5,5}PS_{4,5}Cl_{1,5}$ would have insufficient electronic conductivity. But the contrary is what is shown by the graph since the capacity of the first cycles is actually slightly higher for the batteries without CNF.

This shows that it is not the CNF that is only responsible for the quick battery degradation. But that it might actually be beneficial to leave out the CNF all together for further testing with similar compositions.

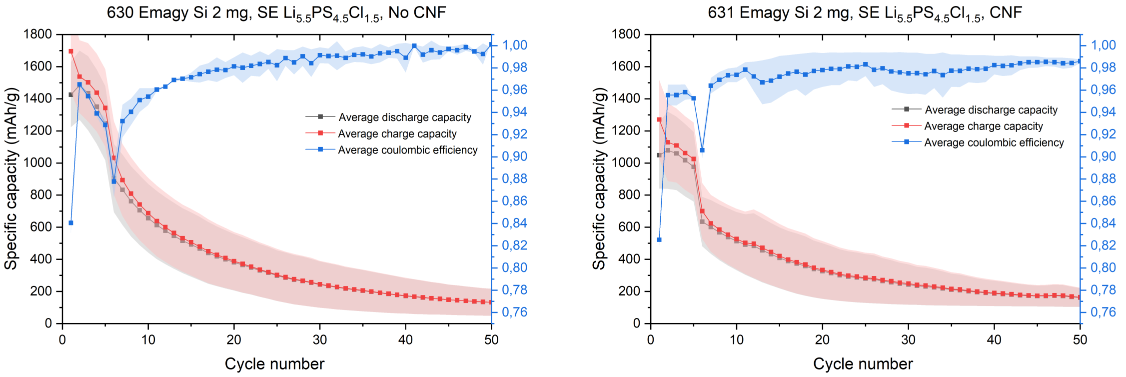

Figure 5.6: The capacity vs cycle number vs coulombic efficiency graphs are shown here comparing the performance of the 6/3/1 Si Emagy/ $Li_{5,5}PS_{4,5}Cl_{1,5}$/ CNF composition with the 6/3/0 composition to see the effects of the CNF on the battery cycling.

5.7. Switch to 2D silicon deposited on Cu

The results we got so far from using a Si/SE/CNF mixture have shown lower battery capacities and quicker degradation for both the Com and E-magy Si then what we where aiming for. And the battery cycling data so far has not yet shown a clear difference between using the regular or nanoporous silicon material. Like mentioned in section(2.7.3) [52] showed promising results with a different technique from the one we are using so far. They mixed the silicon powder with a solvent and binder to make a slurry which can then be evenly spread out over a Cu sheet, after which Si deposited on Cu electrodes can be punched out after drying the sheets. They also advocate for adding no carbon additive to the silicon, and since our previous tests showed that the CNF we had used so far was not improving the battery performance, and might even be hurting it, this seemed like a good choice for us too. There is also no longer any SE added to be mixed with the silicon. Since this slurry making process will be done outside of the glove box in regular air and the solid electrolytes that are being used have poor air stability so cant be used outside of the glove box. And [52] still showed good performance without adding SE and C to the Si.

The first cells that where made with this technique showed a lot of improvement compared to the previous batteries using the powder mixture of Si/SE/CNF, so from this point onward all the results that will be discussed are from batteries with Si deposited on Cu electrodes. The other side of the battery doesn't change, so a LiIn electrode with a Cu current collector is still being used and separated from the Si by either Li_6PS_5Cl or $Li_{5,5}PS_{4,5}Cl_{1,5}$.

For the first series of test that where done in this way, E-magy silicon and commercial silicon are again being compared, in separate cells of course, with $Li_{5,5}PS_{4,5}Cl_{1,5}$ being in between. After the same set of experiments was repeated but now with Li_6PS_5Cl as the SE instead. So this test series compares the performance of the 2 types of silicon and the two types of SE. The results we got from this are shown in figure(5.7), again by showing the capacity vs cycle number vs coulombic efficiency graphs and the potential vs capacity graphs. The batteries from now on only have 2 formation cycles with a C rate of 1/20 instead of the 5 1/10 cycles which where used before. After that the batteries still continue cycling up to 50 cycles with a C-rate of 1/10 just like before.

The table below summarizes the most important parameters of this set of experiments.

Silicon type	Silicon mass	Capacity	Solid Electrolyte	Compositions	Electrode type
E-magy	1.2 mg	3000 mAh/g	$Li_{5,5}PS_{4,5}Cl_{1,5}$	1% PVDF	Si deposited on Cu
Commercial	1.2 mg	3000 mAh/g	$Li_{5,5}PS_{4,5}Cl_{1,5}$	1% PVDF	Si deposited on Cu
E-magy	1.2 mg	3000 mAh/g	Li_6PS_5Cl	1% PVDF	Si deposited on Cu
Commercial	1.2 mg	3000 mAh/g	Li_6PS_5Cl	1% PVDF	Si deposited on Cu

The first 2 Cycles have a C rate of 1/20, all other cycles have a C-rate of 1/10
The cycling is potential limited with a lower and upper limit potential of -0,57 to 0,48 (V vs In/LiIn)

Table 5.7: This table summarizes some of the important parameters of the Si deposited on Cu full capacity testing experiment series.

The results of these tests are shown with capacity vs cycle number vs coulombic efficiency graphs and potential vs capacity graphs in figure(5.7), and this shows us the following
If we compare these results with the results we got from the Si/SE/CNF experiments we can see that:

- Almost all batteries showed better performance then with the mixed Si/SE/CNF that was used before. They show higher initial discharge capacities of around 2800 mAh/g, less capacity fading and higher coulombic efficiencies.
- The coulombic efficiencies stabilize to 98/99 % after the formation cycles really quickly, so already at the third cycle while for the Si powder mixture the Coulombic efficiency would often be lower or take more cycles to reach a stable value.

And if we now look at the new results and compare them to each other we can see that:

- There doesn't seem to be a clear correlation between the initial capacities for the different silicon types, since the E-magy Si showed higher initial capacity values for the $Li_{5,5}PS_{4,5}Cl_{1,5}$ but lower compared to Com Si for Li_6PS_5Cl.

- The E-magy cells seem to show less variance per battery indicated by the smaller colored area around the capacity graph but there has to be kept in mind that these graphs only show 2 battery results each so some more tests would make this point stronger.
- The batteries using $Li_{5,5}PS_{4,5}Cl_{1,5}$ showed higher capacities and also a better capacity retention clearly showcasing the performance improvements made by using $Li_{5,5}PS_{4,5}Cl_{1,5}$ over the regular argyrodite (Li_6PS_5Cl).
- The most stable battery that was made so far showcased a discharge capacity of 2250 after the third cycle, so after the 2 formation cycles and a discharge capacity of 1830 after the remaining 48 cycles. So that gives a capacity faded retention of 81,3% over that period, this is a big improvement compared to the results we got before. It was tried to replicate this performance but the same or better performance was not achieved by making 3 extra batteries with the same composition. This shows that it is still difficult to get consistent results with Si, even with the new technique.

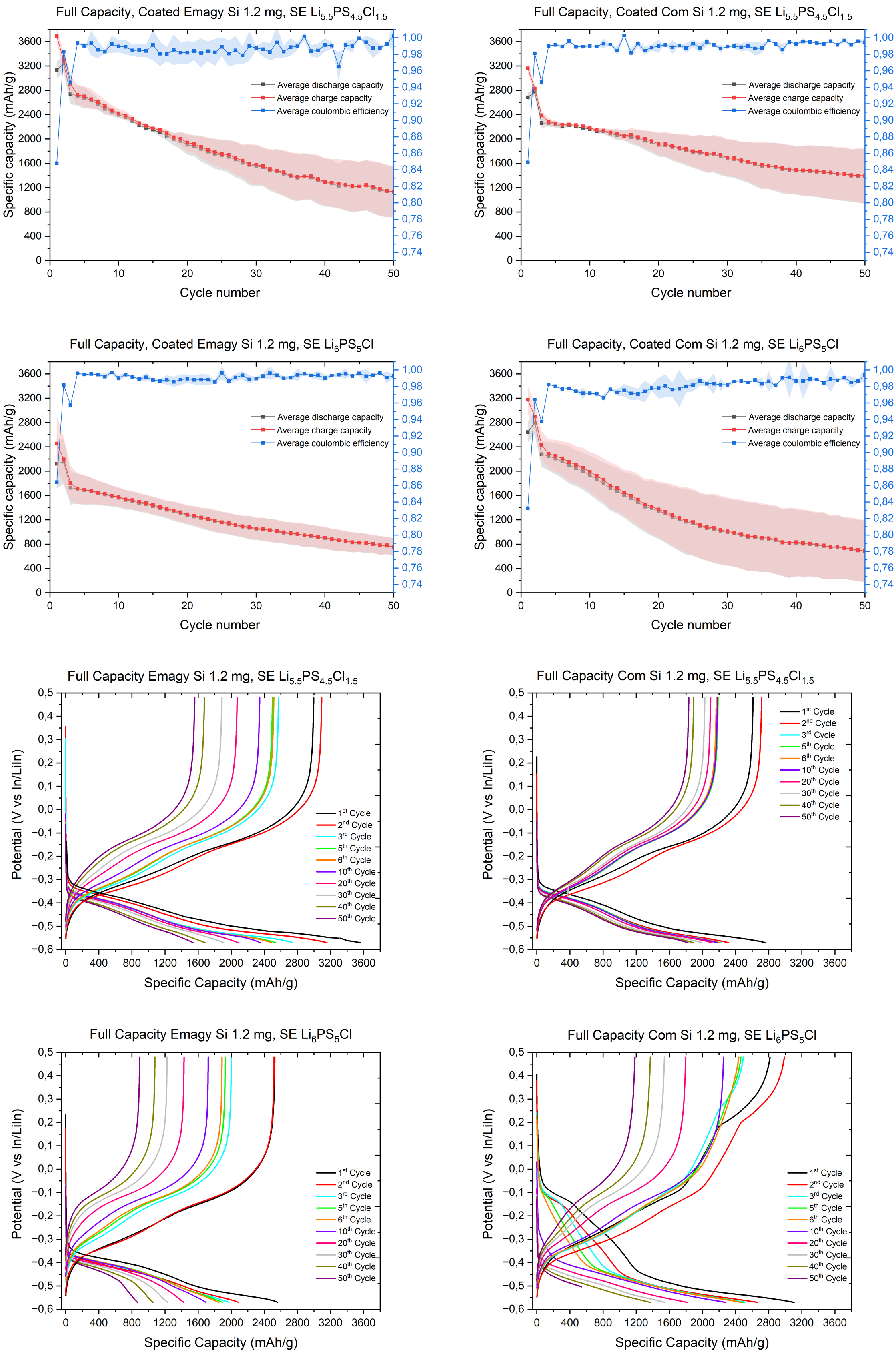

Figure 5.7: The capacity vs cycle number vs coulombic efficiency graphs are shown at the top and the potential vs capacity graphs at the bottom. A comparison is made between E-magy and Com Si and a comparison is made between $Li_{5},{}_{5}PS_{4},{}_{5}Cl_{1},{}_{5}$ and Li_6PS_5Cl.

5.8. limited capacities effect on the life time of the cell

The results so far show that both the Com and E-magy silicon can not reach a sufficient life span because of too much capacity loss when trying to use a capacity of 3000 mAh/g. For the E-magy material this could be explained by the the nanopores being destroyed after the first cycle since the expansion of the material is to much for the pores to take. A application note was shared by the E-magy company at this time, explaining that for the liquid batteries they used to test the material, they also limited the capacity between 1000 and 2000 mAh/g of silicon. This is done to preserve the crystalline backbone to maintain the mechanical integrity of the particles [77]. If charging the silicon fully destroys the pores in the material it makes sense the pores won't be able to fulfill there function anymore and that constant formation of the SEI layer due to it continuously cracking every cycle will continue. To test this, it was decided to try to cycle the E-magy material to limited capacities to see which effect this will have on the capacity fading and the overall battery cycling. To test this 6 new identical cells were made all with 1.2 mg of silicon material just like in all the previous tests. But now we want to charge these cells up to only a part of there maximum capacity to try if this preserves the material structure and therefore decreases the capacity fading.

Before in all tests a certain current was chosen so the batteries would reach a capacity of 3000 mAh/g with a certain C-rate. Now we will test how the batteries perform for 1000, 1500 and 2000 mAh/g. The same current is applied on all batteries to be able to make a fair comparison. The cells have the same current applied to them and they have the same composition, but we don't want to charge all of them to the same capacity, so they will officially have different C-rates. This might seem confusing but it is necessary to make a fair comparison. For example if we want to compare 2 of the same cells charging the material up to 1000 mAh/g and the other to 2000 mAh/g then the same current has to be applied to both of them, but the 1000 mAh/g will of course be be charged and discharged quicker if the same current is applied so the C rate will be twice as large but the current density will be the same.

So the cells are now not only voltage limited, but also time limited to control the capacity with which the silicon is charged. The upper voltage limit is still 0,48 V but the lower voltage limit is now replaced by a time limit chosen with the applied current and C-rates to make sure that the silicon is only lithiated to a point of 1000, 1500 or 2000 mAh/g of silicon. After this time the discharging process starts. These test where later repeated for Com Si too and also with Li6PS5Cl. The parameters of all these tests are summarized in the table below.

Silicon type	Silicon mass	Capacity	Solid Electrolyte	Compositions	Electrode type
E-magy	1.2 mg	1000, 1500, 2000 mAh/g	$Li_{5,5}PS_{4,5}Cl_{1,5}$	1% PVDF	Si deposited on Cu
Commercial	1.2 mg	1000, 1500, 2000 mAh/g	$Li_{5,5}PS_{4,5}Cl_{1,5}$	1% PVDF	Si deposited on Cu
E-magy	1.2 mg	1000, 1500, 2000 mAh/g	Li_6PS_5Cl	1% PVDF	Si deposited on Cu
Commercial	1.2 mg	1000, 1500, 2000 mAh/g	Li_6PS_5Cl	1% PVDF	Si deposited on Cu

The first 2 Cycles have a C rate of 1/20, all other cycles have a C-rate of 1/10
The cycling is time limited to control the amount of capacity that is utilized. There is still a upper voltage limit in place for all batteries at 0,48 (V vs In/LiIn) and for the Li_6PS_5Cl experiments there is also a lower voltage of -0,57 (V vs In/LiIn) in case the potential limit is reached before the time limit

Table 5.8: This table summarizes some of the important parameters of the Si deposited on Cu limited capacities experiment series.

Limited capacity E-magy $Li_{5,5}PS_{4,5}Cl_{1,5}$

The battery cycling results we got from this are shown in figure(5.8) by showcasing the capacity vs cycle number vs coulombic efficiency and by figure(5.9) showing the potential vs capacity graphs again. The images are now shown separately since there are some things to highlight which will be easier when looking at both graph types one by one.

Figure(5.8) shows us the following:

- The charge capacity is constant every cycle for the 1000, 1500 and 2000 mAh/g cells showcased by the flat red line with no colored area around it.

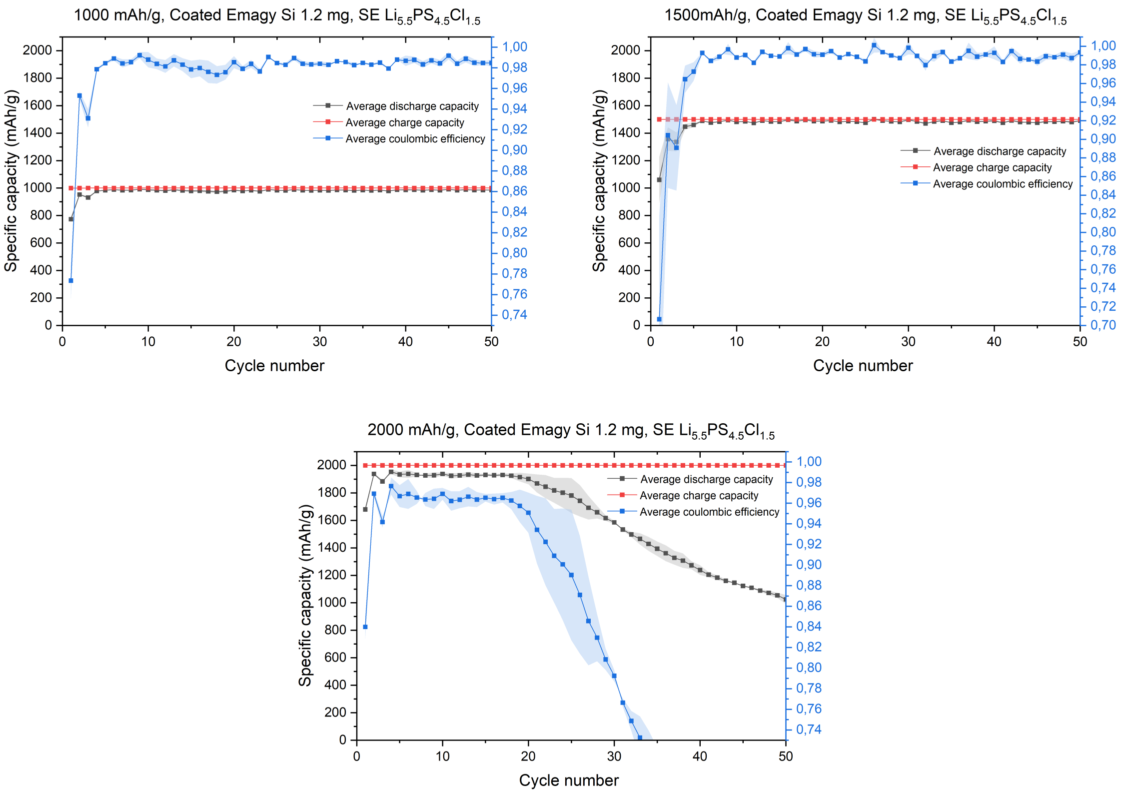

Figure 5.8: Average capacity vs cycle number vs coulombic efficiency graphs of the limited capacity tests with E-magy silicon and $Li_5,_5PS_4,_5Cl_1,_5$ solid electrolyte.

- The 1000 mAh/g batteries showed a first cycle coulombic efficiency of around 78 % which then rises to about 95% for the second cycle, then drops a few percent because of the C-rate increase from 1/20 to 1/10 and then stabilizes to around 98 to 99 %
- The 1500 mAh/g batteries showed the same trend but for one of the batteries showed a lower then expected coulombic efficiency which decreased the average CE in the graph. But if we look at the results form later test series we can see that the CE of the first cycle actually increases when more capacity is used. So the CE of the 1500 mAh/g batteries should lie between the CE of the 1000 and 2000 mAh/g and the lower first and second cycle CE of this one battery can be seen as an outlier.
  After the first cycles the CE stabilizes around 99% for the remaining cycles.
- The 2000 mAh/g batteries CE stabilized to a lower value around 97% until it started to drop after the 20-25th cycle, and this capacity drop kept continuing for the whole duration of the battery cycling process. This behavior was similar for both batteries cycled up to 2000 mAh/g, showing that 2000 mAh/g is still to much for the nano porous material to take and that a value of 1000 or 1500 mAh/g is better suited if the crystalline backbone of the nano porous material has to be preserved.

If we now take a look at figure(5.9) we can see the following from the Potential vs capacity graphs.

- The potential at the top of the graphs is always limited to 0,48 (V vs In/LiIn) as was specified in the cycling program. But the potential that is reached on the bottom right side of the graphs now changes with each cycle. With a higher and higher potential difference being necessary for each cycle to reach the specified capacity. So from only the capacity vs cycle number graph you cant say that the cell is showing no degradation if the capacity is not going down.
- Looking at the first 1000 mAh/g graph we can see that for the first view cycles a voltage of -0,35 is needed to reach the capacity of 1000 mAh/g. This value increases until about -0,5 V at the 20th cycle and then remains -0,5 V for the remainder of the cycling process. Indicating that after the 20th cycle the cell resistance no longer seems to increase, so from this it looks like the battery cycling could have continued stably in this voltage range without the capacity starting to drop.
- The second 1000 mAh/g graph shows a lower negative voltage necessary to reach the capacity for all cycles. But the minimum voltage of the cycles hasn't reached a constant value yet so we can not see if this value will start to remain the same like it did for the first cell after a certain amount of cycles, or that a higher voltage difference will be needed for each following cycle because the resistance in the battery keeps growing.
- For the first 1500 mAh/g battery you can see at the top of the cycling graph that the first cycles capacity is a lot lower then for the other batteries, which is why the average CE in figure(5.8) was so low for the first cycle.
- The voltage needed for charging the Si starts at -0,3 and drops -0,54 V for the first 1500 mAh/g battery but the second battery already needs a voltage of -0,5 which then increases to -0,58 for the 50th cycle. So the second battery starts of with better performance but is less stable.
- The 2000 mAh/g battery already needs a voltage of -0,5 for the first cycle and then the voltage kept getting lower and lower every cycle. Up until a the 30th cycle where the minimum voltage remained around -0,65 but started showing weird sharp spiky behavior at the negative charge potentials, but from the capacity vs cycle number graph (5.8) we can see that the 2000 mAh/g charge potential is still being reached despite this weird behavior.

This spiky behavior at the 2000 mAh/g battery is likely a result of lithium plating and possible dendrite formation. Since no lower potential limit was set in place for these tests the potential of this battery would go as low as -0,62 V vs LiIn which can also be written as 0 V vs Li/Li+. At these low potentials lithium can form as lithium metal on the electrodes instead of alloying into them, which is called lithium plating. And this lithium plating can lead to soft short circuits, which result in voltage irregularities during battery operation. [78]. And theses voltage irregularities can be seen as spiky behavior in the graphs that display the potential.

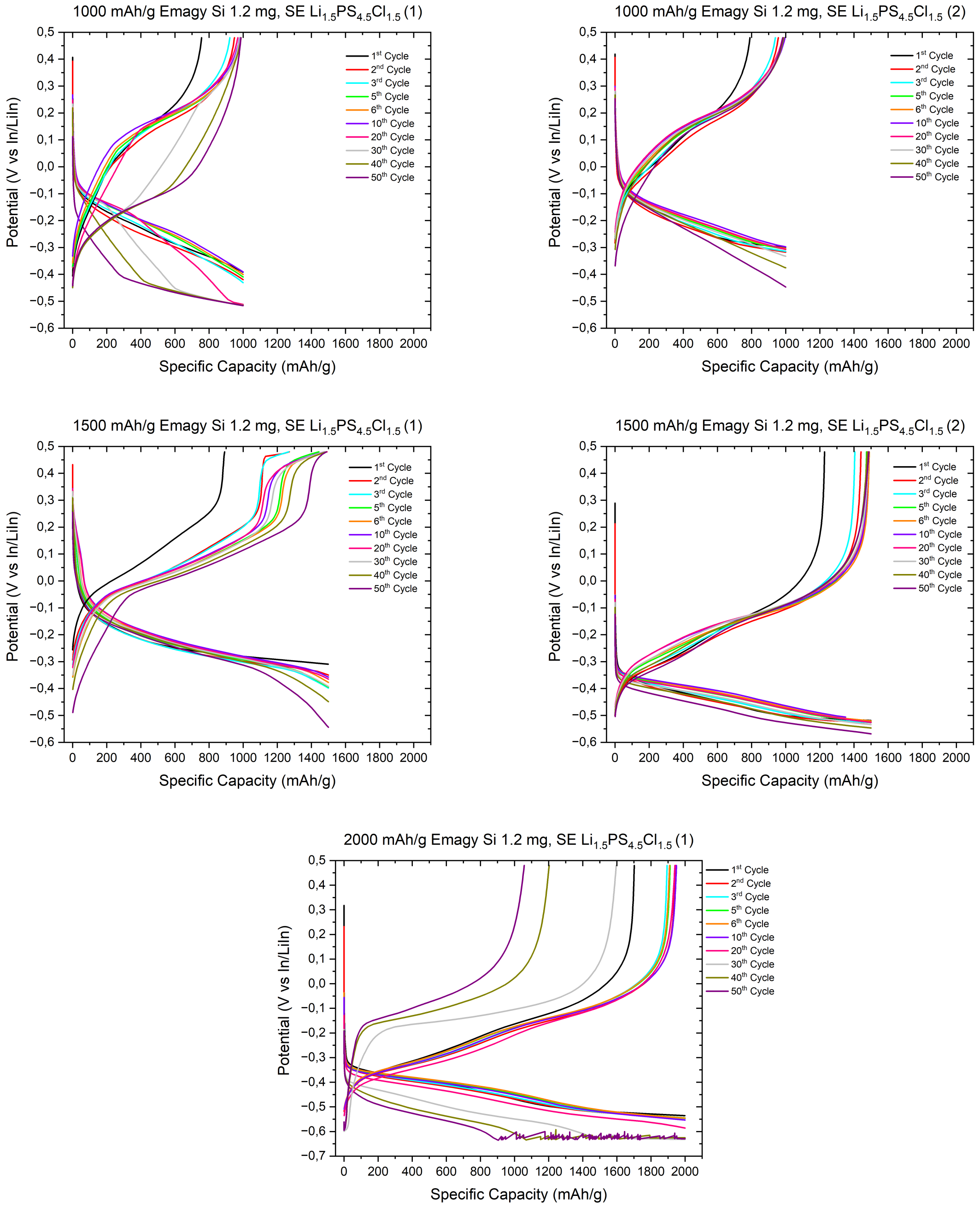

Figure 5.9: Potential vs capacity graphs of the limited capacity tests with E-magy silicon and $\mathrm{Li}_{5,5}\mathrm{PS}_{4,5}\mathrm{Cl}_{1,5}$ solid electrolyte.

Limited Capacity Commercial silicon $Li_{5,5}PS_{4,5}Cl_{1,5}$

From the previous tests we can conclude that a big improvement is seen in the batteries with the E-magy silicon when only part of the capacity is utilized instead of the full capacity of the silicon we where aiming for before. To see if the E-magy material now finally shows improvements compared to the Com Si we will need to do the same set of test with the Com Si. The results of these test can be seen in figure(5.10) and figure(5.11). The capacity vs cycle number graphs of the batteries are now displayed individually without taking the average since there was a lot of variation in the results so taking an average would make the graph less clear.

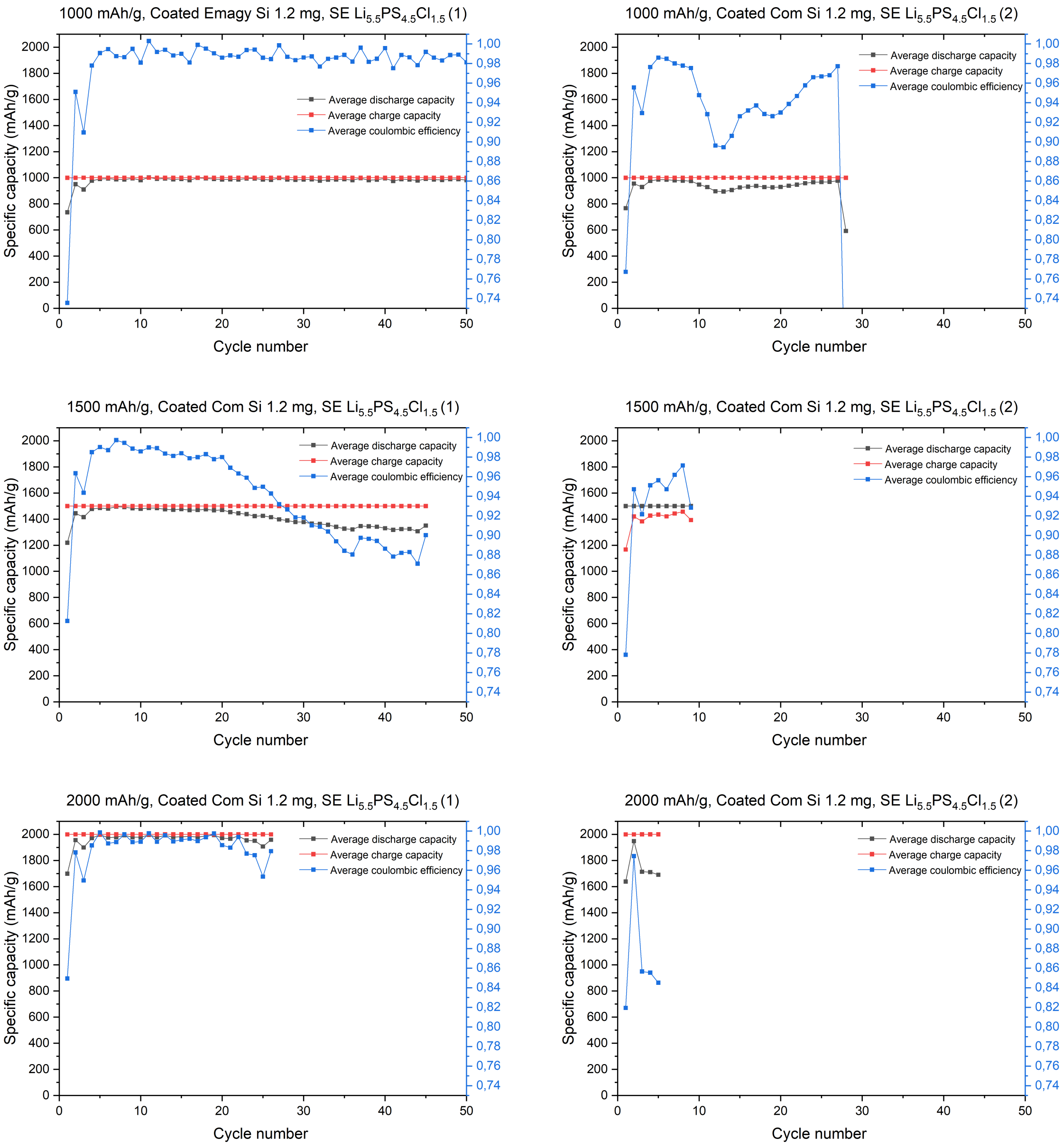

Figure 5.10: Average capacity vs cycle number vs coulombic efficiency graphs of the limited capacity tests with Com silicon and $Li_{5,5}PS_{4,5}Cl_{1,5}$ solid electrolyte.

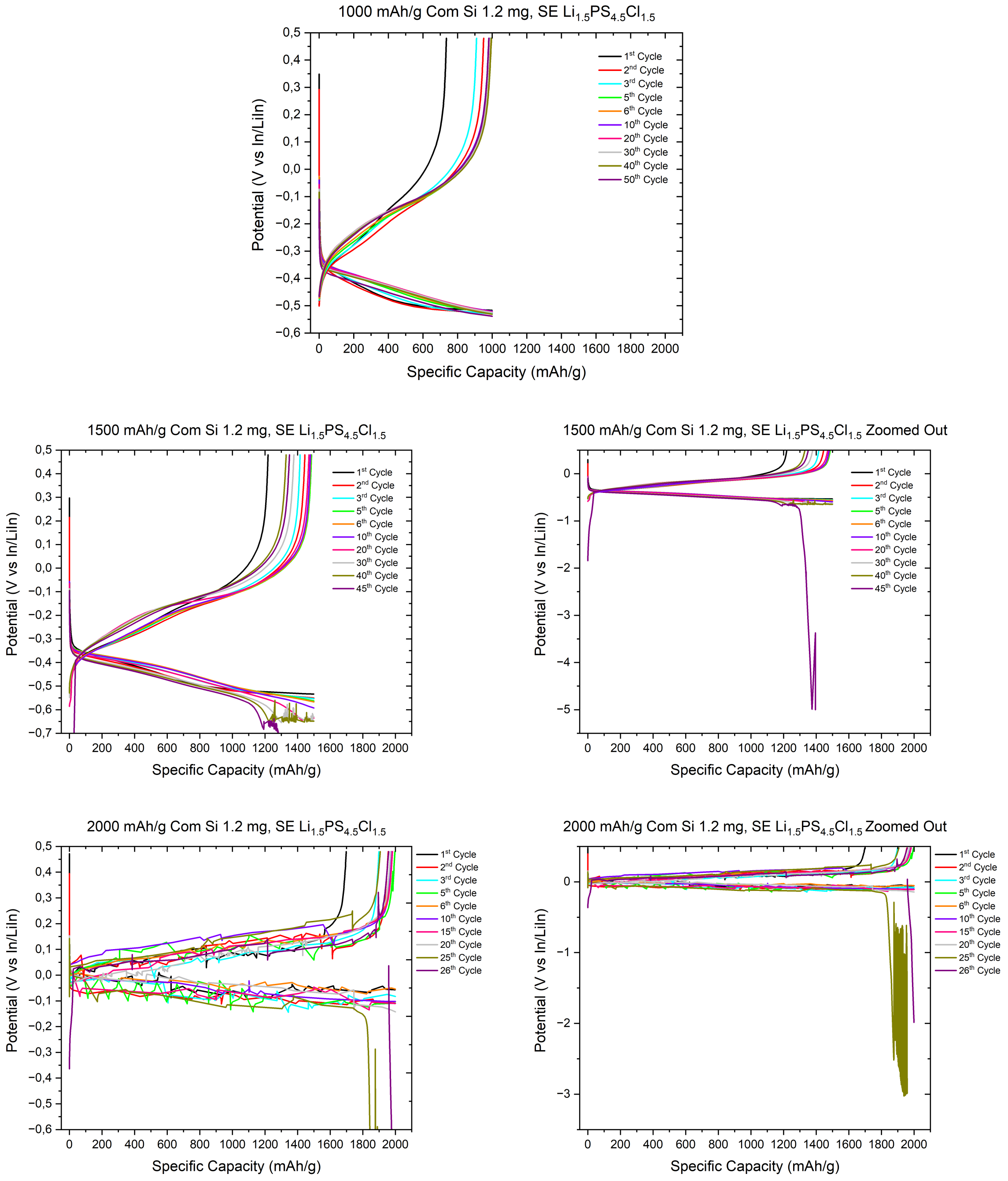

Figure 5.11: Potential vs capacity graphs of the limited capacity tests with Com silicon and $Li_{5,5}PS_{4,5}Cl_{1,5}$ solid electrolyte.

The capacity vs cycle number vs coulombic efficiency in figure(5.10) and the potential vs capacity in figure(5.11) show us the following:

- The charging of the silicon material is now only still limited by a time constraint, and if the resistance in the cell gets higher and higher, this results in a higher voltage difference as a result of the applied current. But with a lot of the cells using the com Si having to high of a resistance the voltage is increasingly being forced more negative until the Maccor battery cycler just cuts of the cycling process. Because these voltages cant be reached anymore or are deemed unsafe. This voltage drop is shown in the 1500 mAh/g and 2000 mAh/g batteries in figure(5.11), the images on the right show a more zoomed out picture then the ones on the left. As you can see the batteries experience a very low voltage value after 45 cycles for the 1500 mAh/g example and the 25th cycle after 2000 mAh/g. This then causes the machine to stop the experiment, but we can still see the behavior before the battery was stopped and how long it takes for it to be stopped still gives us insight into the battery performance.
- The first 1000 mAh/g battery shows stable battery cycling process with a coulombic efficiency around 98/99%. The potential graph also shows that the potential difference is slightly increasing but almost entirely stable remaining only going from -0,5 to -0,53 over the span of 50 cycles.
- The other 1000 mAh/g battery however showed large drops in CE which led up to the battery getting stopped after 28 cycles due to the reasons explained above
- The first 1500 mAh/g batteries showed relatively stable cycling with a CE of around 98% which started to drop after the 20th cycle and finally stopping the battery after 45 cycles. While the capacity of the battery started to drop the the other 1500 mAh/g did not reach a stable CE and already stopped working after 10 cycles. From the potential graph it can be seen that the weird spiky behavior of the potential can be seen again after the 20th cycle, so when the capacity stats to drop, just as it was seen when the potential of the 2000 mAh/g E-magy $Li_{5,5}PS_{4,5}Cl_{1,5}$ started to drop. Like discussed before this is likely a result of lithium plating which is caused by these low potentials being reached when no minimum potential limit is set.
- One of the 2000 mAh/g batteries actually had quite a stable CE of around 99% for the first 20 cycles but then the test was stopped due to the voltage dropping to low. The other battery was unstable form the start causing the capacity to drop after the second cycle and the cycling being stopped after only 5 cycles. The potential curve of the first battery showed very strange behavior with the whole curve being spiky and not just the cycles where the discharge capacities starts to drop. We cant really explain this behavior by the lithium plating since the spiky behavior already occurs before low potentials have ever been reached.
- Something we can see if we compare the CE of the first battery cycle is that this value goes up with increasing the amount of capacity, this behavior was also seen for the E-magy material of the previous tests.

So if we compare the performance of these Com Si batteries with the limited capacity E-magy Si batteries we can see that the E-magy material improves the cycling stability and reduces the capacity loss. But Si remains a tricky material to work with, still giving some variation in batteries with the same composition where you would hope that they would all show the same behavior. So the claim of the E-magy material improving the cycling stability over the commercial silicon is still not that strong. Therefore we are now gonna repeat the past experiments, but with Li_6PS_5Cl instead of $Li_{5,5}PS_{4,5}Cl_{1,5}$ as the SE. This will give us more information about the performance of E-magy vs Com Si and it will showcase the effect that these different solid electrolytes have on the battery cycling.

Limited capacity E-magy Si Li_6PS_5Cl

The same limited capacity tests as before are now repeated with Li_6PS_5Cl instead of the previously used $Li_{5,5}PS_{4,5}Cl_{1,5}$. An additional voltage limit for the negative potentials is now in place as backup in case the voltage limits get reached before the time limit is completed. This will prevent the battery cycling to suddenly stop when to low potential levels are being reached like in the Limited capacity Si Com $Li_{5,5}PS_{4,5}Cl_{1,5}$ experiment. This should also prevent the spiking behavior of the potential caused by lithium plating at low potentials.

The capacity vs cycle number vs coulombic efficiency and the potential vs capacity graphs are both shown together in figure(5.12). The graphs show us the following:

- One of the 1000 mAh/g showed very stable cycling with a a coulombic efficiency around 99% from the 4th cycle onward. The potential difference to reach this capacity was also very constant with a minimum voltage of -0,53 to -0,5 showcasing very stable cycling
- the other 1000 mAh/g battery intimidatingly started losing capacity since the voltage limits now causes the cell to switch charging and discharging before the full capacity is reached if the voltage gets to low. And this capacity kept decreasing during the cycling showcasing ongoing battery degradation.
- The 1500 mAh/g batteries showed a coulombic efficiency of around 99 % too, but started to lose capacity around 25 to 30 cycles since the voltage limit of -0,57 V is reached. The minimum potential started just like the 1000 mAh/g cell at -0,5 V but then did not remain stable like the 1000 mAh/g cell did.
- The 2000 mAh/g cells showed a lower coulombic efficiency of 97-98% and the capacity fade started for one cell at the 13th cycle and for the other on at the 20th cycle due too the voltage limit being reached. Again the first cycle minimum potential was -0,5 V, so the cell resistance increases even more now which was to be expected.

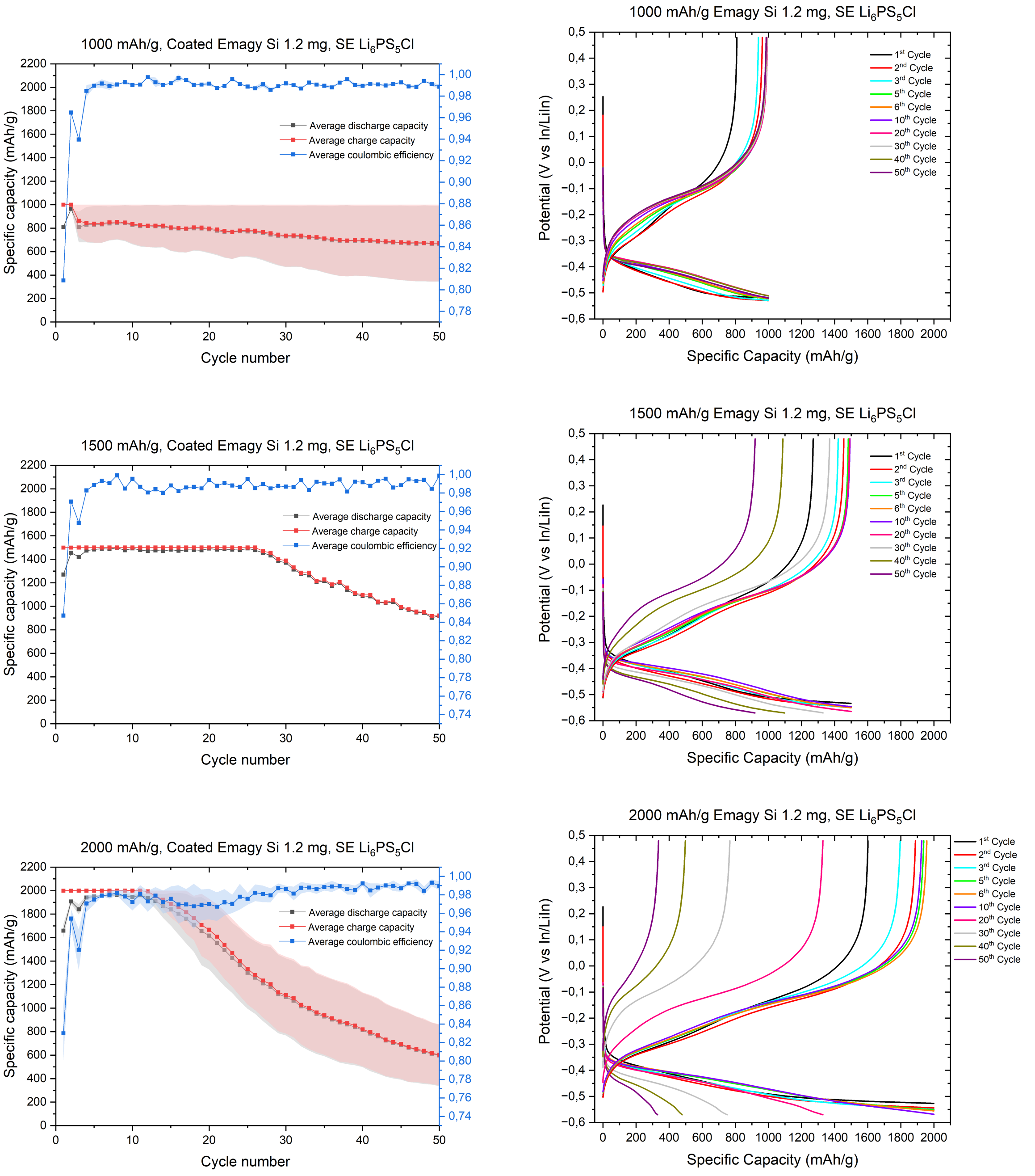

Figure 5.12: Average capacity vs cycle number vs coulombic efficiency graphs of the limited capacity tests with E-magy silicon and $Li_{5,5}PS_{4,5}Cl_{1,5}$ solid electrolyte on the left and potential vs capacity graphs of the better of the two performing batteries on the the right.

Limited capacity Com Si Li_6PS_5Cl
The final test series now repeats the previous experiment but with Com Si instead of the E-magy Si. Again both the capacity vs cycle number vs coulombic efficiency and the potential vs capacity graphs are shown together in figure(5.13) on the next page. From the graphs we can see the following:

- The 1000 mAh/g performance is similar to the E-magy Li_6PS_5Cl test, with the coulombic efficiency being around 99% for the entire cycling duration. And the minimum voltage of the potential curve starting at -0,51 and slowly dropping to -0,55.
- One of the 1500 mAh/g batteries started losing capacity already after the 4th cycle and the other battery followed after 14 cycles. So one battery starts losing a little slower then the other one but the rate at which both batteries lose capacity is almost the same.
- For the the last 2000 mAh/g battery the minimum voltage value of -0,57 was already reached at the third cycle dropping the capacity quickly from that point onward.

Conclusion limited capacity cycling
There is definitely still a lot of variation in performance regarding the battery cycling results from the limited capacity Si on Cu deposited batteries. But looking at the overall results and the trends, we can see an improvement of the battery cycling capacity retention when using the Si E-magy material over the Com Si and using $Li_{5,5}PS_{4,5}Cl_{1,5}$ over Li_6PS_5Cl.

For the 1000 mAh/g batteries, all test series, so E-magy and Com Si and both $Li_{5,5}PS_{4,5}Cl_{1,5}$ and Li_6PS_5Cl had a battery that kept a high discharge capacity for the full 50 cycles with coulombic efficiencies around 99% and the minimum voltage staying stable and not decreasing a lot during the cycling process. But the E-magy Si $Li_{5,5}PS_{4,5}Cl_{1,5}$ batteries where the only ones where a less negative voltage was measured and where no drop of the capacity occurred for both of them.

For the 1500 mAh/g batteries the E-magy Si $Li_{5,5}PS_{4,5}Cl_{1,5}$ where the only batteries that showed no discharge capacity drop, a stable coulombic efficiency of 99% and a minimum voltage value that did not drop quickly. All the other 1500 mAh/g batteries started to reduce in capacity or shut down the measurement because the negative voltage value got to large, or in other words the potential got to low.

For the 2000 mAh/g batteries none of the batteries where able to maintain the 2000 mAh/g capacity and showed lower coulombic efficiencies and quick capacity fade.

When comparing the SE's we can see how using $Li_{5,5}PS_{4,5}Cl_{1,5}$ instead of Li_6PS_5Cl makes the batteries require less of a potential difference to reach the same capacities. Which resulted in less capacity loss and more stable cycling. This highlights the importance of using a high ionic conductivity in Si solid stat batteries.

So this shows us that the nanopores in Si can improve the battery cycling behavior for Si on Cu deposited electrodes as long as the utilized capacity of the silicon is limited to 1000-1500 mAh/g. And it also shows us the importance of a high conductivity solid electrolyte for good battery cycling performance.

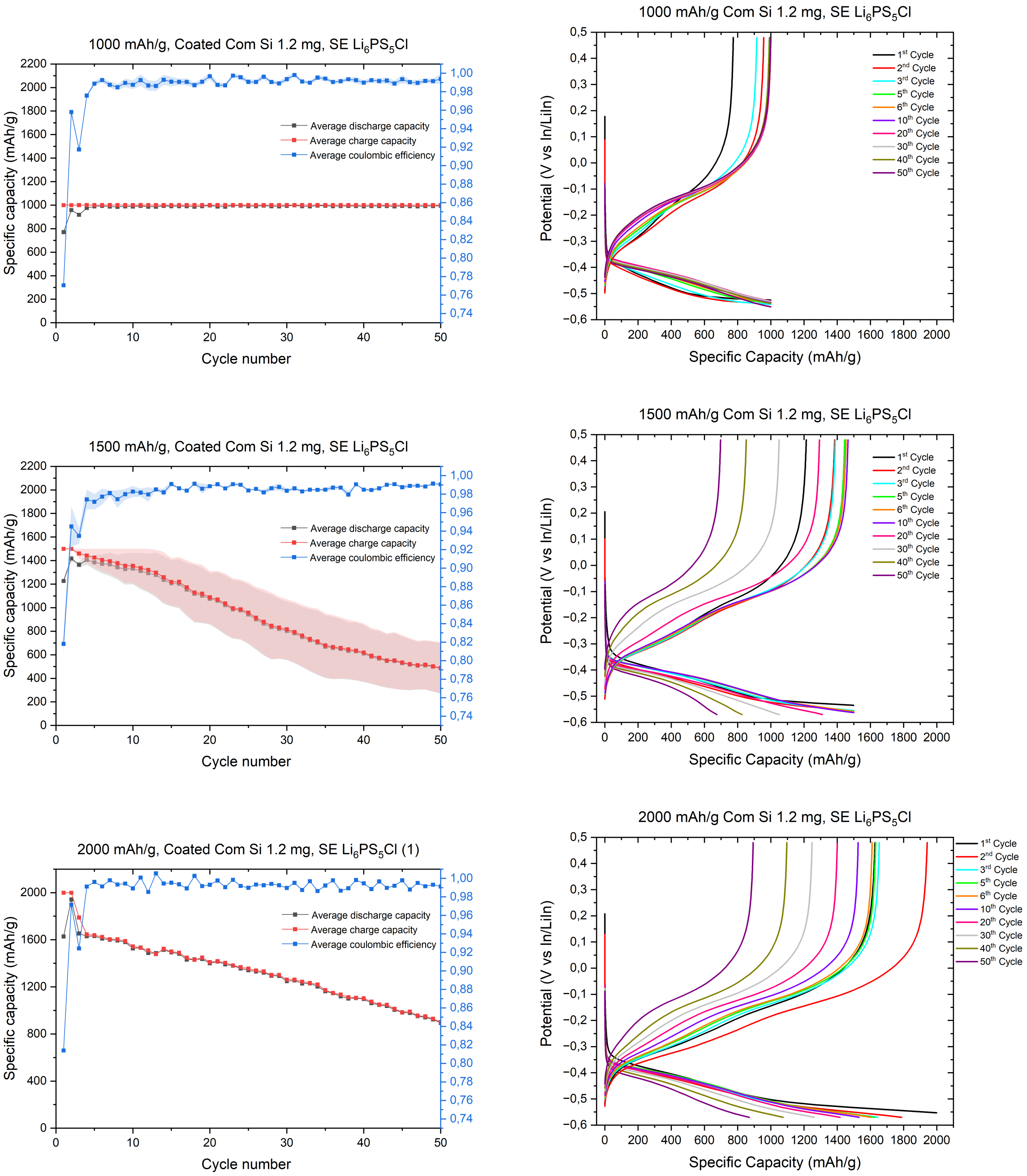

Figure 5.13: Average capacity vs cycle number vs coulombic efficiency graphs of the limited capacity tests with Com silicon and $\text{Li}_{5,5}\text{PS}_{4,5}\text{Cl}_{1,5}$ solid electrolyte on the left and potential vs capacity graphs of the better of the two performing batteries on the the right.

5.9. Impedance limited capacity cycling Si deposited on Cu batteries

EIS measurements of all the limited capacity cycling batteries where done before and after the batteries have been cycled. So this can give us information about how the different SE's, silicon types and amount of lithiation of the Si will influence EIS spectra before and after cycling.

5.9.1. Impedance before Cycling

Lets first take a look at the EIS Nyquist plots we get from doing the measurements before any cycling has taken place in figure(5.15). The measured data is displayed with symbols and the fitted data is displayed with lines, the line colors from the fitted data are the same as the symbol color the fitted data belongs too, how the data was fitted will be explained below. It is important to realize that this measurement took place before the cycling so the only differences are the SE and the Si type since there is no difference in amount of capacity used yet, since no Si has been lithiated at all yet in fresh new battery cells. So the Nyquist plots here should ideally look the same for all batteries that are made up of the same composition.

equivalent circuit before cycling

All the Nyquist plots have the same general shape. First we can see a small step to the right cause by the solid electrolyte resistance as discussed in the section where the solid electrolyte ionic conductivity was determined(4.8). Then you can see the lines going up in a curvature indicating a semicircle, and then at the higher Z' and Z" values at the lower frequencies an other very large semi circle is being formed, the first semicircle can be a bit difficult to distinguish in some of the plots since the second semi circle overlaps with it, and the second one is a lot larger so seems to overpower the first one sometimes.

The bulk solid electrolyte resistance that results in the shift to the right of the spectra can easily be fitted by using a resistor in the circuit. From this resistors value we can easily distinguish between the cells using $Li_{5,5}PS_{4,5}Cl_{1,5}$ and Li_6PS_5Cl. Then a semicircle is being formed which could be modeled using a resistor and a capacitor in parallel. This however models a ideal semicircle with ideal capacitive behavior. If we use a resistor with a constant phase element (CPE) instead of a ideal capacitor we better capture the non-ideal electrochemical behavior that is a result from rough surfaces and non uniformity of the electrode and SE interface [68] [69]. So the semicircle is modeled by a resistor modeling the charge transfer resistance between two interfaces and a CPE modeling the non-ideal double layer capacitance at this same interface, both elements are in parallel. These same combination of circuit elements in parallel is used to model the second semi circle at higher Z' and Z" values (so at lower frequencies).

We attribute the first semicircle at higher frequencies to the charge transfer resistance and non ideal double layer capacitance at the Si/SE interface and the larger semi circle at the lower frequencies to the electrochemical behavior at the SE/LiIn interface. The reason for this is that before cycling the Si/SE typically has faster reaction kinetics and better contact with the SE then the LiIn alloy before any formation cycles have taken place. How this changes after the battery has gone through multiple cycles is discussed in the impedance after cycling section(5.9.2).

This gives us the the following equivalent circuit for fitting the impedance data before the cycling has taken place, which is displayed in figure(5.14)

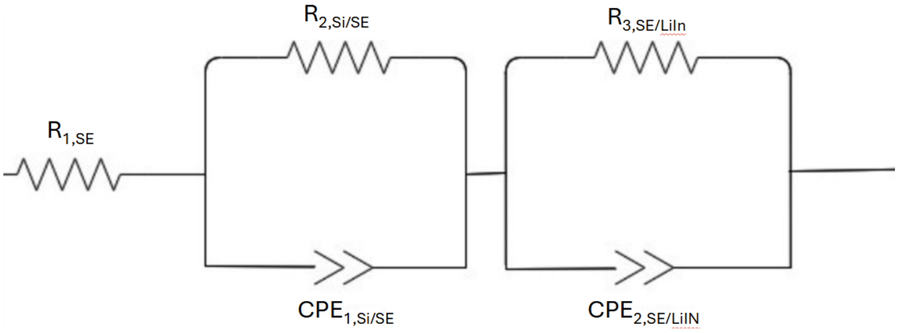

Figure 5.14: Equivalent circuit used for fitting the Impedance data before cycling of the limited capacity Si deposited on Cu test. The circuit consists of a resistor followed by a resistor and CPE in parallel followed by another resistor and CPE in parallel.

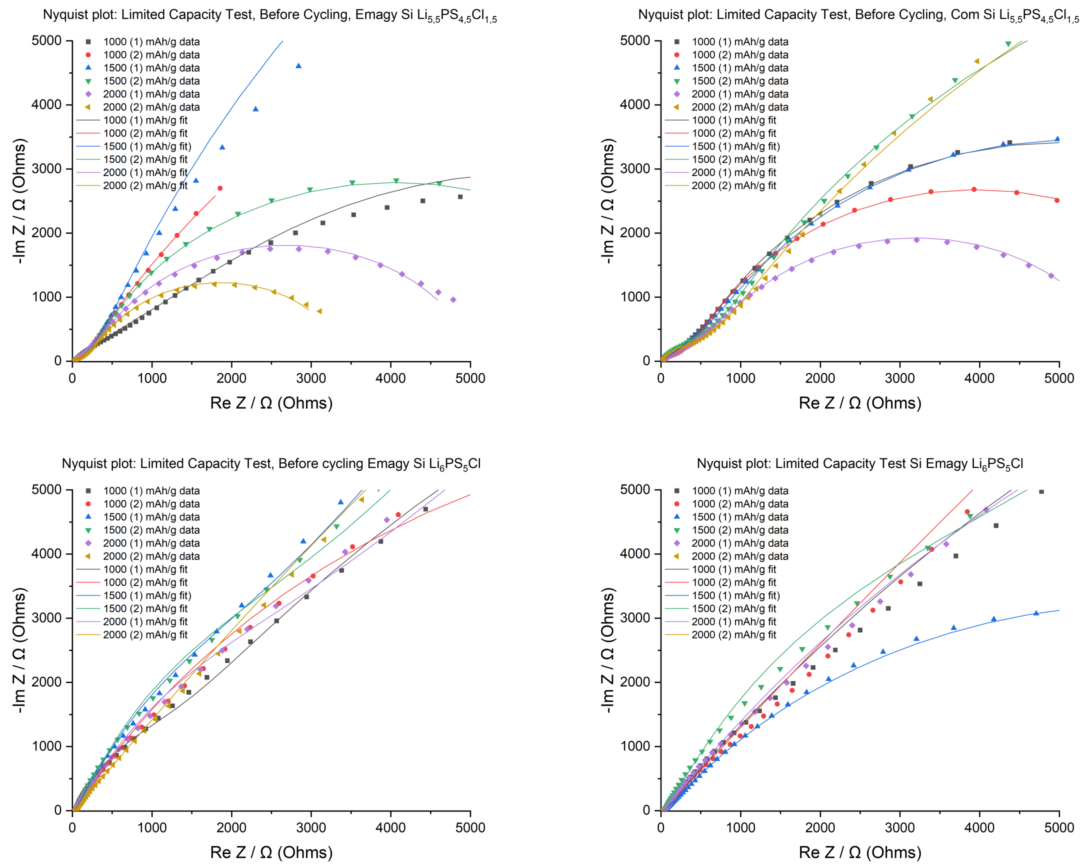

Figure 5.15: The Nyquist plots showcasing the real vs the imaginary impedance of the limited capacity test batteries before they have been cycled, the legend already says which battery will be cycled to a certain capacity in the future to compare them easier to the impedance graph from the batteries after cycling.

Take away from the plots and fitted data before cycling

If we take a look at the the Nyquist plots and the values of the circuit elements the data is fitted to we can see the following:

- The R1 value accounting for the solid electrolyte conductivity is easily distinguishable between the batteries using $Li_{5,5}PS_{4,5}Cl_{1,5}$ and the batteries using Li_6PS_5Cl. With the former showing values of 13-15 for R1 and the lather values of 25-35. This was expected with the respective ionic conductivity of the materials being 7,7 and 2,9 mS/cm.
- The R2 value attributed to the resistance from the Si/SE ($Li_{5,5}PS_{4,5}Cl_{1,5}$) interface has a average value 2,9E+2 for the E-magy Si and a average value of 6,8E+2 for the Com Si. Which could point to the E-magy Si making better contact with the SE then the Com Si before the cycling has started. For both the E-magy and Com Si, most of the batteries using Li_6PS_5Cl showed R2 values of 7E2 to 1,2E3 not really depending on the Si type. So this gives some indication that the E-magy Si and $Li_{5,5}PS_{4,5}Cl_{1,5}$ improve the contact between the SE and Si surfaces.
- The R3 values regarding the SE/LiIn interface for the batteries using $Li_{5,5}PS_{4,5}Cl_{1,5}$ showed values of E3 and E4, while the batteries using Li_6PS_5Cl showed values in the range of E4 and E5. You can also see this from the Nyquist plots where the top graphs showing batteries using $Li_{5,5}PS_{4,5}Cl_{1,5}$ show a lot smaller semi-circles then the bottom Nyquist plots. This shows that using $Li_{5,5}PS_{4,5}Cl_{1,5}$ seems to lower the charge transfer resistance at the SE/LiIn interface before cycling.
- The α value of the CPE of the second semi-circle showed average values of α=7,9 for the $Li_{5,5}PS_{4,5}Cl_{1,5}$ batteries while the Li_6PS_5Cl batteries had a average of α=6,48. Showing closer to ideal capacitive behavior for the $Li_{5,5}PS_{4,5}Cl_{1,5}$ batteries likely caused by less surface roughness and irregularities.

So the $Li_{5,5}PS_{4,5}Cl_{1,5}$ seems to slightly reduce the the charge transfer resistances at the Si/SE interface and greatly reduce it at the LiIn/SE interface. And a slight reduction of the resistance at the Si/SE interface when E-magy Si is used over Com Si was seen.

5.9.2. Impedance after cycling

The impedance including both the measured data and the fitted data from a new equivalent circuit are shown in figure(5.17). Again the measured data is displayed with symbols and the fitted data is displayed with lines, the line colors from the fitted data are the same as the symbol color the fitted data belongs too. Now after cycling, the data of the same battery compositions that have been limited to different capacities of 1000, 1500 and 2000 mAh/g is present. So it will be interesting to see if we can see a difference for the impedance based on the amount of Si capacity used.

equivalent circuit after cycling

The equivalent circuit that best fits the data has changed compared to the circuit that was used before. We still see the shift of the spectrum to the right as a result of the resistance of the solid electrolyte, which can be modeled by a simple resistor. Then we can see that the first semi-circle looks more well defined and shifted to the left of the Nyquist plot and the very large semicircle from the batteries before cycling has been replaced by a straight diagonal line.

The new straight line at the low frequency region can be ascribed to the diffusion of Li+ions [39] now being more limiting then the large semi circle at the SE/LiIn interface that was shown at these frequencies before. But why do we now only have one semi circle you might think? Since even SEI is formed which gives new interfaces and these interfaces have there own charge transfer resistance and double layer capacitance just like the Si/SE and SE/LiIn interfaces had in the batteries before they went through the cycling process. So these new interfaces could have shown up as more semi-circles in the Nyquist plot. So this would give a equivalent circuit of a resistor, modeling the SE bulk resistance, followed by 4 times a resistor in parallel with CPE, modeling the charge transfer resistance and double layer capacitance of the interfaces and then end with a Warburg (W) element to model the resistance caused by diffusion. Such a circuit is also used by [79] for Si/SE/Li coin cells.

But in our Nyquist plots we don't see more semi-circles appear, we actually only see one semi-circle left. The large semi circle at low frequencies has likely disappeared or decreased in size and shifted to the left since the lithium alloying with the indium through the multiple battery cycles reduces the SE/LiIn charge transfer resistance [62] and improves the reaction kinetics at that interface. The reason that the other processes only show up as one semicircle is because they play a role in the same frequency region, and are overpowered by the impedance of only one interface making them appear as only one semi-circle [69]. An other point to note is that a Warburg element can be seen as a 45 degree diagonal line in the Nyquist plot, while in the plots we have the straight lines don't all follow this 45 degrees. This is because a Warburg element models ideal diffusion which is more suitable for liquid electrolytes, but in solid electrolytes it will be better to use a CPE element since this accounts for non-ideal behavior like inhomogeneities, interface roughness and defects in the solid electrolyte.

[80] and [69] both showed that for lithium-ion battery half cells after cycling often 2 semi circles can be distinguished with one containing the resistance and capacitance caused by the SEI and the other resulting from the charge transfer resistance and double layer capacitance of electrode/SE surfaces. We however can only distinguish one semi-circle which will make it difficult to treat these processes separately.

Taking all of this into account, the equivalent circuit that gave the best fit results for the data is shown in figure(5.16) below. The circuit consists of a resistor modeling the ionic resistance of the SE, then a resistor and CPE in parallel representing the resistance from the SEI, the charge transfer resistance, and double layer capacitance of all interfaces, and at the end a CPE representing the Li-ion diffusion.

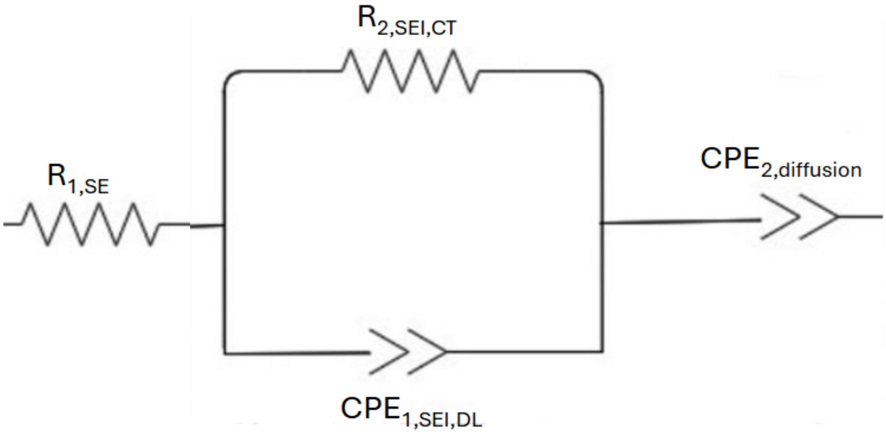

Figure 5.16: The Nyquist plots showcasing the real vs imaginary impedance of the limited capacity test batteries after they have been cycled. The circuit consists of a resistor followed by a resistor and a CPE in parallel and is then followed by another CPE.

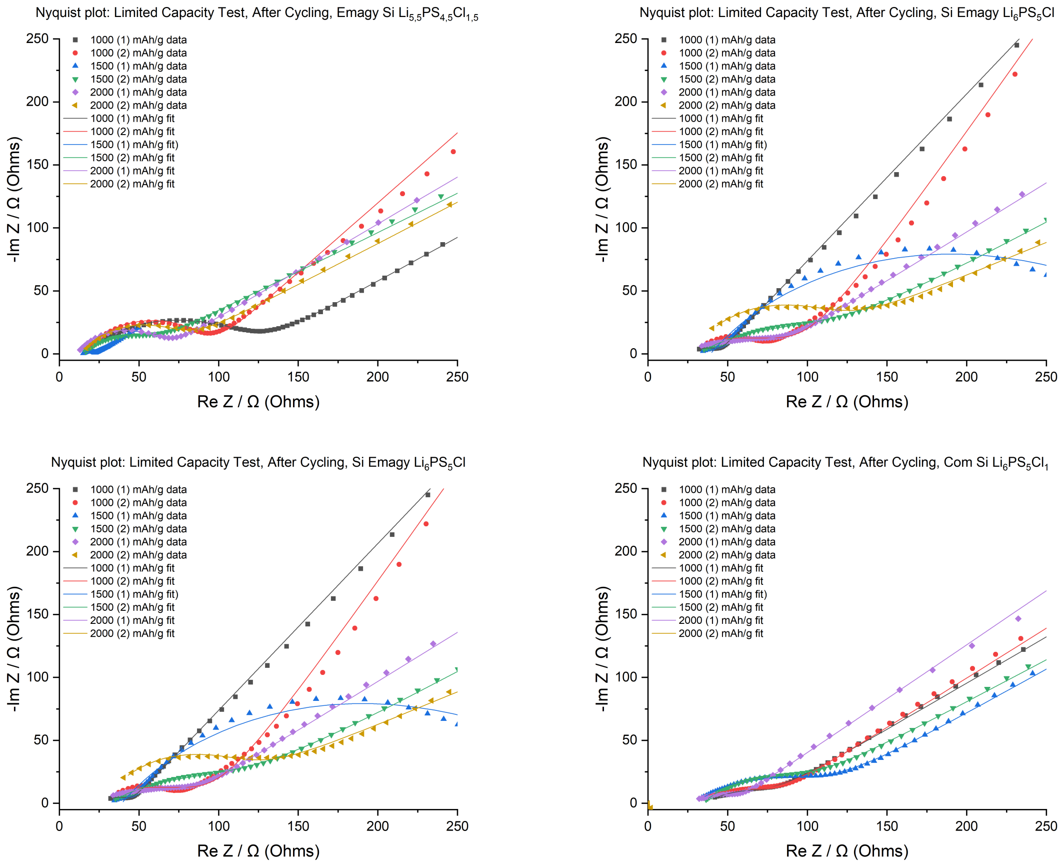

Figure 5.17: The Nyquist plots showcasing the real vs the imaginary impedance of the limited capacity test batteries before they have been cycled.

Take away from the plots and fitted data after cycling

If we now take a look at the Nyquist plots and the values attributed to the components of the equivalent circuit we can see the following:

- The R1 values representing the ionic-conductivity of the SE have not really changed compared to the values from before the cycling. The R1 value of the Li_6PS_5Cl batteries is still about 2,5 times higher as the R1 value from the $Li_{5,5}PS_{4,5}Cl_{1,5}$ batteries.
- From the R2 value we cant really see a difference between the different amounts of capacity used, different SE's and the different Si types. But we can see something interesting for the Com Si $Li_{5,5}PS_{4,5}Cl_{1,5}$ batteries with Si capacity limits of 1500 and 2000 mAh/g. These batteries had very low R values of around 4-7 while the other batteries showed R2 values of 40 to 80. In these low R2 batteries no minimum voltage value was set yet, so they reached lower potentials then the other batteries before the battery cycling procedure was stopped by the Maccor machine. Like discussed before, these low potentials can cause lithium plating to occur and promotes dendrite formation. This was also seen by the spiky behavior in the potential vs capacity plots of section(5.8.0.2). This lithium loss and dendrite formation which could lead to short circuit is of course not good for the health of the battery. But from these lowered R2 values it does reduce the impedance of the interfaces it is formed on. If there would be full dendrite formation between the 2 electrodes the cell would be short circuited and the Impedance would get really small since there is nothing impeding (or blocking) the current anymore.
- from the other circuit elements there couldn't be made a clear distinction between the different values we got for the different capacities, SE's and Si types.

We only have 2 sets of impedance data, one set before the batteries where cycled and one set after the cycling process was completed for 50 cycles. There is a large difference in impedance between these sets since no formation cycles has taken place for the batteries before cycling yet. This resulted in 2 very different sets of impedance data and Nyquist plots which made it difficult to compare the results. In hind-side it would have been more interesting to first let the batteries go through at least 1 formation cycle so all the interfaces in the battery can form and all process can be started. And then cycle the batteries further, and after for example 5 or 10 cycles do an other impedance measurement. If this process is repeated multiple times we could see how the impedance data evolves from cycle to cycle. This could also let us distinguish better between the multiple semi-circles of for example the SEI and the charge transfer after cycling, since now these behaviors had to be captured by one semi-circle(consisting of only 2 circuit elements) which makes it hard to separately discuss what causes the impedance in the battery.

6

Conclusion

6.1. Closing Remarks

A detailed overview of the theory regarding solid state batteries, argyrodite solid electrolytes and the potential and challenges of using silicon in solid state batters was discussed in the the theory chapter. Then research questions where formulated that help us in making a contribution to this theory. Which was followed by the methodology where is explained how this theory is used together with lab equipment to design a set of experiments. And then the results of these experiments where shown. It is now time to see what was learned from these results and to answer the earlier formulated research questions.

6.2. Research Questions

Sub questions where formulated to help answer the main research question, so we will now answer these sub questions first, before answering the main research question.

Research Question 2, Sub-question

Can the use of $Li_{5,5}PS_{4,5}Cl_{1,5}$ help to improve the battery performance when compared to Li_6PS_5Cl in solid state batteries using silicon?

$Li_{5,5}PS_{4,5}Cl_{1,5}$ and Li_6PS_5Cl where synthesized with respective ionic conductivities of 7,5 and 2,9 mS/cm. For Si on Cu deposited electrodes a clear improvement of the battery cycling performance was seen with higher initial capacities being reached and slower capacity fading when $Li_{5,5}PS_{4,5}Cl_{1,5}$ was used. For the limited Si capacity tests the potential differences required to reach targeted capacities where a lot more stable stable throughout the cycling process indicating less battery degradation and resistance growth. The impedance before the battery cycling resulting from the interfaces of the SE with the Si and LiIn electrodes was also shown to be reduced when $Li_{5,5}PS_{4,5}Cl_{1,5}$ was used.

Research Question 3, Sub-question

Will the addition of $Li_{5,5}PS_{4,5}Cl_{1,5}$ and CNF as additives to the powder silicon composite electrode improve the battery cycling results and what composition performs the best?

Multiple compositions of Si/SE/CNF composite powder mixed electrodes where made. Out of the 5/4/1 6/3/1 7/2/1 and 8/1/1 compositions, the 6/3/1 mixed by hand grinding, with 1,2 mg non nanoporous Si, lead to the highest initial capacity of 2410 mAh/g at a current density of 0,229 mA/cm^2. With a capacity retention of 73% from 1680 mAh/g to 1230 mAh/g over 45 cycles at a current density of 0,458 mA/cm^2. The 6/3/1 composition performing the best shows the importance of adding sufficient amount of ionic conductive additive to this type of powder electrode mixture. For some batteries the CNF was also left out of the composition resulting in almost the same but slightly worse battery performance, indicating that adding a carbon electronic conductive additive to this type of electrode mixture is not necessary and could even be hurting the performance.

Research Question 4, Sub-question

How does the battery performance change when silicon deposited on Cu electrodes is used instead of the Si/SE/CNF dry powder mixture electrode?

The battery performance of the Si deposited on Cu electrodes using 1% PVDF binder was shown to give an improvement for the initial capacities, the capacity retention and also for the consistency of the batteries that used Si deposited on Cu electrodes instead the Si/SE/CNF dry power mixture electrodes. The best battery performance was gained with a 1,2 mg non nanoporous Si deposited on Cu electrode showcasing a initial discharge capacity of 2700 mAh/g at a current density of 0,229 mA/cm^2, and a capacity retention of 81% from 2250 mAh/g to 1830 mAh/g for a current density of 0,458 mA/cm^2.

Research Question 5, Sub-question

How does partial lithiation of the silicon by limiting the utilized capacity influence the battery performance?

The partial lithiation of Si for Si deposited on Cu electrodes was shown to be a effective strategy to extend the battery life and minimize the battery degradation. A clear distinction was seen between the battery performance of batteries limited to a capacity of 1000, 1500 and 2000 mAh/g of Si. This where the experiments first where a clear difference was seen between the Si with and without nanopores. The nanoporous silicon showed more stable battery cycling with higher coulombic efficiencies, of up to 99%, and less of a increase in required potential difference for both the 1000 and 1500 mAh/g limited capacity batteries.

The answers to these sub-questions now bring us back to the main research question:

Research Question 1, Main question

How can nanoporous silicon be used to improve the performance of solid state batteries using argyrodite solid electrolyte?

With all the sub question answers in mind we can say that nanoporous silicon (from E-magy) can be used to improve the performance in solid state batteries by:

- Limiting the capacity to an extend where the nanoporous structure stays preserved throughout the battery cycling process, which was up to 1000-1500 mAh/g in our case.
- Choosing a high ionic conductive solid electrolyte such as $Li_{5,5}PS_{4,5}Cl_{1,5}$
- Choosing the best electrode preparation method, which was Si deposited on Cu in our case.
- Choosing the right mixing method and composition of conductive additives for the Si electrode, even if the powder composite Si/SE/CNF electrodes didn't show the best performance, they still showed the importance of finding the right ratio for the battery cycling performance.

6.3. Further research and recommendations

This research could have gone on a lot longer, but it had to end at some point. Below some suggestions are made about what could have been done differently or what could be done in future research regarding the use of nanoporous silicon in solid state batteries.

For the Si/SE/CNF powder composite electrodes:

- Limit the utilized Si capacity for the Si/SE/CNF powder composite electrodes to see if limiting the capacity also shows battery cycling improvements for nano porous Si compared to non porous Si, just like it did for the Si on Cu deposited electrodes.
- This can also be done without the CNF to confirm with more data wether or not that improves or hurts the performance.
- Try less severe ball milling conditions that keep the nanoporous Si structure intact to make another comparison with that and hand grinding.

For the Si deposited on Cu electrodes:

- Further optimize the composition by trying different ratio's and binders like PAA or CMC which have been shown to be effective in combination with silicon and solid electrolytes.
- Try how thick the electrodes can be made while still being effective with the nano porous Si.

Regarding battery cycling:

- Test the material at multiple different C-rates and look if the nano porous Si also shows improvements at higher C-rates.
- Extend the cycle number of the 1000 and 1500 mAh/g Si deposited on Cu nanoporous using $Li_{5,5}PS_{4,5}Cl_{1,5}$ SE batteries and see for how long stable cycling performance is maintained, since in this research we only look at the first 50 battery cycles.
- Also try battery cycling with full cells by changing the LiIn electrode to a commonly used cathode like NMC811

Regarding the impedance:

- Look at how the impedance evolves during the cycling by doing a impedance measurement every few cycles instead of only before and after the completed battery cycling process. This will give a better idea of how the impedance changes during the cycling.
- Use a transmission line model to better account for the porous structure of the Si material.
- Use a 3 electrode set up to better distinguish between the impedance caused by both sides of the battery. This could give us a more precise representation of the impedance on the Si electrode side without the other side of the battery influencing it.

Some other battery characterization techniques that could be used

- Make SEM images of the Si electrodes after the battery cycling to see if the nano pores are still intact after certain amounts of capacity are used. It could also be interesting to see what the Si electrode looks like while it is in the lithiated state.
- Use XRD to look at the Si electrodes after cycling to see how the crystal structure has changed. Operando XRD could also possibly be used to see how the crystal structure changes during the battery cycling.
- Use XPS to look at the Si electrode after cycling to see and quantify the SEI decomposition products. And if this changes when the nanoporous Si is used.
- Use NMR to look at the ionic mobility in the lithiated nano porous silicon and if that is any different for silicon without nanopores.

References

[1] Martina Igini. *Fossil Fuel Comprised 82% of Global Energy Mix in 2023*. en. June 2024. URL: `https://earth.org/fossil-fuel-accounted-for-82-of-global-energy-mix-in-2023-amid-record-consumption-report/` (visited on 10/14/2024).

[2] Hannah Ritchie et al. "Renewable Energy". In: *Our World in Data* (Mar. 2024). URL: `https://ourworldindata.org/renewable-energy` (visited on 10/14/2024).

[3] United Nations. *Net Zero Coalition*. en. Publisher: United Nations. URL: `https://www.un.org/en/climatechange/net-zero-coalition` (visited on 10/14/2024).

[4] EIA. *Battery storage power capacity globally 2022-2050*. en. Jan. 2023. URL: `https://www.statista.com/statistics/1307203/world-battery-storage-electricity-generation-capacity/` (visited on 10/14/2024).

[5] Sina Orangi et al. "Historical and prospective lithium-ion battery cost trajectories from a bottom-up production modeling perspective". In: *Journal of Energy Storage* 76 (Jan. 2024), p. 109800. DOI: `10.1016/j.est.2023.109800`. URL: `https://www.sciencedirect.com/science/article/pii/S2352152X23031985` (visited on 10/17/2024).

[6] R. Borah et al. "On battery materials and methods". In: *Materials Today Advances* 6 (June 2020), p. 100046. DOI: `10.1016/j.mtadv.2019.100046`. URL: `https://www.sciencedirect.com/science/article/pii/S2590049819301201` (visited on 12/29/2024).

[7] Sushyanth Sridhar et al. "Development and Future Scope of Renewable Energy and Energy Storage Systems". en. In: *Smart Cities* 5.2 (June 2022). Number: 2 Publisher: Multidisciplinary Digital Publishing Institute, pp. 668–699. DOI: `10.3390/smartcities5020035`. URL: `https://www.mdpi.com/2624-6511/5/2/35` (visited on 10/16/2024).

[8] R. M. Dell et al. *Understanding Batteries*. en. The Royal Society of Chemistry, July 2001. DOI: `10.1039/9781847552228`. URL: `https://books.rsc.org/books/monograph/390/Understanding-Batteries` (visited on 12/23/2024).

[9] Philip Minnmann et al. "Editors ChoiceQuantifying the Impact of Charge Transport Bottlenecks in Composite Cathodes of All-Solid-State Batteries". en. In: *Journal of The Electrochemical Society* 168.4 (Apr. 2021). Publisher: IOP Publishing, p. 040537. DOI: `10.1149/1945-7111/abf8d7`. URL: `https://dx.doi.org/10.1149/1945-7111/abf8d7` (visited on 10/24/2023).

[10] Yixin Dai et al. "Thermal runaway process in lithium-ion batteries: A review". In: *Next Energy* 6 (Jan. 2025), p. 100186. DOI: `10.1016/j.nxener.2024.100186`. URL: `https://www.sciencedirect.com/science/article/pii/S2949821X24000917` (visited on 10/17/2024).

[11] R. Spotnitz et al. "Abuse behavior of high-power, lithium-ion cells". In: *Journal of Power Sources* 113.1 (Jan. 2003), pp. 81–100. DOI: `10.1016/S0378-7753(02)00488-3`. URL: `https://www.sciencedirect.com/science/article/pii/S0378775302004883` (visited on 10/17/2024).

[12] Ziyang Ning et al. "Visualizing plating-induced cracking in lithium-anode solid-electrolyte cells". en. In: *Nature Materials* 20.8 (Aug. 2021). Publisher: Nature Publishing Group, pp. 1121–1129. DOI: `10.1038/s41563-021-00967-8`. URL: `https://www.nature.com/articles/s41563-021-00967-8` (visited on 10/17/2024).

[13] Tammo K. Schwietert et al. "First-Principles Prediction of the Electrochemical Stability and Reaction Mechanisms of Solid-State Electrolytes". In: *JACS Au* 1.9 (Sept. 2021). Publisher: American Chemical Society, pp. 1488–1496. DOI: `10.1021/jacsau.1c00228`. URL: `https://doi.org/10.1021/jacsau.1c00228` (visited on 12/28/2024).

[14] Hyeon-Ji Shin et al. “New Consideration of Degradation Accelerating of All-Solid-State Batteries under a Low-Pressure Condition”. en. In: *Advanced Energy Materials* 13.40 (2023). _eprint: https://onlinelibrary.wiley.com/doi/pdf/10.1002/aenm.202301220, p. 2301220. DOI: `10.1002/aenm.202301220`. URL: `https://onlinelibrary.wiley.com/doi/abs/10.1002/aenm.202301220` (visited on 12/28/2024).

[15] *(PDF) Fundamental Relationship of Microstructure and Ionic Conductivity of Amorphous LLTO as Solid Electrolyte Material.* URL: `https://www.researchgate.net/publication/331102666_Fundamental_Relationship_of_Microstructure_and_Ionic_Conductivity_of_Amorphous_LLTO_as_Solid_Electrolyte_Material` (visited on 11/15/2024).

[16] Adam Volle. *Solid-state battery | Definition, History, & Facts | Britannica.* en. Nov. 2024. URL: `https://www.britannica.com/technology/solid-state-battery` (visited on 12/27/2024).

[17] John Owen. “21 - Ionic Conductivity”. In: *Comprehensive Polymer Science and Supplements.* Ed. by Geoffrey Allen et al. Amsterdam: Pergamon, Jan. 1989, pp. 669–686. DOI: `10.1016/B978-0-08-096701-1.00058-6`. URL: `https://www.sciencedirect.com/science/article/pii/B9780080967011000586` (visited on 12/23/2024).

[18] Kecheng Zhang et al. “Lithium ion diffusion mechanism in covalent organic framework based solid state electrolyte”. en. In: *Physical Chemistry Chemical Physics* 21.19 (May 2019). Publisher: The Royal Society of Chemistry, pp. 9883–9888. DOI: `10.1039/C9CP02117E`. URL: `https://pubs.rsc.org/en/content/articlelanding/2019/cp/c9cp02117e` (visited on 11/15/2024).

[19] Yubin Zhang et al. “Fundamental Relationship of Microstructure and Ionic Conductivity of Amorphous LLTO as Solid Electrolyte Material”. en. In: *Journal of The Electrochemical Society* 166.4 (Feb. 2019). Publisher: IOP Publishing, A515. DOI: `10.1149/2.0161904jes`. URL: `https://iopscience.iop.org/article/10.1149/2.0161904jes/meta` (visited on 11/15/2024).

[20] Liqun Guo et al. “Interfacial instabilities in halide-based solid-state batteries”. en. In: *MRS Bulletin* 48.12 (Dec. 2023), pp. 1247–1256. DOI: `10.1557/s43577-023-00607-3`. URL: `https://doi.org/10.1557/s43577-023-00607-3` (visited on 11/15/2024).

[21] Rui Martim Salgado et al. “The Latest Trends in Electric Vehicles Batteries”. en. In: *Molecules* 26.11 (Jan. 2021). Number: 11 Publisher: Multidisciplinary Digital Publishing Institute, p. 3188. DOI: `10.3390/molecules26113188`. URL: `https://www.mdpi.com/1420-3049/26/11/3188` (visited on 10/17/2024).

[22] Teresa Insinna et al. “Graphite Anodes for Li-Ion Batteries: An Electron Paramagnetic Resonance Investigation”. en. In: *Chemistry of Materials* 35.14 (July 2023), p. 5497. DOI: `10.1021/acs.chemmater.3c00860`. URL: `https://pmc.ncbi.nlm.nih.gov/articles/PMC10373490/` (visited on 10/17/2024).

[23] Md. Helal Hossain et al. “Advances of lithium-ion batteries anode materialsA review”. In: *Chemical Engineering Journal Advances* 16 (Nov. 2023), p. 100569. DOI: `10.1016/j.ceja.2023.100569`. URL: `https://www.sciencedirect.com/science/article/pii/S2666821123001266` (visited on 05/31/2024).

[24] Robert C. Massé et al. “Energy storage through intercalation reactions: electrodes for rechargeable batteries”. In: *National Science Review* 4.1 (Jan. 2017), pp. 26–53. DOI: `10.1093/nsr/nww093`. URL: `https://doi.org/10.1093/nsr/nww093` (visited on 07/01/2024).

[25] Yuxin Tang et al. “ChemInform Abstract: Rational Material Design for Ultrafast Rechargeable Lithium-Ion Batteries”. In: *Chemical Society reviews* 44 (Apr. 2015). DOI: `10.1039/c4cs00442f`.

[26] M. N. Obrovac et al. “Alloy Negative Electrodes for Li-Ion Batteries”. In: *Chemical Reviews* 114.23 (Dec. 2014). Publisher: American Chemical Society, pp. 11444–11502. DOI: `10.1021/cr500207g`. URL: `https://doi.org/10.1021/cr500207g` (visited on 11/03/2024).

[27] Boran Tao et al. “Halide solid-state electrolytes for all-solid-state batteries: structural design, synthesis, environmental stability, interface optimization and challenges”. en. In: *Chemical Science* 14.33 (Aug. 2023). Publisher: The Royal Society of Chemistry, pp. 8693–8722. DOI: `10.1039/D3SC02093B`. URL: `https://pubs.rsc.org/en/content/articlelanding/2023/sc/d3sc02093b` (visited on 10/25/2024).

[28] Mogalahalli V. Reddy et al. “Sulfide and Oxide Inorganic Solid Electrolytes for All-Solid-State Li Batteries: A Review”. In: *Nanomaterials* 10.8 (Aug. 2020), p. 1606. DOI: `10.3390/nano10081606`. URL: `https://www.ncbi.nlm.nih.gov/pmc/articles/PMC7466729/` (visited on 07/01/2024).

[29] Chuang Yu et al. “Recent development of lithium argyrodite solid-state electrolytes for solid-state batteries: Synthesis, structure, stability and dynamics”. In: *Nano Energy* 83 (May 2021), p. 105858. DOI: `10.1016/j.nanoen.2021.105858`. URL: `https://www.sciencedirect.com/science/article/pii/S2211285521001166` (visited on 10/23/2024).

[30] Thomas Yersak et al. “Moisture Stability of Sulfide Solid-State Electrolytes”. In: *Frontiers in Energy Research* 10 (May 2022), p. 882508. DOI: `10.3389/fenrg.2022.882508`.

[31] Ajay Gautam et al. “On the Lithium Distribution in Halide Superionic Argyrodites by Halide Incorporation in Li7xPS6xClx”. In: *ACS Applied Energy Materials* 4.7 (July 2021). Publisher: American Chemical Society, pp. 7309–7315. DOI: `10.1021/acsaem.1c01417`. URL: `https://doi.org/10.1021/acsaem.1c01417` (visited on 10/31/2023).

[32] Tong-Tong Zuo et al. “Impact of the Chlorination of Lithium Argyrodites on the Electrolyte/Cathode Interface in Solid-State Batteries”. en. In: *Angewandte Chemie International Edition* 62.7 (2023). _eprint: https://onlinelibrary.wiley.com/doi/pdf/10.1002/anie.202213228, e202213228. DOI: `10.1002/anie.202213228`. URL: `https://onlinelibrary.wiley.com/doi/abs/10.1002/anie.202213228` (visited on 04/15/2024).

[33] Chaochao Wei et al. “Tuning ionic conductivity to enable all-climate solid-state LiS batteries with superior performances”. en. In: *Materials Advances* 3.2 (Jan. 2022). Publisher: RSC, pp. 1047–1054. DOI: `10.1039/D1MA00987G`. URL: `https://pubs.rsc.org/en/content/articlelanding/2022/ma/d1ma00987g` (visited on 12/28/2024).

[34] Mingtao Gan et al. “Phytic-Acid-Modified Copper Foil as a Current Collector for Lithium-Ion Batteries”. en. In: *Metals* 14.2 (Feb. 2024). Number: 2 Publisher: Multidisciplinary Digital Publishing Institute, p. 247. DOI: `10.3390/met14020247`. URL: `https://www.mdpi.com/2075-4701/14/2/247` (visited on 10/25/2024).

[35] Jianhui Wang et al. “Superconcentrated electrolytes for a high-voltage lithium-ion battery”. en. In: *Nature Communications* 7.1 (June 2016). Publisher: Nature Publishing Group, p. 12032. DOI: `10.1038/ncomms12032`. URL: `https://www.nature.com/articles/ncomms12032` (visited on 12/28/2024).

[36] Rutooj Deshpande et al. “Battery Cycle Life Prediction with Coupled Chemical Degradation and Fatigue Mechanics”. en. In: *Journal of The Electrochemical Society* 159.10 (Aug. 2012). Publisher: IOP Publishing, A1730. DOI: `10.1149/2.049210jes`. URL: `https://iopscience.iop.org/article/10.1149/2.049210jes/meta` (visited on 07/10/2024).

[37] Christoph R. Birkl et al. “Degradation diagnostics for lithium ion cells”. In: *Journal of Power Sources* 341 (Feb. 2017), pp. 373–386. DOI: `10.1016/j.jpowsour.2016.12.011`. URL: `https://www.sciencedirect.com/science/article/pii/S0378775316316998` (visited on 07/01/2024).

[38] Daxian Cao et al. “Lithium Dendrite in All-Solid-State Batteries: Growth Mechanisms, Suppression Strategies, and Characterizations”. In: *Matter* 3.1 (July 2020), pp. 57–94. DOI: `10.1016/j.matt.2020.03.015`. URL: `https://www.sciencedirect.com/science/article/pii/S2590238520301284` (visited on 11/21/2024).

[39] Yongling An et al. “Green, Scalable, and Controllable Fabrication of Nanoporous Silicon from Commercial Alloy Precursors for High-Energy Lithium-Ion Batteries”. In: *ACS Nano* 12.5 (May 2018). Publisher: American Chemical Society, pp. 4993–5002. DOI: `10.1021/acsnano.8b02219`. URL: `https://doi.org/10.1021/acsnano.8b02219` (visited on 03/01/2024).

[40] Huo Hanyu et al. “Silicon as Emerging Anode in Solid-State Batteries”. In: *ACS Energy Letters* 7 (Oct. 2022), pp. 4005–4016. DOI: `10.1021/acsenergylett.2c01950`.

[41] Jingjing Tang et al. “Two-dimensional porous silicon nanosheets as anode materials for high performance lithium-ion batteries”. en. In: *Nanoscale* 11.22 (June 2019). Publisher: The Royal Society of Chemistry, pp. 10984–10991. DOI: `10.1039/C9NR01440C`. URL: `https://pubs.rsc.org/en/content/articlelanding/2019/nr/c9nr01440c` (visited on 05/08/2024).

[42] Xinyu Chen et al. “Advanced Electrode Materials for Lithium-ion Battery: Silicon-based Anodes and Co-less-Ni-rich Cathodes”. In: *Journal of Physics: Conference Series* 2133 (Nov. 2021), p. 012003. DOI: `10.1088/1742-6596/2133/1/012003`.

[43] Zhefei Sun et al. “Building better solid-state batteries with silicon-based anodes”. In: *Interdisciplinary Materials* 2.4 (July 2023). Publisher: John Wiley & Sons, Ltd, pp. 635–663. DOI: `10.1002/idm2.12111`. URL: `https://onlinelibrary.wiley.com/doi/full/10.1002/idm2.12111` (visited on 12/30/2024).

[44] Hui Wu et al. “Designing nanostructured Si anodes for high energy lithium ion batteries”. In: *Nano Today* 7.5 (Oct. 2012), pp. 414–429. DOI: `10.1016/j.nantod.2012.08.004`. URL: `https://www.sciencedirect.com/science/article/pii/S1748013212000977` (visited on 12/29/2024).

[45] Mok Yun Jin et al. “Optimum Particle Size in Silicon Electrodes Dictated by Chemomechanical Deformation of the SEI”. In: *Advanced Functional Materials* 31 (Feb. 2021). DOI: `10.1002/adfm.202010640`.

[46] Xiuyun Zhao et al. “Challenges and prospects of nanosized silicon anodes in lithium-ion batteries”. en. In: *Nanotechnology* 32.4 (Oct. 2020). Publisher: IOP Publishing, p. 042002. DOI: `10.1088/1361-6528/abb850`. URL: `https://dx.doi.org/10.1088/1361-6528/abb850` (visited on 11/14/2023).

[47] Staff Shaibani Mahdokht. *In search of battery-grade silicon*. en-US. Section: Renewables. May 2020. URL: `https://www.ecogeneration.com.au/in-search-of-battery-grade-silicon/` (visited on 07/10/2024).

[48] E-magy. *E-magy - The Battery Industry Is On With Silicon*. en-US. Sept. 2023. URL: `https://e-magy.com/` (visited on 12/24/2024).

[49] Fabio Maroni et al. “Near-Zero Volume Expansion Nanoporous Silicon as Anode for Li-ion Batteries”. en. In: *Journal of The Electrochemical Society* 169.8 (Aug. 2022). Publisher: IOP Publishing, p. 080506. DOI: `10.1149/1945-7111/ac8628`. URL: `https://dx.doi.org/10.1149/1945-7111/ac8628` (visited on 12/23/2024).

[50] Fei Dou et al. “Silicon/Carbon Composite Anode Materials for Lithium-Ion Batteries”. en. In: *Electrochemical Energy Reviews* 2.1 (Mar. 2019), pp. 149–198. DOI: `10.1007/s41918-018-00028-w`. URL: `https://doi.org/10.1007/s41918-018-00028-w` (visited on 05/08/2024).

[51] Darren H. S. Tan et al. “Elucidating Reversible Electrochemical Redox of Li $_6$ PS $_5$ Cl Solid Electrolyte”. en. In: *ACS Energy Letters* 4.10 (Oct. 2019), pp. 2418–2427. DOI: `10.1021/acsenergylett.9b01693`. URL: `https://pubs.acs.org/doi/10.1021/acsenergylett.9b01693` (visited on 07/11/2024).

[52] Darren H. S. Tan et al. “Carbon-free high-loading silicon anodes enabled by sulfide solid electrolytes”. In: *Science* 373.6562 (Sept. 2021). Publisher: American Association for the Advancement of Science, pp. 1494–1499. DOI: `10.1126/science.abg7217`. URL: `https://www.science.org/doi/full/10.1126/science.abg7217` (visited on 10/27/2023).

[53] Wenbo Zhang et al. “The Detrimental Effects of Carbon Additives in Li10GeP2S12-Based Solid-State Batteries”. In: *ACS Applied Materials & Interfaces* 9.41 (Oct. 2017). Publisher: American Chemical Society, pp. 35888–35896. DOI: `10.1021/acsami.7b11530`. URL: `https://doi.org/10.1021/acsami.7b11530` (visited on 10/16/2024).

[54] Inpil Kang et al. “Introduction to carbon nanotube and nanofiber smart materials”. In: *Composites Part B: Engineering*. JCOM 731 " Nanoengineered composites and Ceramic Laminates" Special Issue 37.6 (Jan. 2006), pp. 382–394. DOI: `10.1016/j.compositesb.2006.02.011`. URL: `https://www.sciencedirect.com/science/article/pii/S1359836806000114` (visited on 11/02/2024).

[55] Fengyu Zhang et al. “A review of the effect of external pressure on all-solid-state batteries”. In: *eTransportation* 15 (Jan. 2023), p. 100220. DOI: `10.1016/j.etran.2022.100220`. URL: `https://www.sciencedirect.com/science/article/pii/S2590116822000650` (visited on 11/16/2024).

[56] Daniela Piper. *(PDF) Effect of Compressive Stress on Electrochemical Performance of Silicon Anodes*. July 2012. URL: `https://www.researchgate.net/publication/257774816_Effect_of_Compressive_Stress_on_Electrochemical_Performance_of_Silicon_Anodes` (visited on 12/30/2024).

[57] Jin Kyo Koo et al. “Detrimental electrochemical behavior caused by excessive high pressure on Li-ion pouch-type full cell”. In: *Electrochemistry Communications* 152 (July 2023), p. 107518. DOI: `10.1016/j.elecom.2023.107518`. URL: `https://www.sciencedirect.com/science/article/pii/S1388248123000929` (visited on 11/16/2024).

[58] Bo Wang et al. “Selecting the Degree of Partial Lithiation for Preventing Fracture in Si Micoparticles”. en. In: *Batteries* 9.6 (June 2023). Number: 6 Publisher: Multidisciplinary Digital Publishing Institute, p. 324. DOI: `10.3390/batteries9060324`. URL: `https://www.mdpi.com/2313-0105/9/6/324` (visited on 12/30/2024).

[59] Stephanie Poetke et al. “Partially Lithiated Microscale Silicon Particles as Anode Material for High-Energy Solid-State Lithium-Ion Batteries”. In: *Energy Technology* 11.3 (Mar. 2023). Publisher: John Wiley & Sons, Ltd, p. 2201330. DOI: `10.1002/ente.202201330`. URL: `https://onlinelibrary.wiley.com/doi/full/10.1002/ente.202201330` (visited on 12/30/2024).

[60] Shuting Luo et al. “Growth of lithium-indium dendrites in all-solid-state lithium-based batteries with sulfide electrolytes”. en. In: *Nature Communications* 12.1 (Nov. 2021). Publisher: Nature Publishing Group, p. 6968. DOI: `10.1038/s41467-021-27311-7`. URL: `https://www.nature.com/articles/s41467-021-27311-7` (visited on 01/03/2025).

[61] Moumita Rana et al. “Toward Achieving High Areal Capacity in Silicon-Based Solid-State Battery Anodes: What Influences the Rate-Performance?” In: *ACS Energy Letters* 8 (June 2023), pp. 3196–3203. DOI: `10.1021/acsenergylett.3c00722`.

[62] Lukas Medenbach et al. “The IndiumLithium Electrode in Solid-State Lithium-Ion Batteries: Phase Formation, Redox Potentials, and Interface Stability”. en. In: *Batteries & Supercaps* 2.6 (2019). _eprint: https://onlinelibrary.wiley.com/doi/pdf/10.1002/batt.201800149, pp. 524–529. DOI: `10.1002/batt.201800149`. URL: `https://onlinelibrary.wiley.com/doi/abs/10.1002/batt.201800149` (visited on 01/17/2024).

[63] Cameron F. Holder et al. “Tutorial on Powder X-ray Diffraction for Characterizing Nanoscale Materials”. In: *ACS Nano* 13.7 (July 2019). Publisher: American Chemical Society, pp. 7359–7365. DOI: `10.1021/acsnano.9b05157`. URL: `https://doi.org/10.1021/acsnano.9b05157` (visited on 11/18/2024).

[64] Mario Birkholz et al. *Thin film analysis by X-ray scattering*. en. Weinheim: Wiley-VCH, 2006.

[65] George F. Harrington et al. “Back-to-Basics tutorial: X-ray diffraction of thin films”. en. In: *Journal of Electroceramics* 47.4 (Dec. 2021), pp. 141–163. DOI: `10.1007/s10832-021-00263-6`. URL: `https://doi.org/10.1007/s10832-021-00263-6` (visited on 11/18/2024).

[66] Yannik Rudel et al. “Investigating the Influence of the Effective Ionic Transport on the Electrochemical Performance of Si/CArgyrodite SolidState Composites”. en. In: *Batteries & Supercaps* 6.8 (Aug. 2023), e202300211. DOI: `10.1002/batt.202300211`. URL: `https://chemistry-europe.onlinelibrary.wiley.com/doi/10.1002/batt.202300211` (visited on 01/17/2024).

[67] Anix Casimir et al. “Silicon-based anodes for lithium-ion batteries: Effectiveness of materials synthesis and electrode preparation”. In: *Nano Energy* 27 (Sept. 2016), pp. 359–376. DOI: `10.1016/j.nanoen.2016.07.023`. URL: `https://www.sciencedirect.com/science/article/pii/S2211285516302622` (visited on 06/25/2024).

[68] Pooja Vadhva et al. “Electrochemical Impedance Spectroscopy for All-Solid-State Batteries: Theory, Methods and Future Outlook”. en. In: *ChemElectroChem* 8.11 (2021). _eprint: https://onlinelibrary.wiley.com/doi/pdf/10.1002/celc.202100108, pp. 1930–1947. DOI: `10.1002/celc.202100108`. URL: `https://onlinelibrary.wiley.com/doi/abs/10.1002/celc.202100108` (visited on 07/01/2024).

[69] Woosung Choi et al. “Modeling and Applications of Electrochemical Impedance Spectroscopy (EIS) for Lithium-ion Batteries”. en. In: *Journal of Electrochemical Science and Technology* 11.1 (Feb. 2020), pp. 1–13. DOI: `10.33961/jecst.2019.00528`. URL: `http://jecst.org/journal/view.php?doi=10.33961/jecst.2019.00528` (visited on 01/11/2025).

[70] RelaxIS. *RelaxIS 3: THE software for impedance spectroscopy analysis*. en-US. Oct. 2025. URL: `https://rhd-instruments.de/solutions-and-products/for-eis-data-analysis/relaxis/` (visited on 01/03/2025).

[71] Alexandros Ch. Lazanas et al. “Electrochemical Impedance SpectroscopyA Tutorial”. In: *ACS Measurement Science Au* 3.3 (June 2023). Publisher: American Chemical Society, pp. 162–193. DOI: `10.1021/acsmeasuresciau.2c00070`. URL: `https://doi.org/10.1021/acsmeasuresciau.2c00070` (visited on 12/05/2024).

[72] Parvin Adeli et al. “Boosting Solid-State Diffusivity and Conductivity in Lithium Superionic Argyrodites by Halide Substitution”. en. In: *Angewandte Chemie International Edition* 58.26 (2019). _eprint: https://onlinelibrary.wiley.com/doi/pdf/10.1002/anie.201814222, pp. 8681–8686. DOI: `10.1002/anie.201814222`. URL: `https://onlinelibrary.wiley.com/doi/abs/10.1002/anie.201814222` (visited on 12/05/2024).

[73] Linfeng Peng et al. “Enhancing Moisture and Electrochemical Stability of the Li5.5PS4.5Cl1.5 Electrolyte by Oxygen Doping”. In: *ACS Applied Materials & Interfaces* 14.3 (Jan. 2022). Publisher: American Chemical Society, pp. 4179–4185. DOI: `10.1021/acsami.1c21561`. URL: `https://doi.org/10.1021/acsami.1c21561` (visited on 04/15/2024).

[74] Roby Gauthier et al. “The amorphization of crystalline silicon by ball milling”. In: *Heliyon* 10.15 (July 2024), e34881. DOI: `10.1016/j.heliyon.2024.e34881`. URL: `https://www.ncbi.nlm.nih.gov/pmc/articles/PMC11320443/` (visited on 12/16/2024).

[75] Axel Durdel et al. “Modeling Silicon-Dominant Anodes: Parametrization, Discussion, and Validation of a Newman-Type Model”. en. In: *Batteries* 9.11 (Nov. 2023). Number: 11 Publisher: Multidisciplinary Digital Publishing Institute, p. 558. DOI: `10.3390/batteries9110558`. URL: `https://www.mdpi.com/2313-0105/9/11/558` (visited on 12/10/2024).

[76] Elad Pollak et al. “In Situ Conductivity, Impedance Spectroscopy, and Ex Situ Raman Spectra of Amorphous Silicon during the Insertion/Extraction of Lithium”. In: *The Journal of Physical Chemistry C* 111.30 (Aug. 2007). Publisher: American Chemical Society, pp. 11437–11444. DOI: `10.1021/jp0729563`. URL: `https://doi.org/10.1021/jp0729563` (visited on 12/10/2024).

[77] *E-magy - The Battery Industry Is On With Silicon.* URL: `https://e-magy.com/` (visited on 12/11/2024).

[78] Svetlana Menkin et al. “Insights into soft short circuit-based degradation of lithium metal batteries”. In: *Faraday Discussions* 248 (), pp. 277–297. DOI: `10.1039/d3fd00101f`. URL: `https://www.ncbi.nlm.nih.gov/pmc/articles/PMC10823489/` (visited on 01/12/2025).

[79] Ke Pan et al. “Comprehensive electrochemical impedance spectroscopy study of Si-Based anodes using distribution of relaxation times analysis”. In: *Journal of Power Sources* 479 (Dec. 2020), p. 229083. DOI: `10.1016/j.jpowsour.2020.229083`. URL: `https://www.sciencedirect.com/science/article/pii/S0378775320313781` (visited on 01/24/2024).

[80] Andika Pandu Nugroho et al. “Vertically Aligned n-Type Silicon Nanowire Array as a Free-Standing Anode for Lithium-Ion Batteries”. en. In: *Nanomaterials* 11.11 (Nov. 2021). Number: 11 Publisher: Multidisciplinary Digital Publishing Institute, p. 3137. DOI: `10.3390/nano11113137`. URL: `https://www.mdpi.com/2079-4991/11/11/3137` (visited on 01/11/2025).